

**Framework for the quantitative analysis of the interplay between
cyanobacterial physiology and photosynthesis-driven biocatalysis**

Dissertation

Zur Erlangung des

Doktorgrades der Ingenieurwissenschaften (Dr.-Ing.)

der Naturwissenschaftlichen Fakultät I – Biowissenschaften –

der Martin-Luther-Universität Halle-Wittenberg,

vorgelegt von

Dipl.-Ing. Marcel Grund

geb. am 17. Juli 1986 in Hagen

Gutachter:

Prof. Dr. Bruno Bühler

Prof. Dr. Markus Pietzsch

Prof. Dr. Rene Wijffels

Tag der Verteidigung: 31.01.2020

Selbstständigkeitserklärung

Hiermit erkläre ich, Marcel Grund, an Eides statt, dass ich die vorliegende Dissertation selbstständig und ohne fremde Hilfe verfasst habe, dass keine anderen als die von mir angegebenen Quellen und Hilfsmittel verwendet und die den verwendeten Werken wörtlich oder inhaltlich entnommenen Stellen als solche kenntlich gemacht worden sind.

Die Dissertation hat in der gegenwärtigen bzw. in einer anderen Fassung noch keiner Prüfungsbehörde vorgelegen.

Leipzig, 25.06.2019

Danksagung

An dieser Stelle möchte ich allen, die direkt oder indirekt zum erfolgreichen Abschluss dieser Arbeit beigetragen haben, danken. Ein ganz besonderer Dank gilt meinem Doktorvater Prof. Dr. Bruno Bühler. Nach dem Umzug an das UFZ hat er mich in seine Gruppe aufgenommen und mich im Folgenden in jeder Situation uneingeschränkt unterstützt und gefördert. Dein unglaublich scharfes wissenschaftliches Denken, die beispiellose Expertise in der Biokatalyse und das Erkennen tieflyingender Zusammenhänge sind eine Inspiration. Danke für Deine Geduld in den vielen langen Meetings und wissenschaftlichen Diskussionen, die diese Arbeit mitgeprägt haben, aber auch bei den kläglichen Versuchen von mir auf, zunächst zwei Brettern, und später einem Brett, heil die Pisten von Davos hinunterzukommen.

Eine besondere Rolle nahm auch Prof. Dr. Andreas Schmid ein. Er ermöglichte diese Arbeit in einem spannenden und sich schnell entwickelnden Forschungsgebiet. Ohne seine Unterstützung und das Schaffen der notwendigen Infrastruktur wäre die erfolgreiche Durchführung dieser Arbeit nicht möglich gewesen. Besonders geschätzt habe ich unseren offenen Umgang miteinander und den gewährten Freiraum während der Entwicklung und Durchführung dieser Arbeit.

Einen ganz herzlichen Dank möchte ich an Prof. Christian Wilhelm und Dr. Torsten Jakob von der Universität Leipzig richten. Als ich mit dem Projekt begonnen habe, begannen wir von Null an die Fundamente und Voraussetzungen für die Arbeit mit Cyanobakterien zu schaffen. Die Kooperation im Rahmen dieser Arbeit ermöglichte mir mich schnell und tief in das Gebiet der phototrophen Physiologie einzuarbeiten. Danke Euch beiden für die vielen Diskussionen und die Unterstützung.

Die Arbeit wurde ungemein erleichtert durch die offene und produktive, aber gleichzeitig freundschaftliche Atmosphäre in der BT und später in SoMa. Danke an alle, die dies leben und dazu beigetragen haben: Adrian, Anna, Babu, Bart, Bin, Birgitta (die mir während meiner Studienarbeiten die wissenschaftliche Basis vermittelt hat), unseren Sekretärinnen Christine, Anja K. und Anja S. (die in jeder organisatorischen Notlage eine große Hilfe waren), Christian D. (wir haben es geschafft!) und Christian W., Carolin, Caroline, Dani, Düse, Eleni, Fabian, Francesco, Heiko, Inge, Jan, Jenny, Jens A. und Jens K., Jochen, dem „*Ur-Leipziger*“ Jörg, Kamila und Diego (*¡Muchas gracias por los tiempos locos!*), Karo, Karsten, Katja, Katrin, Kerstin, Kirsten, Kristin, Linde, Lisa, Lollo und Mona, Magda, Mahir, Mani, Martin, Marvin, Mattijs, Nadine, Olli, Patty, Peter, Pfützchen, Rohan, Ron (ein Hoch auf unsere Vorliebe für koffeinhaltige *Limonaden*), Samuel, dem Schirmchen, Paulchen, Sebastian, Stephan, Verena, Vu.

Meinen Studenten Dominik, Marco und Philipp möchte ich für Ihren großen Einsatz und die Begeisterung beim Bearbeiten Ihrer wissenschaftlichen Fragestellungen danken und wünsche Ihnen viel Erfolg auf Ihrem zukünftigen Weg.

Mani und Rohan sind zu engen Weggefährten geworden. Danke für die vielen wissenschaftlichen Diskussionen, das Entertainment in guten wie in schwierigen Zeiten und die vielen gute Ratschläge in den vergangenen Jahren.

Hmmm, Anna und Magda: bei Euch möchte ich mich hier ganz besonders bedanken: Ihr seid zu einem wichtigen Teil in meinem Leben geworden. Danke für Eure Unterstützung, fürs Da-Sein in guten wie in schwierigeren Zeiten sowohl im Labor/Büro als auch im *realen* Leben. An unsere gemeinsamen Zeiten in unserem gemeinsamen Wohnzimmer, beim Luft-Schnappen, beim *Was-Was'n*, an unserem Hausstrand und auch sonst überall werde ich immer gerne zurückdenken.

Ein großer Dank gilt auch meiner Familie, insbesondere meinem Bruder Dennis, meiner Oma Elisabeth und meinem Opa Paul, der leider zu früh von uns ging, Edith und Martin. Abschließend möchte ich meinen tiefen Dank für die unermüdliche Unterstützung meiner Eltern auf diesem langen Weg ausdrücken. Ihr habt immer, egal ob in Dortmund, Indianapolis, Brisbane oder Leipzig, hilfreich, verständnisvoll und mitfiebernd hinter mir gestanden. Vielen Dank dafür.

*Zwei Dinge sind zu unserer Arbeit nötig:
Unermüdliche Ausdauer und die Bereitschaft, etwas, in das
man viel Zeit und Arbeit gesteckt hat, wieder wegzuwerfen.*

Albert Einstein

Funding and support

This work was performed in the facilities of the Centre for Biocatalysis (MiKat) at the Helmholtz Centre for Environmental Research which is supported by European Regional Development Funds (EFRE - Europe funds Saxony, 10096171), and the Helmholtz Association. Additional support was provided by the Helmholtz Impulse and Networking Fund through the Helmholtz Interdisciplinary Graduate School for Environmental Research (HIGRADE).

Table of contents

List of Abbreviations	VII
Summary	VIII
Zusammenfassung	IX
Chapter 1: General introduction	1
Chapter 2: Electron balancing under different sink conditions reveals positive effects on photon-efficiency and metabolic activity of <i>Synechocystis</i> sp. PCC 6803	23
Chapter 3: Heterologous lactate synthesis in <i>Synechocystis</i> sp. PCC 6803 causes a condition-dependent increase of photosynthesis rates	47
Chapter 4: Accessing the efficiency of the hydroxylation of cyclohexane to cyclohexanol in a continuous photo-biotransformation	69
Chapter 5: General Discussion	91
Chapter 6: Conclusion and Outlook	102
References	104
Supplemental Information	118
Curriculum Vitae	123

List of Abbreviations

AEF	alternative electron flux
A^*_{phy}	chlorophyll <i>a</i> dependent cellular absorption coefficient
CEF	cyclic electron flux
C	carbon
°C	degree Celsius
CCM	carbon concentration mechanism
CDW	cell dry weight
chl <i>a</i>	chlorophyll <i>a</i>
DoR	degree of reduction
e ⁻	electron
ETC	electron transport chain
Fd	ferredoxin
Flv	flavodiiron proteins
LEF	linear electron flux
LIC	light induction curve
N	nitrogen
ncAEF	non cyclic alternative electron flux
OD ₇₅₀	optical density at 750 nm
PAR	photosynthetically active radiation
PSI	photosystem I
PSII	photosystem II
Q _{phar}	photon uptake rate
r	specified rate
r _{AEF}	ate of alternative electron flux
r _F	fluorescence based PSII rate
r _O	oxygen evolution rate
r _{O,gross}	oxygen evolution rate corrected for the respiration rate
r _{Resp}	respiration rate
rH	relative humidity
Y(PSII)	effective quantum yield around PSII

Abbreviations are introduced in the text when used the first time within a chapter.

Summary

Photo-biotechnology gains increasing attention for its capability to contribute to a substitution of fossil resource utilization and a decarbonized economy. Consequently, much effort is spent in engineering photosynthetically active cells as whole-cell biocatalysts for the synthesis of value-added products directly from CO₂ and/or light. Nevertheless, successful and rational strain and process engineering is hampered by insufficient knowledge on the physiology of photosynthetically active cells.

This study focuses on biocatalyst characterization, which is an essential aspect in bioprocess development. A methodological framework was developed to enable a systematic and quantitative investigation of the physiological properties of the model cyanobacterium *Synechocystis* sp. PCC 6803. Combination of continuous cultivation strategies with an advanced set of analytics allowed the quantitative characterization of light reactions and carbon metabolism within defined and controlled steady states. The established framework was applied to investigate the physiological response of *Synechocystis* sp. PCC 6803 to three different additional electron and/or carbon sinks, i.e., the assimilation of differently reduced nitrogen sources, the fermentative synthesis of lactate from CO₂, and the hydroxylation of cyclohexane to cyclohexanol.

The results confirm a carbon sink effect, which is the metabolic stimulation of photosynthetically active cells by an additional sink, e.g., a biocatalytic reaction. Increased effective quantum yields and enhanced metabolic rates (reflected by carbon fixation, water oxidation, and linear electron transfer rates) were observed for all model systems. Strikingly, stimulating effects were not found under all tested conditions but depended strongly on light and carbon availability. In this respect, additional sinks are hypothesized to enable an optimization of the cellular ATP and NAD(P)H balances and thus enhance photosynthesis rates within the given environmental and metabolic constraints. Additionally, investigation of photosynthesis-driven biotransformation of cyclohexane to cyclohexanol revealed a tremendous impact of the metabolic state on the whole-cell activity, emphasizing the importance of systematic and quantitative approaches in photo-biotechnology.

This study contributes to the fundamental understanding of photosynthetically active cyanobacterial cells and demonstrates the potential of and necessity for systematic and quantitative biocatalyst characterization in photo-biotechnology.

Zusammenfassung

Die Photo-Biotechnologie hat das Potenzial, durch die Substitution von fossilen Rohstoffen zur Dekarbonisierung der industriellen Ökonomie beizutragen. Die Entwicklung von photosynthetisch aktiven Ganzzell-Biokatalysatoren zur Produktion von Wertstoffen und Energieträgern ausgehend von CO₂ und/oder Licht befindet sich dabei im Zentrum wissenschaftlicher und industrieller Forschung. Limitiertes Wissen über die grundlegenden Mechanismen und quantitativen Potenziale photosynthetisch aktiver Zellen erschwert jedoch die rationale und effiziente Biokatalysator- und Bioprozessentwicklung.

Die vorliegende Studie setzt an der quantitativen und systematischen Untersuchung der Physiologie des Modell-Organismus *Synechocystis* sp. PCC 6803 als Ganzzell-Biokatalysator an. Dazu wurde ein integrierter Kultivierungs- und Analytik-Ansatz verfolgt, der es ermöglicht die Physiologie von *Synechocystis* sp. PCC 6803 in definierten und reproduzierbaren Fließgleichgewichten quantitativ zu erfassen. Neben grundlegenden physiologischen Effekten unter verschiedenen Licht- und CO₂-Verfügbarkeiten wurde der Einfluss von biokatalytisch bedingtem Kohlenstoff- oder Elektronen-Abzug auf die Zellphysiologie untersucht. Dazu wurden drei verschiedene Ansätze verfolgt: i. die Variation der zellulären Stickstoff-Assimilierungskosten durch die Verwendung von Stickstoffquellen mit unterschiedlichem Reduktionsgrad, ii. Kohlenstoffabfluss durch Laktat-Synthese ausgehend von CO₂ und iii. Elektronenabzug durch eine an die Photosynthese gekoppelte Hydroxylierung von Cyclohexan zu Cyclohexanol.

Die Ergebnisse dieser Studie bestätigen die in der Literatur diskutierten Hinweise auf eine Erhöhung von Photosynthese- und Kohlenstofffixierungsraten durch das Einbringen zusätzlicher Elektronen- und Kohlenstoff-Senken in Form biokatalytischer Reaktionen. Dieser Effekt wird in der Literatur als *Carbon Sink Effect* beschrieben und diskutiert. In allen untersuchten Ansätzen konnte eine Erhöhung der Raten für Wasseroxidation, linearen Elektronentransfer und/oder Kohlenstofffixierung festgestellt werden. Diese Effekte waren stark von der CO₂- und Lichtverfügbarkeit wie auch von der Art der zusätzlichen Senke abhängig. Somit wird die Hypothese aufgestellt, dass eine zusätzliche Senke unter geeigneten Umweltbedingungen (Licht- und CO₂-Verfügbarkeit) zur Optimierung der zellulären ATP/NAD(P)H Bilanz beitragen und innerhalb bestimmter metabolischer Grenzen, wie z.B. die maximale Kohlenstofffixierungsrate, zu einer Erhöhung der metabolischen Aktivität führen kann. Untersuchungen zur Biotransformation von Cyclohexan zur

Cyclohexanol zeigten zudem großen Einfluss der Kultivierungsbedingungen und somit der metabolische Zustand der Zellen auf die Ganzzellaktivität.

Zusammenfassend zeigt diese Arbeit die Bedeutung von quantitativer und systematischer Analyse der Physiologie von Photo-Biokatalysatoren für die Stamm- und Prozessentwicklung auf. Sie leistet auf Basis eines entwickelten quantitativen Ansatzes einen fundamentalen Beitrag zum Verständnis der Wechselbeziehung von photosynthetischem Metabolismus und biokatalytischer Aktivität.

Chapter 1: General introduction

Fossil resource use and climate change: the need for low- and zero-carbon resources and energy carriers

The ability to exploit fossil resources as a cheap and abundant energy source has accelerated human development at the beginning of the 17th century, peaking in industrialization and modern lifestyle as present today. Consequently, fossil resources are the basis for human development and wealth, and most energy and chemical supply chains rely on them. Worldwide, a total of 4622 Mt refined oil equivalents were used in 2017 [1]. Most of it is utilized as energy carrier for electricity generation or as fuel in the mobility sector. 676 Mt fossil resources are used by the chemical industry as feedstock or energy source for chemical production (in 2013 [2]), which is a significant share of the overall global fossil resource use. Most of the carbon in the exploited fossil resources is consequently introduced as carbon dioxide (CO₂) to the global carbon cycle and severely interferes with the global carbon budget [3]. As a result, the global atmospheric carbon dioxide concentration raised from 277 ppm in 1750, the onset of the industrial era [4], to 410.6 ppm in May 2019 [5] in accordance to the fossil resource use. Overall, it is estimated that mankind released a total of more than 400 billion metric tons of carbon into the atmosphere in the time span from 1751 to 2014 due to fossil resource utilization [6]. In 2017, the total emitted CO₂ was estimated between 11.3 ± 0.9 Gt carbon (combined fossil resource use and land-use) [3] and 33.4 Gt CO₂ (equivalent to 9.1 Gt carbon) [1]. This and the simultaneous increase in the abundance of other greenhouse gases is the main cause for the climate change phenomena and especially global warming as we are experiencing since a few decades. The resulting changes in global and/or local weather and/or climate in terms of extremes such as storms [7, 8], excessive rain and floods [7, 9, 10], heat waves [11], and, droughts [12, 13] are, or will be, apparently occurring more heavily and frequently. The human-induced changes are so severe that the present time is already considered as an era determined by mankind, the Anthropocene [14, 15]. It has the potential to fully destroy the planet and consequently the basis of life and mankind [16, 17], and ultimately yielding in mass distinction [18]. This prompts politics regularly to initiate means to reduce negative climate change effects due to global warming [19]. The “Paris Agreement” in 2015 declares to take all measures to limit the average global warming to a maximum of 2°C above the pre-industrial era by reduction of carbon and greenhouse gas emissions [20].

Replacing fossil resources by renewable resources

Different strategies for the transition of the fossil-resource based economy to a sustainable carbon neutral economy are under debate. The main focus is the substitution of fossil resources as energy carriers by renewable fuels and respective sources. While controversial debates are ongoing regarding a comeback of nuclear power [21-23] or the development of atomic fusion as low-carbon energy source of the future [24], we already have the technology for the sustainable generation of electricity by exploiting natural energy sources in hand: geothermal, solar, wind, and water energy can be transformed efficiently into electricity [25-28]. The potential of such technologies is enormous and enables the coverage of the global electricity and heating demand by far: solely the solar radiation reaching earth would be sufficient to cover the global demand approximately 2850 times, and, wind power could be used to cover 200 times the global energy demand [28]. To access this potential and to overcome challenges such as balancing anti-cyclic demand for energy and its generation phases, which in case of solar and wind power is highly dependent on daytime, weather and region, a plethora of solutions are under debate. Those include local electricity storage and transformation of generated electricity to energy carriers such as methane or hydrogen [29, 30]. The transition towards a low-carbon energy generation system appears, considering the potential of natural energy resources, feasible.

The transition towards a fossil resource free mobility sector seems more challenging. While electricity can be introduced into the existing grid infrastructure, fuels have to be provided at the place needed. Electricity and hydrogen-based technologies are discussed as the main alternatives. Vehicles powered by electric engines captivate by the charming idea that the potential of renewable electricity can be directly used for mobility, but severe challenges such as (in the moment) low energy density in the required batteries and critical resource demand/availability have to be overcome to build up a broad electrified mobility sector [31, 32]. Hydrogen-based mobility is discussed as an alternative [33]. It can be burned in fuel cells to generate electricity, which can, in turn, be used to power engines. Hydrogen is also a potential energy carrier for decentralized energy and power generation systems [34, 35]. The above-mentioned coupling of hydrogen production as energy storage for renewable energy resources could further contribute to a low carbon hydrogen supply chain [30, 35].

Bioeconomy

The path to a low or even zero carbon economy is long and challenging. But as discussed, technological solutions to replace fossil resources for electricity generation are on the way. Keywords found at multiple levels within the transition process away from fossil resource use are, besides the above-mentioned utilization of natural energy sources, *bio-economy* and *biofuels*. The term biofuel gained significant attention when fossil resource prices increased and the fossil resource dependent climate change debates started and is a substantial puzzle piece in future energy mix considerations [36]. Bio-economy concepts aim at gaining biofuels, such as bioethanol from natural resources like sugars, and oils derived from biomass (first generation biofuels) or plant waste material (second generation), or oils from algal biomass (third generation). Such biologically derived energy carriers are CO₂ neutral since the CO₂ which is released was fixed before by the feedstock plants or algae from the atmospheric CO₂ [37]. Considering the dimension of fossil resources to be replaced, it is under debate if first and second generation biofuels have the potential as a sustainable resource, mainly due to a land use conflict with food production [38, 39]. Irrespective of that, it is estimated that biomass-based energy has the potential to cover the global energy demand by a factor of 20 [28]. The third biofuel generation tries to overcome the land use conflict by utilizing algae as feedstock, which can be cultivated on non-arable land and with higher efficiencies than plants [40, 41]. But even the potential of third generation biofuels is under debate, mainly regarding the whole life cycle energy balance [42].

The fourth biofuel generation shall overcome such limitations by decoupling biomass and fuel production. By applying genetic engineering, cells can be “designed” to produce hydrogen from sunlight and water directly or utilize CO₂ and metabolize it directly into a fuel component, for example, ethanol or certain alkanes [37, 43, 44]. In this way, not only energy carriers, but also components synthesized in chemical processes, can be produced by using CO₂ as feedstock in a low-carbon or even zero-carbon manner. Consequently, biotechnology offers not only an option to substitute fossil resource dependent energy generation but also fossil feedstocks in chemical production and thereby contributing to a de-carbonization of the industrial chemical sector.

Milestones in microbial biotechnology

The UNESCO defines biotechnology as the following [45]:

Biotechnology is the term given to the use of plants, animals, micro-organisms and biological processes to achieve advancement in the areas of industry, medicine and agriculture. It is the utilization of living organisms to promote development for the benefit of mankind.

According to this definition, the use of microorganisms for food processing, i.e. fermentation of beverages and curing of food, can be considered as the first biotechnological applications. The earliest evidence for fermentation processes for food conservation purposes, in this case, fish, was found in Scandinavia and reaches approx. 9200 years back [46]. Hints for fermented (alcoholic) beverages reach back 9000 years in China, and even as far as 13000 years in the Middle Eastern area [47]. In those times, biotechnology was conducted rather in an “empirical” way without knowledge of the involved microbial processes.

The initial starting point towards microbiology and “rational” biotechnology by applying genetic manipulation techniques was set by the work of Antoni Van Leeuwenhoek and Robert Hooke with the development of the first microscopes and the first characterization of microorganisms in the 1660's [48, 49]. The next milestone was the understanding of heritage and consequently of genes as code for living processes. The basis for that was set already in 1866 by Gregor Mendel, who described in his studies heritage rules of certain characteristics in pea plants over multiple generations [50]. But Mendel was way ahead of his time and it took until 1906 that William Bateson seized on Mendel's ideas and framed the field of genetics [51, 52]. The breakthrough was the elucidation of the structure of DNA in 1953 by Francis Crick and James Watson [53]. From this point on, the mechanistic and structural building plan for living processes was known, and, consequently, in principle also the knowledge what would have to be done to manipulate and “design” (microbial) cells. And indeed, Herbert Wayne Boyer succeeded only about twenty years later with the attempt to transfer and express heterologous DNA in another cell [54]. This can be considered as the beginning of rational cell design and modern biotechnology. Based on that technology, Boyer himself founded already in 1976 the first commercial (industrial) biotechnology company, Genentech. Genentech was in the following the first company to announce a heterologous synthesized commercial product: insulin [55].

Photo-biotechnology: exploiting CO₂ and (sun) light as substrates

The knowledge basis in the field of microbial biotechnology increased steadily over the following years, and by today, many products are produced in biotechnological processes with genetically modified, or engineered, microorganisms or enzymes as biocatalysts: for example amino acids, enzymes, bulk chemicals, food additives, antibiotics and pharmaceuticals [56-58]. Most microbial biotechnological processes depend on organic feedstocks, for example sugars, which are derived from plants. The use of biological feedstocks can be considered CO₂ neutral, but the competition for arable land between biotechnological utilization of biomass for fuel production or as chemical feedstock with food production demonstrates that this is not an entirely sustainable and reasonable solution. The utilization of CO₂ as a substrate, in contrast, is a more elegant solution to combine chemical and fuel synthesis in the context of de-carbonization. Nature offers a solution to enable both, the synthesis of value-added products and energy carriers, and the simultaneous utilization of CO₂.

Photosynthetically active cells, such as algae and cyanobacteria, are ubiquitous organisms which evolved 3.5 billion years ago [59, 60]. They exhibit two distinct features: 1. they are able to use light as energy source and transform it into biochemically available energy, and, 2. they can utilize “thermodynamically dead” CO₂ as sole carbon source and precursor for biomass formation (Fig. 1). In the above-outlined context, this makes photosynthetically active cells highly interesting as chassis organisms for “green” and zero-carbon biotechnological applications. Consequently, much effort is taken to evaluate and demonstrate cyanobacteria as a chassis for biofuel and chemical production directly from CO₂ and sunlight [61-64]. In the last decades, it was demonstrated that cyanobacteria can be engineered for the conversion of CO₂ into all relevant chemical classes such as alcohols [65-71], carbohydrates [72], organic acids [73, 74], alkanes and fatty acids [75-77], terpenes [78-80], and amino acids [81]. Furthermore, it was shown that cofactor dependent enzymes can be coupled directly to the photosynthetic electron transport chain, exploiting the electrons derived from water-splitting for the reduction of a specific reaction substrate [82]. Examples are reactions mediated by P450 monooxygenases [83-85] or enoate reductase [86] and the synthesis of hydrogen via hydrogenases [87-89].

Even though the potential of photosynthetically active cells was demonstrated, not many concepts reached a large production scale. Multiple startups tried to establish

photosynthetic CO₂ conversion into value-added products, especially in the context of sustainable biofuels. A prominent example is Joule Unlimited, formerly known as Joule Biotechnologies, which claimed the concept of “*Hyperphotosynthetic Organisms*” for the synthesis of ethanol or other carbon-based fuels such as alkanes from CO₂ and innovative bioprocess solutions for biofuel production [90, 91]. While the company and its strategy was widely celebrated (among others as “GoingGreen Top 100 Winner” [92], one of the “World's 10 Most Important Emerging Technologies” [93] and as one of the “50 Most Innovative Companies in the World” [94]), it did not exceed the stage of demonstration plants towards commercialization. Instead, Joule Unlimited was closed in 2017 because financing of the first commercial scale plant was not feasible within the low-price frame of biofuels and bulk products [95]. Other companies, such as Solazyme Inc. and Algenol LCC, experienced similar challenges with similar concepts to synthesize carbon-based products and biofuels directly from CO₂. Today, both companies shifted the main focus of operations to biomass-based food additives and personal care products, which allows operation in an economically feasible frame. The next round in attempting commercialization is taken by Photanol BV, which uses modified cyanobacteria to produce chemicals from CO₂. It recently announced to build a demonstration plant for the production of organic acids which can be used in biodegradable plastics, personal care products and as intermediates for the chemical industry [96].

Efficient bioprocess development

The examples of failed commercialization and scale-up of photo-biotechnological processes reveal that economic compatibility is one of the main challenges towards commercialization. This is especially true for low price products including fuels and bulk chemicals. Bioprocesses are considered to be economically feasible depending on the character of the product: typical threshold production values are 0.5 – 10 € kg_{product}⁻¹ for bulk chemicals, 10 – 50 € kg_{product}⁻¹ for fine chemicals, and >100 € kg_{product}⁻¹ for pharmaceuticals [97, 98]. As biofuels and bioplastics, as targeted by Photanol BV, are bulk chemicals, it is clear that the economic pressure on such a bioprocess is key. To achieve compatibility, certain process and reaction parameters have to be met. Most relevant are productivity, product titer and yield [99]. Values of >10 g_{product} L_{reactor}⁻¹ h⁻¹, >300 g_{product} L_{reactor}⁻¹ and between 10³ - 10⁵ g_{product} g_{catalyst}⁻¹ are considered to enable economic feasibility for bulk chemicals [97]. In

order to reach those parameters in an efficient and straight forward manner, rational bioprocess development is required.

Each bioprocess consists of three stages (Fig. 1.1, [100]): Upstream, midstream and downstream process. In the upstream process development, a suitable biocatalyst has to be identified and the product formation and yield have to be optimized on cellular or enzyme level for the synthesis of the product. The midstream process development deals with the optimization of the product yield and titer and the product formation rate by identifying ideal cultivation and process conditions. At last, the downstream process has to be designed for efficient and effective product removal and purification from the cultivation broth.

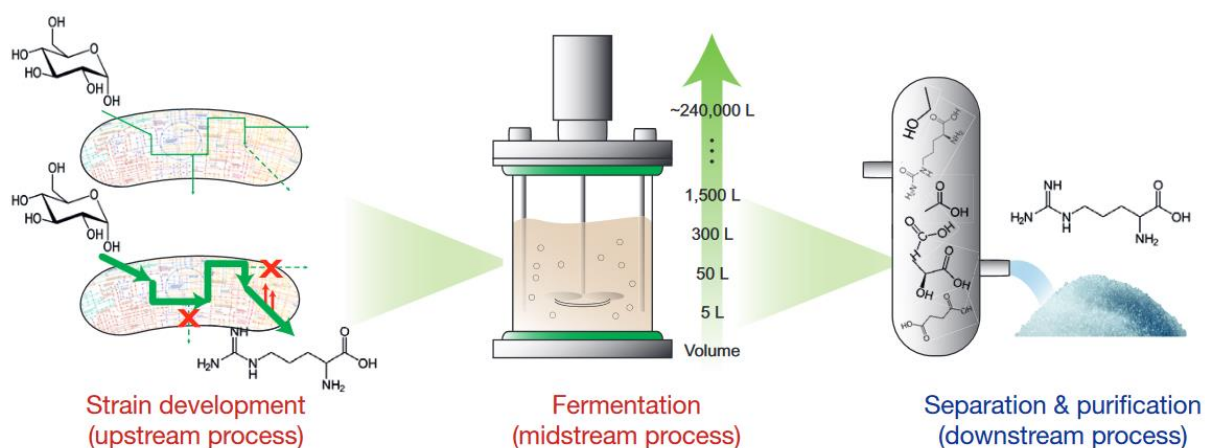


Figure 1.1: Stages of bioprocess development. Each bioprocess can be divided into three stages: Upstream, midstream and downstream process. Figure is taken from [100].

Efficient and rational bioprocess development profits from iterative and integrated approaches as proposed by Schmid and coauthors via the circle of biocatalysis (Fig. 1.2, [101]). The main objective is to develop an economically competitive and ecologically friendly bioprocess for the synthesis of the product of interest. The example of Joule Unlimited thereby underlines the importance of the economic considerations for a successful bioprocess implementation. But it should also be evaluated if the bioprocess is ecologically friendlier than a chemical process, which is not the case for all bioprocesses [102].

Every bioprocess development starts with an initial evaluation of suitable biocatalysts, which can be either whole cells or enzymes as biocatalytic units. Both have opposite characteristics [103]: Isolated enzymes, either immobilized or free in solution, as biocatalysts have the advantage of often less complex downstream processing and high specific rates due to the

direct proximity to the substrate. The reaction environment around the free, isolated enzyme on the other hand goes along with a reduced life-time of the enzyme. Contrary to that, whole-cell biocatalysts provide a stable, self-reproducing and maintaining reaction compartment which simultaneously often results in reduced reaction rates due to mass transfer processes of the substrate and product into the cell and out. The cofactor regeneration capacity of the cells is thereby a particular advantage over isolated enzymes, as those are a significant cost-factor. Approaches for screening for biocatalytic activity in microorganisms or enzyme libraries are widely established (see [104, 105] for an overview).

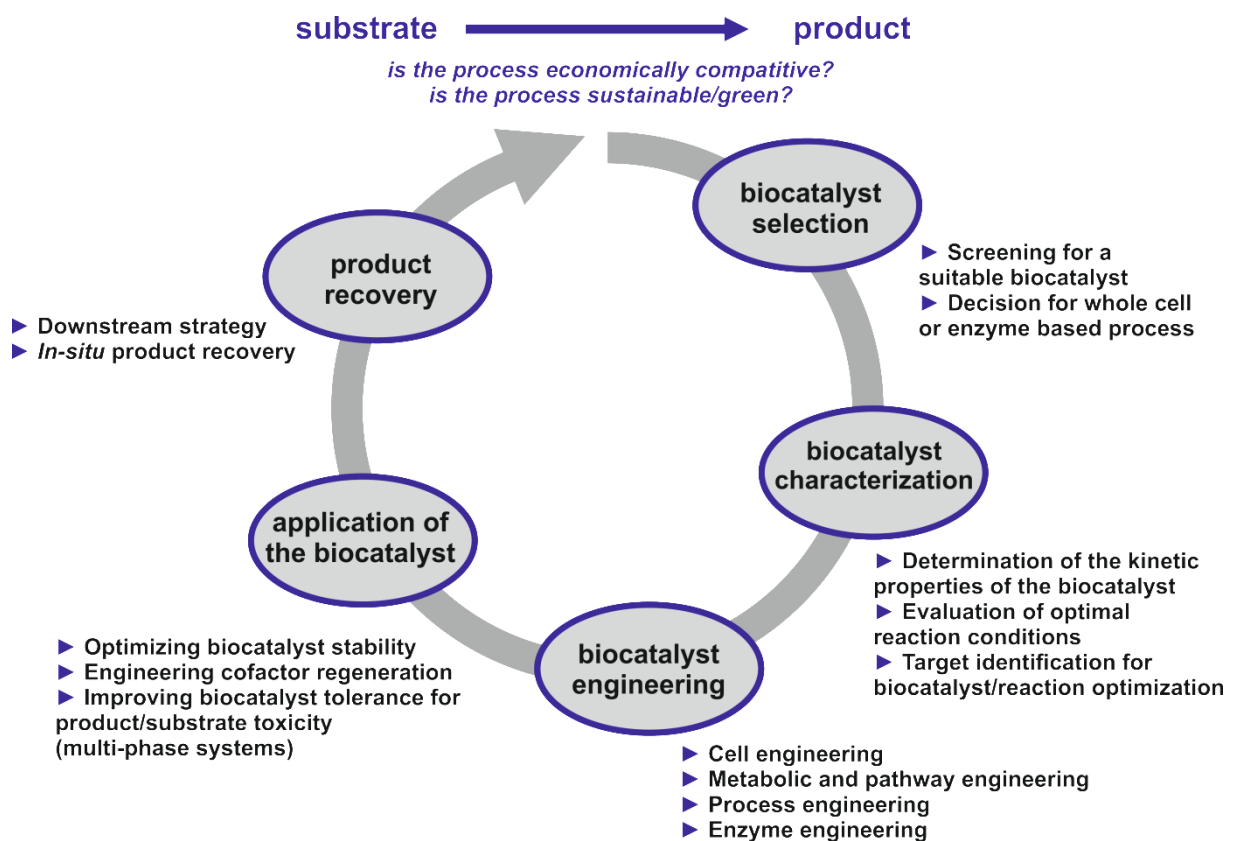


Figure 1.2: Iterative and integrated bioprocess development based on the circle of biocatalysis. Modified from [101].

In future, engineering a *de-novo* enzyme for a certain target reaction with tailored enzyme characteristics by computational means might be a promising approach. This was demonstrated for example for retro-aldolases [106] and a phenol oxidase reaction [107]. Further host selection, either for the production of a biocatalytically active enzyme, or as a whole-cell biocatalyst, remains, however, highly limited due to a small number of well-characterized organisms with established genetic tools and good cultivation characteristics. Consequently, the well-characterized *Synechocystis* sp. and *Synechococcus* sp. strains remain

as the most used organisms as (model) prokaryotic host organisms in photo-biotechnological studies.

After identification of a suitable biocatalyst, its properties have to be characterized in order to gain an understanding about the kinetics and cellular limits for an application and for the identification of optimization targets to enhance product formation rates and yields. Limited insight into cellular systems and especially underlying regulatory networks is still considered to be a major burden in applied biocatalysis and hindering a rational and straight forward process and cell design as known from other engineering principles [100]. Here, the advances in systems biology provide tools for a significant increase in knowledge and systems understanding of cellular functions and capabilities [100, 108]. Qualitative and quantitative omics technologies enable the characterization of the cellular state on each functional level, from metabolites (metabolomics), cellular fluxes (fluxomics), translation pattern (proteomics), transcription pattern (transcriptomics), to the genetic equipment (genomics). Successful examples for systems biology-driven identification of targets for cell optimization are the metabolic engineering of *Escherichia coli* for L-valine production by combined transcriptome analysis and *in silico* driven knockout and overexpression strategy [109], the metabolic flux analysis assisted rerouting of cellular fluxes for optimizing cofactor regeneration rates in *Escherichia coli* for the whole-cell biotransformation from styrene to styrene oxide [110], the genome scale *in silico* knock out strategy for the engineering of a succinic acid producing *Saccharomyces cerevisiae* [111], and the transcriptomics based improvement of the butanol tolerance of *Synechocystis* sp. PCC 6803 [112].

Based on the identified bottlenecks and optimization targets, cellular, metabolic, pathway and enzyme engineering can be applied to enhance biocatalyst performance, i.e. enzyme specificity and selectivity, titer and reaction rate. Cell engineering is the structural engineering of the cell to improve catalyst performance, mostly to overcome limitations in mass transfer over the cell membranes. Successful examples are the integration of a porine to enable better transfer of a hydrophobic substrate and product through the cell membrane for the omega-oxyfunctionalization of dodecanoic acid methyl ester in *Escherichia coli* [113] and the integration of a sucrose permease in a sucrose producing *Synechococcus elongatus* PCC 7942 [72].

Classic approaches in metabolic engineering are the knock out/down of competing pathways as in the case of the before mentioned L-valine production in *Escherichia coli* [109] and the

1,4-butanediol production in *Escherichia coli* [114], and the overexpression of rate-limiting enzymes in a diaminopentane producing *Corynebacterium glutamicum* [115].

Pathway engineering is the fine-tuning of the heterologous pathway in a cell. Codon optimization and promoter design can improve functional and enhanced expression of the catalytic enzyme and reduce the accumulation of toxic compounds within a cascade pathway, as shown for the oxyfunctionalization of fatty acid methyl esters in *Escherichia coli* [116]. Enzyme engineering allows optimization of the catalyst on enzyme level. This can be facilitated by evolutionary methods to improve for example substrate specificity and enantiomeric excess (reviewed in [117]).

In the next step, the applicability of the biocatalyst has to be ensured. The most important aspect is in many processes the substrate and product toxicity. Such effects can be minimized by applying a second phase, such as in the process development of the monooxygenase mediated oxidation of styrene to styrene oxide in *Pseudomonas putida* [118] or the hydroxylation of cyclohexane in *Synechocystis* sp. PCC 6803 [85] in which the toxic compounds accumulate in an organic phase. Another aspect of biocatalyst applicability is the cofactor regeneration capability under reaction conditions, which can be addressed by modulation of cellular fluxes, as mentioned above already [110]. Besides optimizing redox cofactor availability and enhancing biocatalyst stability, the most suitable reaction mode has to be identified and implemented. Whole-cell biocatalysis can be facilitated in batch, fed-batch, continuous and resting cell mode. Each of those process modi has distinct advantages and impacts on cellular performance during the catalysis. In case of the electron demanding oxyfunctionalization of dodecanoic acid methyl ester in *Escherichia coli* based whole-cell biotransformations, for instance, it was demonstrated that initial specific whole-cell activities are higher under resting cell conditions compared to growing cells, where the reaction competed with biomass formation for the available cofactors [119]. Limonene production in a recombinant *Escherichia coli* could be optimized by applying a resting cell biotransformation under simultaneous medium optimization [120].

In the last step, the downstream process design has to be optimized to enable an efficient product recovery. A multi-phase approach does not only improve biocatalyst stability, but it can simultaneously simplify product separation from the reaction broth. Such integrated product recovery can be widely applied [121]. Besides of classical downstream processing unit operations, such as distillation or crystallization (an overview can be found here [122-

124]), novel methodologies such as product recovery from second phases by supercritical CO₂ are investigated [125, 126].

The term circle of biocatalysis implies an iterative linear process, but all engineering levels are in fact highly interconnected as each parameter has an impact on the others, especially when considering the biocatalyst and reaction properties with the process design. Consequently, successful bioprocess development profits from the combination of all available tools at each level. Examples for integrated bioprocess optimization are described in detail by Lee and Kim for the development of a L-arginine producing *Corynebacterium glutamicum* and an 1,4-butanediol producing *Escherichia coli* [100].

Photo-biotechnological bioprocess development

Biocatalyst engineering approaches are well established, covering enzyme [105, 127, 128], pathway and metabolic engineering principles [129-131] and are widely applied to enhance carbon partitioning into a carbon-based product and thereby increase production rate and titer in photosynthetically active cells [61, 132, 133]. The engineering of *Synechocystis* sp. PCC 6803 for the synthesis of lactate from CO₂ represents the most intensive engineering of a phototropic cell towards an efficient phototrophic biocatalyst, involving, among others, codon optimization (enzyme engineering), optimizing translation by promotor selection (pathway engineering), and debottlenecking of the fluxes to the precursor and minimizing alternative carbon fluxes (metabolic engineering) [71, 74, 134, 135].

As seen in the previous section, a quantitative and systematic characterization of cellular metabolism can not only accelerate and simplify cell optimization targets. It is in fact even a fundamental requirement to evaluate and characterize the effects of conducted engineering steps. Even though systems biology and quantitative physiology approaches are applied for photosynthetically active cells, its use is not as common as for heterotrophic cells (see below), resulting in a still trial-and-error approach in strain and process development.

Reaction engineering and process engineering are, in contrast to biocatalyst engineering, not a focus in photo-biotechnological research, even though it is widely known that reaction conditions, such as substrate, or nutrient in general, availability and the process mode (batch, fed-batch, continuous) can have tremendous impact on the production rate and product yield. Examples for a systematic evaluation of the impact of reaction conditions and process modes are the biotransformations mediated by an alkane monooxygenase AlkBGT and a P450 monooxygenase in recombinant *Synechocystis* sp. PCC 6803 strains, where

whole-cell activities were increased by optimized light and carbon supply and suitable cultivation modes including the implementation of a second phase to reduce the toxic impact of the substrates and products, respectively [85, 136]. The reason that most studies focus on biocatalyst engineering might result from the still low production rates and titers, offering additional potential for cell and metabolic optimization.

Another means to enhance the space-time yield of a reaction and volumetric titer of a product is the increase of the biocatalyst concentration. This is in case of photosynthetically active cells a critical point as it is a challenge to supply cells in high-density cultivations with the energy source, i.e. light. One concept aims at maximizing the cell concentration by applying surface bound layers of the active cells in the form of biofilms in capillary bioreactors [137]. Consequently, the development of suitable cultivation technologies and strategies for photosynthetically active cells, enabling cost-efficient cultivation at high cell densities, is in focus of photo-biotechnological bioprocess research. Two main concepts are in focus: open systems and enclosed bioreactors [138, 139]. The first enable cost efficient cultivation of algal and cyanobacterial biomass in systems with a low degree of complexity and process regulation and lacks the applicability for genetically modified organisms (GMO) as biocatalysts. Closed bioreactors, in contrast, enable the use of GMOs and offer highly defined process conditions on the expense of high systems complexity, difficult upscaling characteristics and consequently high costs. Morweiser and coauthors review recent developments in photo-bioreactor design [140]. Suitable economically feasible large scale solutions are consequently a major challenge in photo-biotechnological bioprocess development.

Systems biology for a knowledge driven strain and bioprocess development

Rational and straight forward biocatalyst and reaction engineering relies on an in-depth knowledge about the cell, especially its metabolism and the underlying regulatory networks. Due to the complexity of a cell, we are still far away from a true rational strain and consequently bioprocess development. As seen in the previous sections, systems analysis of cells can accelerate biocatalyst development and enable a more targeted and rational optimization strategy [100, 131]. Such omics approaches are also more frequently applied in photo-biotechnology. Examples are the transcriptomics based improvement of the butanol tolerance of *Synechocystis* sp. PCC 6803 [112], the proteome analysis of lactate and ethanol producing *Synechocystis* sp. PCC 6803 strains [141], and the C-13-based metabolic flux

analysis and *in silico* analyses to understand the quantitative metabolism of cyanobacteria in order to find future optimization targets [142-147].

However, quantitative physiology data of phototrophic organisms is scarce. One reason for that is the underlying complexity in phototrophic cell cultivation. Two different main substrates determine growth: carbon dioxide and light. During batch cultivation, the availability of light and carbon is permanently changing, resulting in cellular responses according to the environment and a characteristic growth curve reflecting the substrate limitation (light limitation due to shading and carbon limitation due to insufficient carbon intake into the medium) in form of a linear growth after rather a short exponential growth phase (Fig. 1.3 [148, 149]).

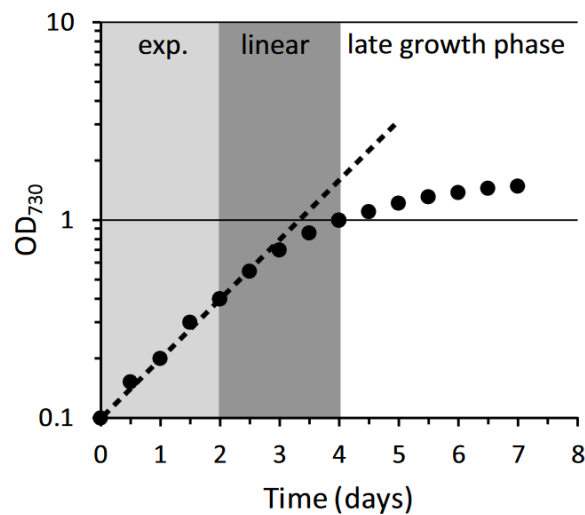


Figure 1.3: Growth phases of *Synechocystis* sp. PCC6803 as proposed by Schuurmans and coauthors Figure taken from [148].

In chemotrophic strain and process development, the exponential growth phase is used to gain quantitative insights into cellular rates and thereby cellular capabilities. This is possible as the cells can be assumed to be in a pseudo-steady state under unlimited substrate availability. Due to the character of light supply from outside the cultivation vessel, this is not true for phototrophic cells as increasing cell density causes self-shading effects. While this is not a substantial issue in the investigation of qualitative biological questions, it hinders a systematic and quantitative understanding of phototrophic metabolism, where well-defined and reproducible environmental conditions are required to achieve steady metabolic states. This was recognized in the community and yielded in an increasing number of quantitative studies to characterize systematically phototrophic metabolism. This includes the systematic and quantitative investigation of media components on the growth of

Synechocystis sp. PCC 6803 [150, 151], and the characterization of physiological parameters in steady states by applying (semi-) continuous cultivations [152-154].

Phototrophic metabolism

The photoautotrophic metabolism can be considered as an interconnected system with the two modules *carbon fixation and carbon metabolism* (dark reactions, blue color in Fig. 1.4) and *energy and reduction power generation* (light reactions, orange color in Fig. 1.4), which are linked by the cofactors NAD(P)H and ATP (green color in Fig. 1.4) [155, 156].

The biochemical energy and electron carrier ATP and NAD(P)H are regenerated by the photosynthetic light reactions, which take place in the thylakoid membranes. Photons are absorbed by photoactive pigments, mainly chlorophyll *a* (chl*a*), carotenoids and phycobilins, and transferred to the reaction center of photosystem II (PSII), where a chlorophyll molecule (P680) is excited [156]. The excited electron is transferred to plastoquinone Q_B. The electron hole at P680 is in turn filled with an electron gained from water oxidation in the water oxidation center (WOC). Reaction products are O₂ and protons, from which the latter contribute to the thylakoid proton gradient.

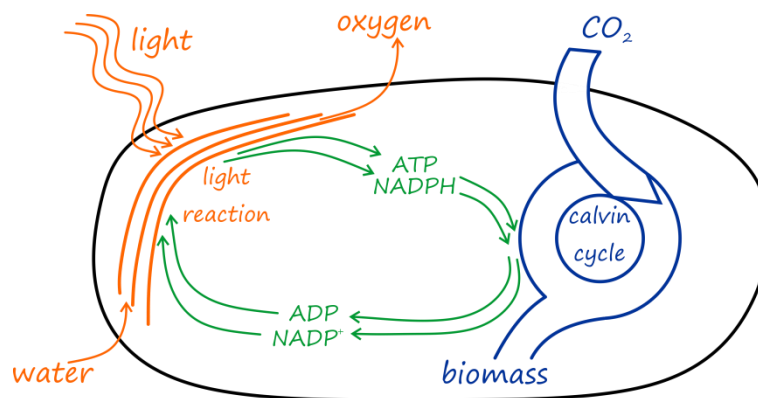


Figure 1.4: Simplified scheme of the photoautotrophic metabolism of a cyanobacterial cell. Absorbed photons fuel the “light reactions” of photosynthesis (the source side of photosynthetically active cells, orange). The energy is used to regenerate ATP and the electrons from the water splitting reaction are transferred to NAD(P)⁺. NAD(P)H and ATP are used to fuel metabolic reactions (green), mainly cell maintenance and nutrient assimilation such as nitrogen and carbon, and for biomass formation (the sink side of photosynthetically active metabolism, blue).

The electrons from water oxidation are channeled from Q_B over the plastoquinone pool (PQ) through complex III (cytochrome *b₆f* complex) to plastocyanine (PC) and finally to PSI, where they are excited at the chlorophyll P700 and finally transferred to ferredoxin (Fd), which

serves as the main hub to distribute the photosynthetically derived electrons [157]. The whole pathway is referred to as the photosynthetic electron transport chain (ETC). Overall, different electron fluxes within the ETC can be distinguished: i. the linear electron flux (LEF), ii. alternative electron fluxes (AEF), and, iii. non-photosynthesis related respiratory electron fluxes. The AEF can be distinguished in the cyclic electron flux around PSI (CEF) and non-cyclic alternative electron fluxes (ncAEF).

LEF comprises electrons gained from water oxidation which are channeled to metabolic electron acceptors, either via NADPH/H⁺ or directly via Fd. The main electron sinks are the Calvin-Benson cycle, which facilitates the carbon assimilation, and other nutrient assimilation and reduction processes such as nitrate assimilation (Fig. 1.5). The CEF represents a shortcut from Fd back to cytochrome *b₆f*, resulting in a cyclic electron flux around PSI (Fig. 1.5). The energy which is generated in that cycle contributes to the proton gradient across the thylakoid membrane. The proton gradient fuels the regeneration of ATP in the ATPase. In contrast to the CEF, where electrons are cycled around PSI, ncAEF relies, as the LEF, on electrons gained from water splitting. Therefore, the sum of ncAEF and LEF equals the PSII, or water splitting, rate. However, ncAEF are characterized by the fact that other final electron acceptors, typically O₂, are used and as a consequence, those electrons are not biochemically available via Fd or NAD(P)H/H⁺ for metabolic reactions. The main ncAEF is the Mehler reaction (or Mehler cycle) [158]. In that reaction, electrons gained from water splitting reduce O₂ at photosystem I. As water functions as electron donor and end product of the Mehler reaction, it is also referred to as water-water cycle. In cyanobacteria, Mehler-like reactions are considered as the main ncAEF (reviewed in [159]), constituting up to 20% of the electron flux from PSI in *Synechocystis* sp. PCC 6803 under carbon excess conditions, and under carbon limited conditions even 50-60% of the photosynthetically evolved O₂ were reduced [160]. Here, electrons are either transferred directly from PSII to the Flv2/4 system, which mediates a transfer to an unknown final electron acceptor (hints point to O₂ as acceptor under certain environmental conditions [161]), or from NADPH to Flv1/3, which catalyzes also the reduction of O₂ [162, 163]. All ncAEF have in common that they do not contribute to NAD(P)H regeneration, but to the proton gradient and consequently to ATP regeneration.

From Fig. 1.4 and 1.5 can be seen that a phototrophic cell has a “sink” and a “source” side of metabolism. The source-side comprises the water oxidation as electron generating reaction

and the electron fluxes, which are contributing to the generation of ATP. The sinks, on the other hand, comprise all acceptors after PSI for the photosynthetically derived electrons and ATP (Fig. 1.5). It is necessary to balance the electron and ATP generation according to the availability and capacity of the respective sinks and sources. In general, a photosynthetically active cell is considered to be limited by metabolic constraints to fully exploit the light energy, in other words, the photosynthesis is sink limited [164, 165]. Excess electron generation can lead to severe cell damages, known as photo-inhibition and -toxicity. To prevent excess generation of electrons, the AEFs play a central role, as they function as electron futile pathways (Fig. 1.4). If the metabolic sinks are getting limiting, for example due to a reduced carbon fixation and a respective reduced nutrient assimilation rate, excess NAD(P)H/H⁺ could be used by Flv1/3 or electrons could be quenched in the Mehler reaction. If, on the other hand, an excess PSII rate yields in an over-reduced ETC, the Flv2/4 valve might relieve the electron pressure. Other measures are the downregulation of the photosystems and the light uptake [164].

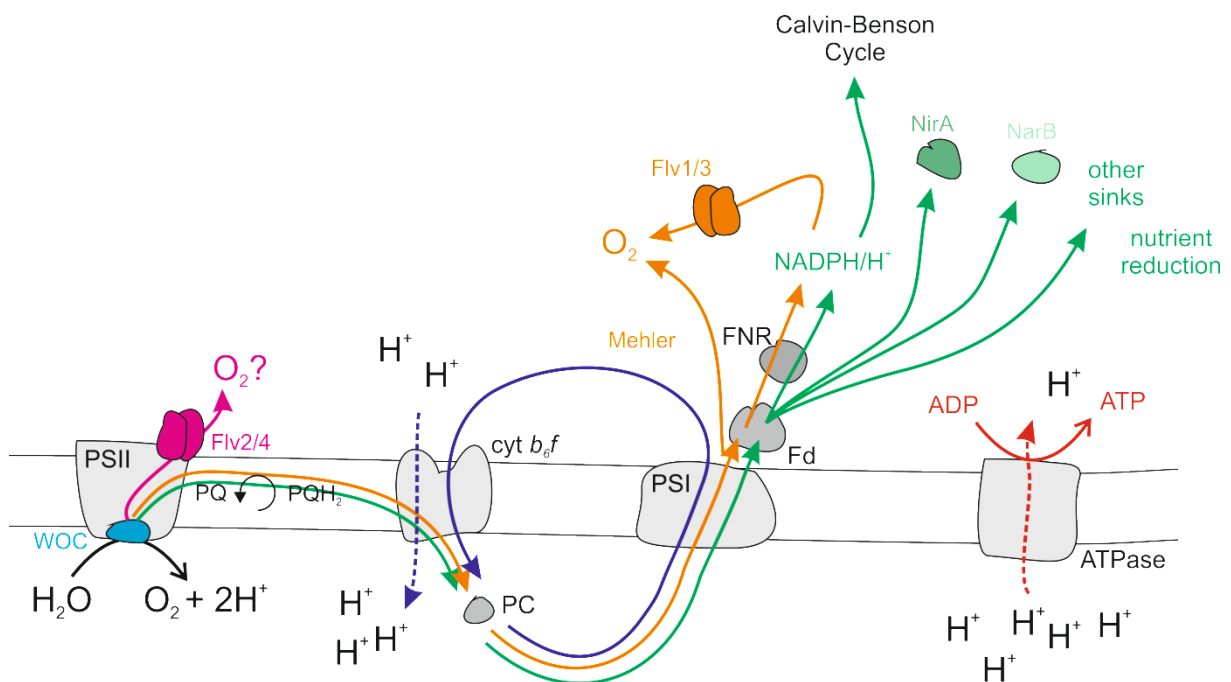


Figure 1.5: Photosynthetic electron fluxes and main metabolic electron sinks. See text for details (modified from [166]).

Another important function of the AEFs is the balancing of the NAD(P)H/H⁺ and ATP regeneration rates. The LEF does not provide ATP and NAD(P)H/H⁺ in a sufficient ratio to fuel all metabolic processes [167]. Instead, additional ATP has to be provided. This is facilitated by optimizing the flux ratios of LEF, nAEF and, most importantly, the CEF.

Quantitative physiology in the context of the sink hypothesis

As discussed before, systematic and quantitative approaches are shifting into the focus of photo-biotechnological studies and were already successfully applied to fill knowledge gaps or revise old assumptions. An example is the ongoing debate on the functional modes of the TCA cycle. While it was believed long time that cyanobacteria, including the model organism *Synechocystis* sp. PCC 6803, have a dysfunctional cycle due to the lack of the 2-oxoglutarate dehydrogenase complex (OGDH). However, recent metabolic modelling approaches and considerations indicate that diverse metabolic bypasses might result in a functional TCA cycle [143]. This demonstrates that a systematic and quantitative analysis of cyanobacterial metabolism, or the cells in general, can help to solve old questions in cyanobacterial research.

Another fundamental knowledge gap is the limited knowledge regarding the physiological responses of a phototrophic cell to a biocatalytic reaction. As seen in the previous section, the cell is permanently balancing the energy and electron supply in dependency of the available light and the maximum rate of metabolic sinks (growth, Calvin-Benson Cycle and other nutrient assimilation and reduction). Under light saturating conditions, which are predominant in nature, the photosynthesis has to be downregulated and a significant share of absorbed light energy has to be dissipated so that the cell is not flooded by excess electrons (Fig. 1.6, [164, 165]).

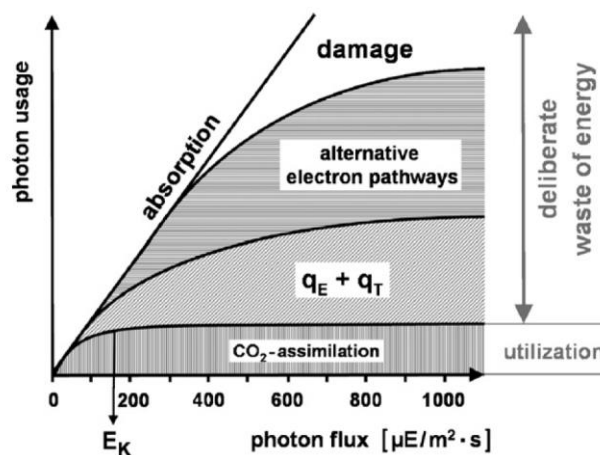


Figure 1.6: Photon usage in a phototrophic cell in dependency of the light availability. While the absorption of photosynthetically active radiation (PAR) depends on the photon flux, is the actual photon usage constrained by the availability of metabolic sinks, i.e., carbon fixation and nutrient assimilation. All absorbed radiation exceeding this capacity has to be dissipated in order to prevent cell damage due to excess electrons and ROS. For that, different mechanisms have developed, including AEF for reducing LEF and quenching to reduce the photon flux guided to the reaction center of PSII. Figure taken from [164].

A biocatalytic reaction is in principle nothing else than an artificial additional sink, i.e. electron acceptor and/or carbon valve (Fig. 1.7). Consequently, the question arises if such an additional sink can relieve the sink limitation, resulting in enhanced photosynthesis rates. On the other hand, one can ask the question if the theoretical surplus in electron availability can directly be exploited for productive reactions in photo-biotechnology or if and what regulatory mechanisms obstruct such exploitation.

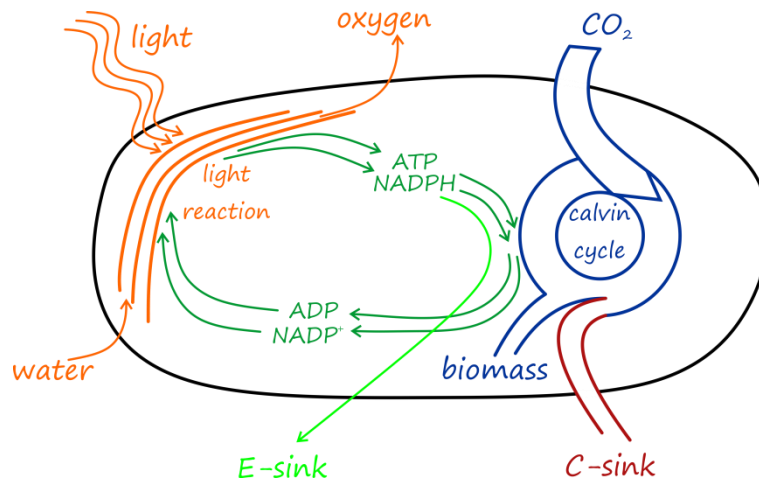


Figure 1.7: Simplified scheme of the photoautotrophic metabolism of a cyanobacterial cell. A heterologous reaction functions as an electron and/or sink and competes with natural, metabolic sinks. According to the photosynthesis sink limitation, such sinks should have the potential to relieve this limitation and enable increased photosynthesis rates.

Indeed, distinct physiological responses to the additional sink were observed in many studies focusing on the engineering of cyanobacterial cells for the production of carbon-based products. In some cases, cells with an additional carbon sink showed in comparison to respective wild-type strains increased photosynthetic rates (oxygen evolution and effective quantum yield at PSII) [70, 72, 168-170]. In a few other cases, not only a stimulated photosynthesis was registered, but furthermore even enhanced carbon fixation rates [65, 70-72, 170-172].

Quantitative physiological data on an additional electron sink is not available due to the lack of suitable electron sinks, i.e. biocatalytic reactions mediated by an electron demanding enzyme. The only hint is an observed increased quantum yield and maximum electron transport rate in a recombinant *Synechococcus* PCC 7002 expressing the mammalian cytochrome P450 CYP1A1 [169].

Knowledge about the physiological responses of a phototrophic cell would provide an understanding of the cellular limits (Which electron and carbon withdrawal rates are

achievable?) and responses to such sinks would provide new targets for a rational and more efficient strain and process development. Consequently, the systematic and quantitative investigation of such responses, in literature referred to as carbon sink effect, was identified as a main target in cyanobacterial research [173].

***Synechocystis* sp. PCC 6803 as a model organism in photo-biotechnology**

Most studies in the field of photo-biotechnology, that is the rational design and use of phototrophic microorganisms, are conducted with the unicellular work-horse *Synechocystis* sp. PCC 6803 (Fig. 1.8). The genome of *Synechocystis* sp. PCC 6803 was the first cyanobacterial, and the third overall, to be sequenced [174]. It should be noted at this point that lab evolution of *Synechocystis* sp. PCC 6803 generated a variety of sub-strains with different geno- and phenotypes [175-177]. This complicates the transfer of knowledge and comparability between studies and hinders scientific progress in the field. Even in this thesis, two different wild-type strains were used: a type strain from the Pasteur strain collection, *Synechocystis* sp. PCC 6803 (ATTC-27184), and a wild-type strain originating from the Bhaya Lab from the University of Stanford (USA), *Synechocystis* sp. PCC 6803 (Stanford).

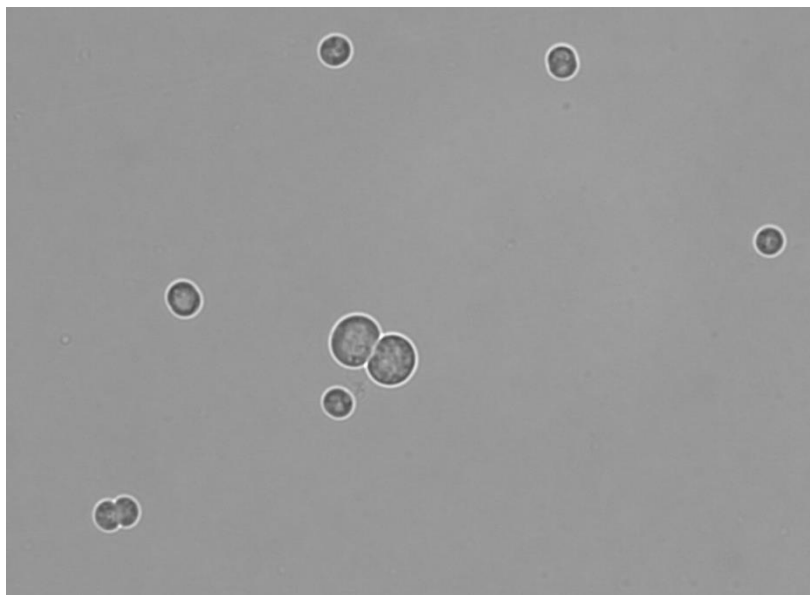


Figure 1.8: Microscopic picture of *Synechocystis* sp. PCC 6803 under bright field conditions.

The early availability of its genome sequence set the starting point for this organism towards becoming a photosynthetic unicellular model organism. A rich genetic manipulation toolbox was developed and established for cyanobacteria and *Synechocystis* sp. PCC 6803 in particular [133, 178-185] which allowed in the following to gain significant knowledge on

genome [186, 187], metabolic network and fluxome [143, 145, 146, 188-190], proteome and transcriptome level [191, 192]. Today, it is even considered as the green *E. coli* [193, 194]. *Synechocystis* sp. PCC 6803 was selected as model organism in this study as it is, as seen above, well characterized and already widely used as model organism in photosynthesis and photo-biotechnological research.

Scope of this thesis

The goal of this thesis was to establish an integrated cultivation and analysis platform to systematically access quantitative physiology data of photosynthetically active *Synechocystis* sp. PCC 6803. Lacking quantitative physiology tools were identified as a major limitation in photo-biotechnological catalyst and bioprocess development. Especially quantitative data on the physiological response of photosynthetically active cells to a biocatalytic reaction, that is carbon or electron withdrawal, is scarce. Angermayr and coauthors addressed the need to understand such effects very clearly: *a precise and quantitative analysis of the carbon sink effect and its molecular basis is highly desired to apply it systematically to cyanobacterial biotechnology* [173].

This thesis follows that call and describes a framework to cultivate photosynthetically active cells under defined conditions, to establish steady metabolic states, and to characterize major physiological parameters allowing electron and photon balancing.

In the second chapter, the developed framework was applied to evaluate physiological changes induced by nitrogen sources differing in their reduction degree and thereby assimilation costs. Such nutrient assimilation was found to constitute a major cellular electron sink with the potential to cause sink effects.

In the third chapter, the carbon sink effect is systematically investigated under different environmental conditions. For this purpose, lactate synthesis was chosen as a model system. The carbon sink effect was found to depend strongly on light and CO₂ availability.

Chapter 4 describes the quantitative characterization of photosynthetically active cells catalyzing a P450 mediated biotransformation on bioreactor scale. This study gave insights into the interaction between physiology, reaction conditions, and biocatalysis-related electron withdrawal (electron sink).

Finally, the outcomes of the thesis are discussed in a wider context in chapter 5, followed by a conclusion and outlook on future developments in chapter 6.

**Chapter 2: Electron balancing under different sink conditions
reveals positive effects on photon-efficiency and metabolic activity
of *Synechocystis* sp. PCC 6803**

Marcel Grund, Torsten Jakob, Christian Wilhelm, Bruno Bühler, Andreas Schmid

This chapter was published in *BMC Biotechnology for Biofuels*, 12, 43.

Marcel Grund performed all experiments and wrote the manuscript. Torsten Jakob and Marcel Grund measured the light induction curves and photosynthetic quotient. Christian Wilhelm, Bruno Bühler and Andreas Schmid coordinated the project and corrected the manuscript.

Abstract

Cyanobacteria are ideal model organisms to exploit photosynthetically derived electrons or fixed carbon for the biotechnological synthesis of high-value compounds and energy carriers. Much effort is spent on the rational design of heterologous pathways to produce value-added chemicals. Much less focus is drawn on the basic physiological responses and potentials of phototrophs to deal with natural or artificial electron and carbon sinks. However, an understanding of how electron sinks influence or regulate cellular physiology is essential for the efficient application of phototrophic organisms in an industrial setting, i.e., to achieve high productivities and product yields.

The physiological responses of the cyanobacterium *Synechocystis* sp. PCC 6803 to electron sink variation were investigated in a systematic and quantitative manner. A variation in electron demand was achieved by providing two N-sources with different degrees of reduction. By additionally varying light and CO₂ availabilities, steady state conditions with strongly differing source-sink ratios were established. Balancing absorbed photons and electrons used for different metabolic processes revealed physiological responses to sink/source ratio variation. Surprisingly, an additional electron sink under light and thus energy limitation was found not to hamper growth, but was compensated by improved photosynthetic efficiency and activity. In the absence of carbon and light limitation, an increase in electron demand even stimulated carbon assimilation and growth.

In conclusion, the metabolism of *Synechocystis* sp. PCC 6803 is highly flexible regarding the compensation of additional electron demands. Under light limitation, photosynthesis obviously does not necessarily run at its maximal capacity, possibly for the sake of robustness. Increased electron demands can even boost photosynthetic activity and growth.

Introduction

The photosynthetic machinery is well conserved among phototrophic organisms. Cells are assumed to optimize energy and carbon utilization capacities for efficient biomass formation. Yet, recent studies revealed that only a minor part of the light available and absorbed by the cells is actually used for biomass formation. Even micro-algal cells, which are considered to be more efficient compared to plant cells (compare [195] and references therein), display a poor light efficiency. This is believed to be a consequence of the general sink limitation of photosynthesis when the cells are exposed to a surplus of light [164, 165, 196-200]. The kinetics of biomass formation depends on a rate-limiting metabolic step or a developmental process during cell growth. Among others, these can be replication and cell division rates, the carbon fixation capacity, diffusion processes within the cell, or limiting nutrient or energy availability [164, 195]. Any absorbed light energy exceeding the metabolic sink demands or sink utilization capacity has to be dissipated to prevent cellular damage and photoinhibition. Thus, phototrophic microorganisms continuously balance the cellular source/sink ratio of energy assimilation (light harvesting and photosynthetic electron flux) and the metabolic energy demand (mainly for nutrient assimilation and biomass formation) under changing environmental conditions. A phototrophic cell can be forced into an unbalanced state by, e.g., sudden light limitation, excessive irradiance, nutrient limitation, or a combination thereof. Phototrophs possess a number of mechanisms to react to such an unbalanced state on short-term, including non-photochemical quenching and alternative electron quenching pathways as for example Mehler and Mehler-like reactions (reviewed in [158, 159]). On the long term, a new balance is reached mainly by the adjustment of the Chl*a* content, the reduction of PSII rates, the variation of the PSI to PSII reaction rates, the regulation of the cellular RubisCO content, and changes in carbon allocation (reviewed in [164, 196-200]). Cyanobacteria possess a variety of alternative electron sink pathways mediated by, e.g., flavodiiron proteins [162, 163]. This indicates that cyanobacteria strongly rely on alternative electron sinks such as O₂ to cope with unbalanced and suboptimal growth conditions as described above. Such dissipation of photosynthetic energy restricts the quantum use efficiency of photosynthetic biomass formation.

During recent years, microalgae and particular cyanobacteria gained increasing attention as catalysts for the synthesis of (fine) chemicals and fuels ultimately from CO₂ in climate-friendly processes to replace fossil resources (for comprehensive reviews see [61, 132, 173,

201]). In addition, the direct draining of photosynthetically activated electrons derived from water splitting for biotransformations (examples are [83, 84, 86, 169, 202-205]) and ultimately hydrogen production (reviewed in [43, 44]) constitutes an interesting approach for a future bioeconomy. These approaches, however, depend on answers to the following questions: What is the true (biological) potential of phototrophic cells? How can we exploit this potential more efficiently for biomass or product formation? To answer these questions, we need to understand the mechanisms and general metabolic concepts determining the regulation of the light reaction and general cell physiology by a (metabolic) sink. It is widely accepted that photosynthesis is highly sink-limited. Metabolic sinks/processes or nutrient availability are limiting, if light is available in excess [164, 165]. The main hypothesis is that additional sinks have the potential to relieve this limitation and unleash higher photosynthetic capacities. It was observed in cyanobacteria that additional electron/carbon sinks can indeed relieve such a limitation to a certain extent and result in increased photosynthetic activity/efficiency and even elevated carbon fixation rates. This was shown *inter alia* for additional carbon sinks in cyanobacteria excreting 2,3-butanediol [171], glycerol [206], sucrose [72, 168], and isoprene [79], but also for the draining of photosynthetic electrons by electron demanding enzymes [169]. Despite of such findings indicating positive effects of sinks on photosynthesis efficiency, quantitative descriptions in terms of energy balances are not available. The focus so far has been set on the engineering of strains regarding enzymatic/cellular activities, product titer and formation rate, and strain stability. A deeper understanding is missing on how the cells balance metabolic sinks (biomass formation and product formation) with available resources (harnessing of light and photosynthetic electron activation) in the presence of additional sinks.

Nitrate and ammonium constitute two nitrogen (N) sources with strongly differing degrees of reduction. In comparison to ammonium, nitrate requires eight additional electrons per assimilated nitrogen atom and thus represents a significant electron sink [207]. Phototrophs typically prefer the assimilation of ammonium when supplied with both nitrate and ammonium simultaneously [208-210]. Nitrate assimilation, as compared to ammonium assimilation, can thus be expected to have significant effects on cell physiology [211]. Surprisingly, growth rates and quantum yields upon cultivation with ammonium or nitrate as N-source did not give a consistent picture such as a higher quantum yield for growth with ammonium as N-source (reviewed in [207]). This could be due to secondary effects of

ammonium/ammonia, such as photo-damage at PSII, decoupling of cyclic and linear electron flow, or global regulatory effects [212-216].

In this study, we compared the assimilation of nitrate and ammonium based on a broad set of physiological parameters and photon/electron balancing [217-220]. This approach was followed to investigate long-term acclimation responses to differing electron demands in the model cyanobacterium *Synechocystis* sp. PCC 6803 (hereafter referred to as PCC6803) and included the analysis of three steady metabolic states based on differing source-sink (light-CO₂) availabilities. The respective experimental setup involved continuous bioreactor cultivation at low biomass concentrations and constant and defined environmental conditions. Thereby, this study sets a basis for future systematic analyses of electron sink effects on the physiology of PCC6803 and respective underlying regulatory mechanisms.

Materials and Methods

Bacterial strain and growth conditions

A wild-type *Synechocystis* sp. PCC 6803 strain, in the following referred to as PCC6803, was used in this study. The strain was obtained from the Pasteur Culture Collection of Cyanobacteria (Paris, France) and stored as cryo-culture at -80°C in BG11 medium supplemented with 20% (v/v) DMSO.

PCC6803 was cultivated in BG11 or YBG11. For cultivation on solid medium, BG11 according to Rippka et al. [221] was supplemented with 1.5% (w/v) agar and 0.03% (w/v) sodium thiosulfate. A modified YBG11 medium according to Kwon et al. [150] was used for liquid cultivations in shake flasks or bioreactors. For shake flask cultivation, YBG11 was supplemented with 50 mM HEPES and adjusted to pH 8.0 by titration with 10 M NaOH. For continuous bioreactor cultivations, YBG11 was supplemented with 2 mM HEPES and the respective nitrogen source and adjusted to pH 8.0 by titration with 10 M NaOH. Ammonium chloride or sodium nitrate was provided in a concentration of 17.8 mM.

For the bioreactor experiments, PCC6803 was streaked out on BG-11 agar plates from cryo-cultures and cultivated in a plate incubator (poly klima GmbH, Freising, Germany) at 20 $\mu\text{mol photons m}^{-2} \text{ s}^{-1}$, 30°C and 75% relative humidity (rH). Emerging colonies were used to inoculate liquid pre-cultures in 250ml baffled flasks filled with 40 ml YBG-11, which were cultivated in a photoincubator equipped with LED panels (INFORS AG, Bottmingen, Switzerland) at 140 rpm, 30°C, 50 $\mu\text{mol photons m}^{-2} \text{ s}^{-1}$ and 75% rH. These cultures were

further used to inoculate flat panel bioreactors (Labfors 5 Lux, INFORS AG, Bottmingen, Switzerland) as described below.

Bioreactor setup and conditions for continuous cultivation

The experiments were conducted in a flat-panel airlift bioreactor system (Labfors 5 Lux, INFORS AG, Bottmingen, Switzerland, Switzerland) with controlled aeration rate (pressurized air or pressurized air enriched with CO₂), illumination intensity, pH, and temperature. Besides light input, CO₂ enrichment, and nitrogen source, all environmental parameters were kept constant. The reactors were operated at pH 8.0, controlled by 1 M sodium hydroxide and 15% (v/v) phosphoric acid addition, 30°C, and 0.5 vvm aeration, which was sufficient for mixing the cell suspension. Light was provided by a LED panel on one side of the reactor (Supplemental Information, Fig. S1). The other side of the reactor was covered to prevent environmental light to enter the reactor.

The bioreactors were operated continuously, i.e. the biomass concentration was kept constant by providing fresh medium at the same rate as culture broth was removed. The initial dilution rate was set as the growth rate during the batch phase of the cultivation at the respective applied conditions and manually adjusted until the biomass concentration remained stable. The medium was pumped into the reactor with a peristaltic tube pump (IPC-series, ISMATEC, Cole-Parmer GmbH, Wertheim, Germany). The working volume was set to 1.8 l during the cultivations. The filling level was kept constant by pumping culture through a fixed efflux tube at the top of the reactors. The growth rate was derived from the dilution rate according to

$$D = \mu = \frac{\dot{V}}{V}$$

with a working volume of $V=1.8$ L and the feeding rate \dot{V} .

Three different conditions were tested for both ammonium and nitrate grown cells:

- aeration with 1% (v/v) CO₂ and a low light intensity of 65 $\mu\text{mol photons m}^{-2} \text{s}^{-1}$ (LLHC),
- aeration with 1% (v/v) CO₂ and a high light intensity of 250 $\mu\text{mol photons m}^{-2} \text{s}^{-1}$ (HLHC),
- aeration with air and a high light intensity of 250 $\mu\text{mol photons m}^{-2} \text{s}^{-1}$ (HLLC). As soon as the physiological parameters of the cells remained stable for at least a day, the cells were considered to be in a stable metabolic state and were characterized via photon/electron balancing as described below.

Determination of cell dry weight (CDW) and biomass concentration

OD₇₅₀ was measured in duplicates at least 14 times per steady state in a photo-spectrometer (Libra S12, Biochrom Ltd, Cambridge, Great Britain) at 750 nm. Samples for the determination of the biomass concentration were diluted to an OD₇₅₀ between 0.1 and 0.3. The correlation between OD₇₅₀ and cell dry weight (CDW) concentration was determined for each analyzed metabolic state independently as a mean of three independent measuring days. Fifty ml of cell suspension from the reactor were centrifuged (Centrifuge 5810R, rotor FA-45-6-30, Eppendorf AG, Hamburg, Germany) for 10 min at 10°C and 7000 *g*. The supernatant was discarded and the pellet washed with distilled water. After a second centrifugation step at the same conditions, the cells were resuspended in 0.5 ml distilled water and transferred to a glass tube. The cells were dried at 70°C until a constant weight was reached. The weight of the dry biomass was used to calculate the correlation factor between OD₇₅₀ and CDW concentration.

Estimating cellular composition

Biomass composition was evaluated on the elemental level. The C/N ratio was analyzed in duplicates on three different measuring days for each metabolic state. Fifty ml were sampled from the reactor and centrifuged for 10 min at 10°C and 7000 *g* (Centrifuge 5810R, rotor FA-45-6-30, Eppendorf AG, Hamburg, Germany). The supernatant was discarded and the pellet washed with distilled water. After a second centrifugation step for 10 min at 10°C and 7000 *g*, the cells were resuspended in 1 ml distilled water and transferred to an Eppendorf cup. The samples were lyophilized (Freezone 2.5, Labconco, Kansas City, USA) and stored until further measurement. The measurement of the carbon and nitrogen content of the dried biomass was performed with a Vario EL Cube elemental analyzer (Elementar Analysegeräte GmbH, Langenselbold, Germany).

Determination of the cellular Chl_a content

The Chl_a content of the cells was determined spectroscopically for each metabolic state on three different measuring days. Three samples of a defined volume were centrifuged for 10 min at 10000 *g* and 4°C (Heraeus Fresco 17, Thermo Scientific, Waltham, USA). The pellet was resuspended in 1.5 ml ice-cold methanol and homogenized in a bead-mill (Precellys Evolution, BERTIN Technologies, Saint Quentin en Yvelines Cedex, France) for 30 sec at 8000 rpm. The homogenized cells were kept on ice for 20 min followed by centrifugation for 10 min at 17000 *g* and 4°C (Heraeus Fresco 17, Thermo Scientific, Waltham, USA). The

absorption of the extract was measured at 666 nm against a methanol blank. The Chl a concentration was calculated using the specific correlation factor of 79.95 l g $^{-1}$ cm $^{-1}$ [222].

Measurement of the effective quantum yield at PSII

Fluorescence analysis was performed with a Multi-Color PAM [223] (Heinz Walz GmbH, Effeltrich, Germany) to determine the quantum yield at PSII (Y(PSII)), i.e. the number of quanta productively used within PSII for charge separation divided by the number of quanta absorbed. The effective quantum yield at PSII is defined as

$$Y(\text{PSII}) = \frac{F'_q}{F'_m},$$

with F'_q being the photochemical quenching of fluorescence by open PSII centers and F'_m the level of fluorescence when QA is maximally reduced and all PSII centers are closed [224]. This procedure is well established for algae [219, 224]. For cyanobacteria, Y(PSII) is considered to be underestimated due to additional fluorescence emission caused by the light harvesting phycobilisomes upon excitation [225-228]. To minimize this underestimation of Y(PSII), the analysis was modified, using 400 instead of 625 nm for the measurement light in order to avoid excitation of the phycobilins. White light was used as actinic light and for the saturation flash. A light induction curve (LIC) was recorded with increasing light intensities. Supernatant from the reactor was used to blank the basal fluorescence of the medium. Y(PSII) was interpolated for the light intensity provided in the bioreactor. 9-12 LIC were measured for each metabolic state. The measurements were conducted at least 9 times per steady state (minimum 3 times per measuring day) on three independent measuring days.

Determination of photosynthetic rates

The photosynthetic capacity and activity of PCC6803 was characterized by determining the cellular quantum absorption rate (Q_{phar}), the net O $_2$ evolution rate (r_o), as well as the maximum electron flux at PSII (r_F) estimated from Y(PSII). These parameters were determined as described by Jakob et al. and Wagner et al. [217, 218]. r_o and r_F are given as O $_2$ evolution rates. Q_{phar} is given as a quantum uptake rate.

Q_{phar} can be estimated based on the emission spectrum of the LED panel of the reactor (see Supplemental information, Fig. S1) and the specific *in vivo* Chl a -specific absorption spectrum of the cells. The theoretical background for the use of the Chl a specific absorption

coefficient is described by Blache et al. [229]. The wavelength dependent Chl α -specific absorption coefficient of the cells (see Supplemental Information 3, Fig. S3) is defined as

$$a^*(\lambda) = 2.3 \cdot \frac{A(\lambda)}{d \cdot c(\text{Chl}\alpha)}$$

with the wavelength-dependent absorption A of the sample, the conversion factor 2.3 for the transformation of log₁₀ to ln, the path length of the cuvette d, and the measured chl α concentration c(chl α). The absorption spectra of the cells were measured with a dual beam spectrophotometer equipped with an adapter for dispersive samples to correct for light scattering (Zeiss M500, Carl Zeiss AG, Oberkochen, Germany). The absorption spectra were normalized to OD₇₅₀. The emission spectra of the light sources were determined using a spectroradiometer (Tristan 4.0, m-u-t GmbH, Wedel, Germany). These two spectra form the basis for the calculation of the photosynthetically active quantum absorption rate Q_{phar} (the wavelength-dependent Q_{phar} is depicted in Supplemental Information 4, Fig. S4). According to Gilbert et al. [230], Q_{phar} was estimated via the equation

$$Q_{phar} = \int_{400 \text{ nm}}^{700 \text{ nm}} Q(\lambda) - Q(\lambda) \cdot e^{-(a^*(\lambda) \cdot c(\text{Chl}\alpha) \cdot d)} d\lambda$$

with Q_{phar} and Q standing for the photosynthetically absorbed quanta and the photosynthetically available quanta, respectively.

The net O₂ evolution rate r_O in the different metabolic states was measured in triplicates on three different days using a Clark-type electrode (MI-730, Microelectrodes Inc., Bedford, USA). A LIC was performed, determining the O₂ evolution rates at the cultivation light intensity and respiration rates in a following dark phase. The net O₂ formation rate was calculated by correcting the measured O₂ evolution rate for the corresponding respiration rate.

The maximum electron flux through PSII r_F, expressed as an O₂ evolution rate, was estimated based on the measured Y(PSII) at the applied cultivation light intensity (see above) by applying the equation

$$r_F = \frac{Y(\text{PSII}) \cdot Q_{phar} \cdot 0.5 \cdot 0.25 \cdot \text{Chl}\alpha_{CDW}}{d \cdot c(\text{Chl}\alpha)}$$

with d standing for the reactor vessel diameter and Chl α _{CDW} for the specific chlorophyll content of the cells based on cell dry weight (CDW). The factors 0.5 and 0.25 account for the

assumptions that two quanta are required to feed one electron into the ETC and that four electrons are required to form one molecule of O₂, respectively.

The photosynthetic quotient PQ was determined for bioreactor samples by measuring the CO₂ and O₂ exchange rates in a respirometer (Biometric Systems, Weiterstadt, Germany) as described in Wagner et al. [218]. The carbon fixation rate was derived according to [231] based on PQ and was derived from the formula

$$r_C [\mu\text{mol d}^{-1} \text{mg}_{CDW}^{-1}] = \frac{r_O}{PQ}$$

PQ, Q_{phar} and r_O were determined on three independent measuring days.

Results

Establishment of different metabolic states in PCC6803 by modulating source and sink availability

This study aimed at the characterization of the physiological responses of PCC6803 to the replacement of the N-source ammonium with nitrate functioning as an additional electron sink. For this purpose, a photon/electron balancing approach was applied. This approach was used previously to investigate the physiological response and the metabolic electron partitioning in unicellular algae in response to changing environmental conditions [217-220]. For the reproducible characterization of cell physiology via a photon/electron balance, it is important to cultivate the cells under steady state conditions, i.e., constant and controlled environmental conditions, in a well-defined bioreactor setup. This included steady illumination and low turbidity to minimize self-shading. First, the cells were grown in batch mode up to an OD₇₅₀ of approx. 0.5. Then, a feed with fresh growth medium was started and adjusted to maintain constant turbidity and thus cell concentration (turbidostat) for each experimental condition. The established steady state biomass concentrations did not exceed 120 ± 4 mg_{CDW} l⁻¹ (Table 2.1).

In order to investigate and quantify possible electron sink effects, three continuous cultivation conditions differing in electron source and sink availabilities were applied: i) Low light (LL) with excess supply of CO₂ (1% CO₂, HC) to induce light and thus source limitation, ii) high light (HL) with limiting CO₂ supply (ambient air, LC) to induce an electron sink limitation, and iii) unlimited conditions with high light (HL) and excess CO₂ supply (1% CO₂, HC) (Fig. 2.1). Under the assumption that the cells objective is to maximize growth [232], the cells should operate at maximum light harvesting capacity and quantum efficiency upon light

limitation (LLHC). The additional costs for nitrate assimilation should consequently lead to a reduced growth rate as less electrons are available for carbon fixation in the Calvin-Benson cycle. Under HLLC conditions, which force the cells into a carbon dioxide limited state, nitrate, as compared to ammonium as N-source, can be expected not to affect the growth rate, but to cause an increase in light reaction activity to meet the higher electron demand. A similar behavior can be expected for the HLHC condition, which served as a reference condition.

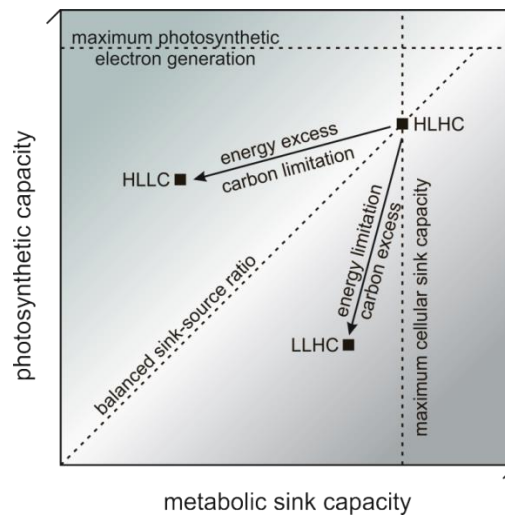


Figure 2.1: Metabolic states induced by the selected light and carbon dioxide availabilities. In the reference condition HLHC (high light and high carbon), light and carbon are supplied in excess ($250 \mu\text{mol photons m}^{-2} \text{s}^{-1}$, $1\% \text{CO}_2$). The cells can be expected to optimize resource utilization for optimal growth. Under HLHC conditions, growth is restricted by cellular limitations, i.e., saturation of metabolic pathways as for example the Calvin-Benson cycle or other molecular constraints (compare text). Limiting light availability and excess carbon dioxide supply ($65 \mu\text{mol photons m}^{-2} \text{s}^{-1}$, $1\% \text{CO}_2$, LLHC) will force the cells into an electron source limited metabolic state. In this case, the available light has to be exploited as efficiently as possible to achieve optimal growth. Growth is determined by the light harvesting capacity and PSII efficiency. If light is provided in excess, but carbon availability is limiting ($250 \mu\text{mol photons m}^{-2} \text{s}^{-1}$, ambient CO_2 , HLLC), the cells are expected to reduce expenses for photosynthetic source utilization in order to optimize sink utilization. In both cases, LLHC and HLLC, cells are expected to respond with reduced growth compared to the HLHC reference state.

Under unlimited HLHC conditions, when cellular processes and capacities are expected to limit growth, a constant growth rate of 2.45 d^{-1} was obtained, which, as expected, was the highest among the three conditions applied (Table 2.1). LLHC conditions resulted in a 47% reduced growth rate of PCC6803 compared to the reference HLHC condition (Table 2.1). This indicated that a light limitation was achieved, which was confirmed by the light induction curve (LIC, Fig. 2.2) showing that the photosynthetic oxygen evolution rate at the applied light intensity of $65 \mu\text{mol photons m}^{-2} \text{s}^{-1}$ was within the linear alpha slope (Fig. 2.2). The

specific chlorophyll a (Chl a) content remained at a similar level as under HLHC conditions (Table 2.1).

Table 2.1: Basic physiological parameters of PCC6803 under different steady conditions with ammonium or nitrate as N-source.

	LLHC		HLHC		HLLC	
	NH $_4$	NO $_3$	NH $_4$	NO $_3$	NH $_4$	NO $_3$
D [d $^{-1}$]	1.15	1.13	2.45	2.83	0.77	0.74
X [mg $_{CDW}$ l $^{-1}$]	107 ± 10	111 ± 7	63 ± 1	58 ± 1	120 ± 4	91 ± 3
c(Chl a) [mg $_{Chl a}$ l $^{-1}$]	2.18 ± 0.29	2.64 ± 0.22	1.50 ± 0.07	1.63 ± 0.10	1.41 ± 0.09	1.05 ± 0.03
Chl a $_{CDW}$ [μ g $_{Chl a}$ mg $_{CDW}^{-1}$]	20.4 ± 4.6	23.8 ± 3.5	23.8 ± 1.5	27.7 ± 2.2	11.7 ± 1.1	11.5 ± 1.1
Y(PSII) [-]	0.50 ± 0.01	0.60 ± 0.01	0.34 ± 0.01	0.52 ± 0.01	0.16 ± 0.01	0.21 ± 0.03
a^*_{phy} [m 2 g $_{Chl a}^{-1}$]	15.0 ± 0.8	14.0 ± 0.4	14.5 ± 0.1	15.2 ± 0.2	18.3 ± 1.3	17.9 ± 1.6
Q $_{phar}$ [mmol quanta mg $_{CDW}^{-1}$ d $^{-1}$]	1.28 ± 0.16	1.36 ± 0.09	6.20 ± 0.37	7.28 ± 0.59	3.56 ± 0.55	3.73 ± 0.38
r $_F$ [μ mol O $_2$ mg $_{CDW}^{-1}$ d $^{-1}$]	81.5 ± 10.8	102.3 ± 6.6	260.6 ± 23.0	469.4 ± 48.3	68.1 ± 7.4	108.3 ± 11
r $_O$ [μ mol O $_2$ mg $_{CDW}^{-1}$ d $^{-1}$]	28.9 ± 7.7	34.2 ± 7.9	84.5 ± 16.1	142.8 ± 21.2	39.9 ± 6.4	44.8 ± 4.9
r $_{resp}$ [μ mol O $_2$ mg $_{CDW}^{-1}$ d $^{-1}$]	7.7 ± 1.7	13.3 ± 3.0	19.7 ± 3.3	24.3 ± 4.5	5.2 ± 1.0	5.9 ± 0.4
PQ [mol mol $^{-1}$]	1.8 ± 0.1	1.9 ± 0.1	1.5 ± 0.1	1.7 ± 0.1	1.6 ± 0.1	1.6 ± 0.1
C/N [mol mol $^{-1}$]	4.67 ± 0.02	4.69 ± 0.13	4.61 ± 0.01	4.86 ± 0.07	5.23 ± 0.14	5.39 ± 0.14

Mean values and standard deviations correspond to 3-12 samples (depending on the parameter, see Materials and Methods section) taken during at least 3 different days for the same metabolic state. LLHC, low light (65 μ mol photons m $^{-2}$ s $^{-1}$) and high carbon (1% CO $_2$) condition; HLHC, high light (250 μ mol photons m $^{-2}$ s $^{-1}$) and high carbon condition (1% CO $_2$); HLLC, high light (250 μ mol photons m $^{-2}$ s $^{-1}$) and low carbon condition (ambient CO $_2$); D, dilution rate equaling the specific growth rate μ in the respective steady state; X, biomass concentration; c(Chl a), volumetric chlorophyll a concentration; Chl a $_{CDW}$, biomass specific Chl a content; Y(PSII), effective quantum yield at PSII; a^*_{phy} , Chl a dependent absorption coefficient of the cells; Q $_{phar}$, rate of quantum uptake; r $_F$, fluorescence-based electron flux at PSII; r $_O$, net O $_2$ evolution rate; r $_{resp}$, respiration rate; PQ, photosynthetic quotient defined by the ratio of O $_2$ evolution and CO $_2$ uptake; C/N, molar ratio of carbon and nitrogen in biomass.

The decrease of carbon dioxide supply from 1% to ambient air concentrations under HLLC conditions resulted in a strong decrease of the growth rate by 69% compared to HLHC conditions, which confirms the C- and thus sink limitation. As expected, the biomass-specific Chl*a* content decreased by 50% compared to HLHC (Table 2.1). The cells decreased their absorption capacity, which also was reflected by the 50% decrease of the rate of absorbed quanta and the severely lower Y(PSII) in comparison to HLHC conditions (Table 2.1 and Fig. 2.3).

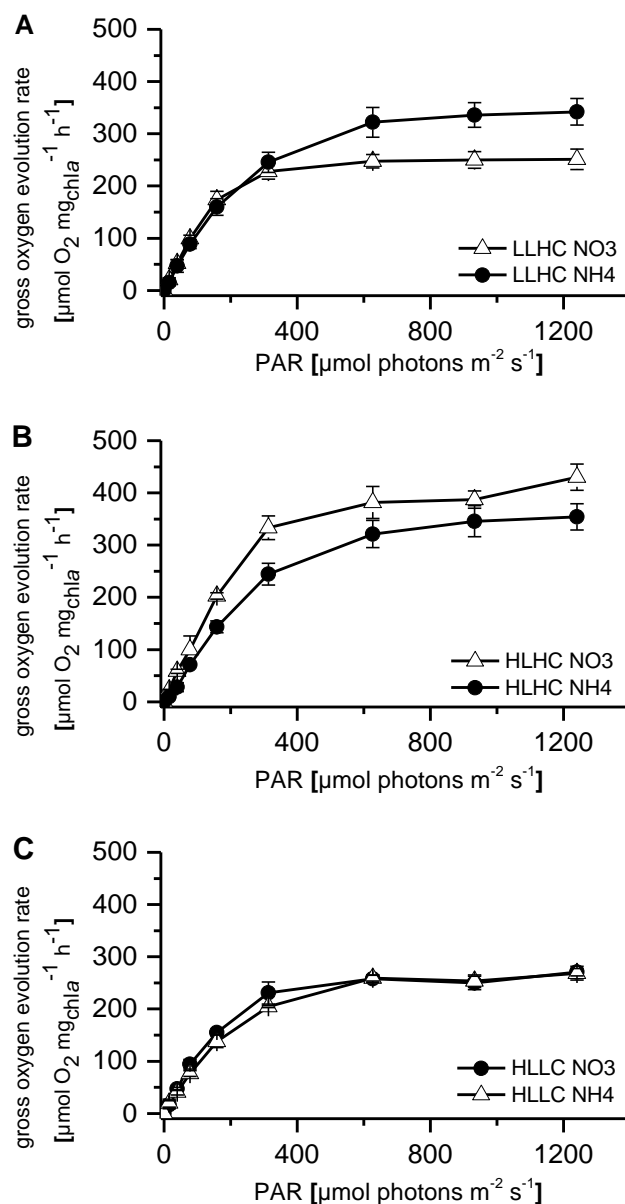


Figure 2.2: Light induction curves (LIC) of PCC6803 under different sink-source availabilities. LICs were performed for cells grown in the conditions low light high carbon (LLHC, panel A), high light high carbon (HLHC, panel B), and high light low carbon (HLLC, panel C). See Materials and Methods section for further experimental details.

In conclusion, the three selected combinations of light and carbon availability forced the cells into three different sink-source balanced metabolic states. A clear physiological response to sink-source modulation without any effects of fluctuating light and short term adaptation effects was achieved. The following sections describe in detail the impact of replacing ammonium with nitrate as an additional electron sink on the physiology of PCC6803 under these different sink-source balances.

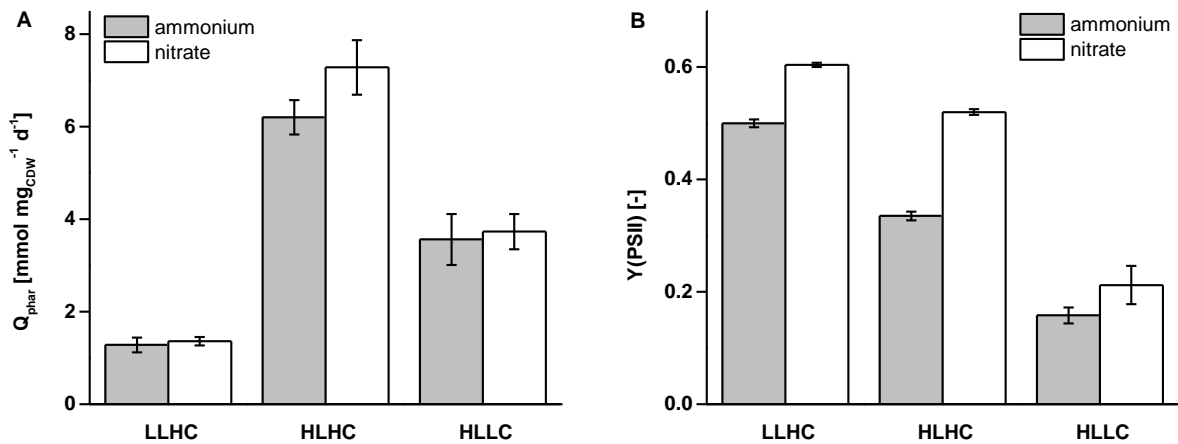


Figure 2.3: Quantum absorption rates Q_{phar} (A) and effective quantum yields at PSII $Y(\text{PSII})$ (B) under different steady state conditions. PCC6803 was grown with ammonium (striped bars) or nitrate (white bars) as N-source under LLHC (low light high carbon), HLHC (high light high carbon), and HLLC (high light low carbon) conditions. Cells were cultivated in a bioreactor setup in a continuous (turbidostat) mode to achieve stable steady metabolic states. Light and carbon supply were varied in order to force the cells into different sink-source balances. The light intensity was set to either 65 (LL) or 250 (HL) $\mu\text{mol photons m}^{-2} \text{s}^{-1}$, and carbon was supplied with ambient CO_2 concentration in air (LC) or air enriched with 1% CO_2 (HC). Mean values and standard deviations were calculated for three different measurement days. See Materials and Methods for details on the measurements.

Effect of an additional electron sink under source limitation

Under source-limited conditions (LLHC), cell growth is restricted by the light availability fueling water splitting and thus the electron transport chain to regenerate NADPH and ATP. Consequently, the cells should possess a maximized light-harvesting capacity and the photosynthetic electron transport should operate at maximum efficiency at the given irradiance. Any additional electron sink is expected to consume electrons at the expense of the electrons available for carbon fixation and finally growth. We tested this hypothesis under steady state LLHC conditions with the supply of nitrate instead of ammonium as N-source.

In contrast to the expectations, nitrate instead of ammonium supply did not affect growth and carbon assimilation rates (Table 2.1 and Fig. 2.4A). The light harvesting capacity is defined by the Chl*a* dependent absorption coefficient of the cells (a^*_{phy}) and finally by the quantum absorption rate of the cells (Q_{phar}). Cells fed by either nitrate or ammonium did not differ regarding specific Chl*a* content and a^*_{phy} (Table 2.1), resulting in similar quantum absorption rates (Table 2.1 and Fig. 2.3A). This met the expectation that cells should display maximum light harvesting capacity in a light limited regime irrespective of the presence of an additional electron sink. It was further expected that the quantum efficiency $Y(PSII)$, i.e., the efficiency of quantum usage at PSII for photochemistry, is maximized in LL and, consequently, should not be influenced by the different electron demand with nitrate and ammonium as N-source. $Y(PSII)$, however, increased from 0.50 ± 0.01 to 0.60 ± 0.01 , if nitrate instead of ammonium was supplied (Table 2.1 and Fig. 2.3A). The increased quantum efficiency in combination with the constant uptake of quanta (Q_{phar}) resulted in increased photosynthetic rates. The net oxygen evolution rate (r_o) increased by 18% and the fluorescence-based electron flux at PSII (r_F) by 26% (Table 2.1).

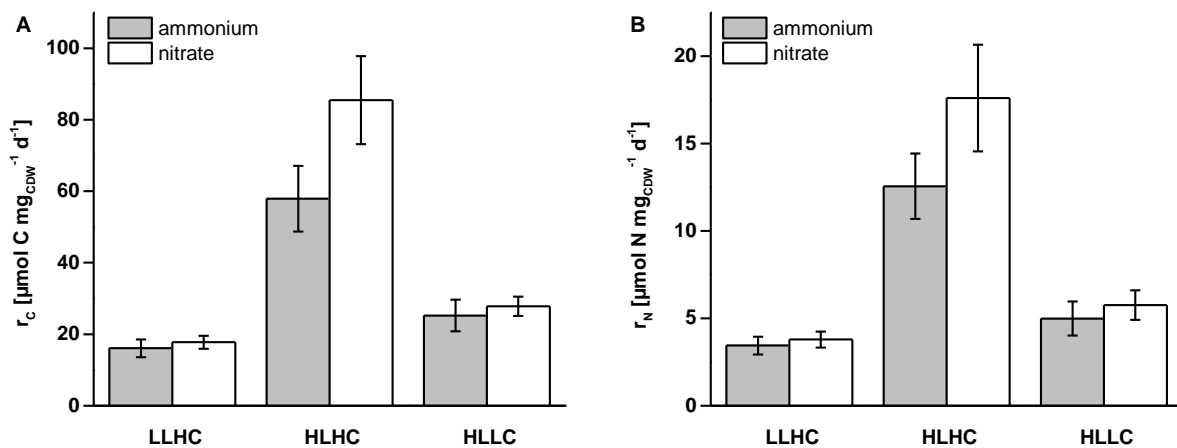


Figure 2.4: Molar carbon (r_C , A) and nitrogen (r_N , B) assimilation rates of PCC6803 under different steady state conditions. Cells were grown with ammonium (striped bars) or nitrate (white bars) as N-source under LLHC (low light high carbon), HLHC (high light high carbon), and HLLC (high light low carbon) conditions. Growth conditions are described in the legend of Fig. 2.3. Mean values and standard deviations were calculated for three different measurement days. See Materials and Methods for details on the measurements.

In the next step, the metabolic sink capacity, i.e., the metabolic electron demand, and the photosynthetically provided electrons were calculated in order to gain a deeper understanding of the cellular sink-source balancing. Table 2.2 depicts the calculated cellular electron demand for biomass formation and electron fluxes in the electron transfer chain

(ETC) under the conditions investigated. The O₂-based electron supply rate, $r_{O,gross}$, was based on r_O and corrected for the respective measured respiration rate ($r_{O,gross} = r_O + r_{resp}$). r_O and r_{resp} were measured at the light intensity applied under the respective cultivation condition. The alternative electron flux (r_{AEF}) was defined as the difference between oxygen- and fluorescence-based electron fluxes through PSII ($r_{AEF} = r_F - r_{O,gross}$). The total electron demand was estimated from the N- and C-assimilation rates. Two assumptions were made: i) Eight additional electrons are required for the assimilation of one molecule of nitrate as compared to ammonium and ii) a minimum of 4 electrons is required for the assimilation and reduction of one molecule CO₂.

Table 2.2: Electron demands and supply in PCC6803 at the investigated sink-source ratios with ammonium or nitrate as N-source.

	LLHC		HLHC		HLLC	
	NH	NO	NH	NO	NH	NO
r_C	64 ± 10	71 ± 7	232 ± 37	342 ± 49	101 ± 18	111 ± 11
$r_{nitrate}$	-	30 ± 4	-	141 ± 24	-	41 ± 6
r_D	64 ± 10	101 ± 11	232 ± 37	483 ± 74	101 ± 18	153 ± 17
$r_{O,gross}$	147 ± 6	190 ± 5	417 ± 13	668 ± 17	180 ± 6	203 ± 5
r_{AEF}	179 ± 17	219 ± 12	626 ± 36	1209 ± 65	92 ± 13	231 ± 16

All rates are given in $\mu\text{mol electrons mg}_{CDW}^{-1} \text{d}^{-1}$. Mean values and standard deviations were calculated for three different measurement days. See Materials and Methods for details on the measurements. The cellular electron demand (r_D) was calculated from the electron demand for carbon fixation (r_C) and nitrogen assimilation ($r_{nitrate}$). The electron supply rate ($r_{O,gross}$) is derived from the sum of r_O and r_{Resp} . The alternative electron flux (r_{AEF}) is calculated by subtracting $r_{O,gross}$ from the fluorescence-based electron flux (derived from r_F).

Under the LLHC condition, nitrate assimilation resulted in a significantly higher cellular electron demand (r_D) of $101 \pm 11 \mu\text{mol electrons mg}_{CDW}^{-1} \text{d}^{-1}$ compared to $64 \pm 10 \mu\text{mol electrons mg}_{CDW}^{-1} \text{d}^{-1}$ for ammonium fed cells. Accordingly, the nitrate reduction costs accounted for 16% of the oxygen-based electron supply rate at PSII, $r_{O,gross}$. The net increase of $r_{O,gross}$ upon nitrate compared to ammonium assimilation (Table 2.2, Fig. 2.5) covered the additional net electron demand for nitrate assimilation. However, $r_{O,gross}$ was significantly higher than the calculated metabolic demand. This gap is a consequence of the assumption that the cellular electron demand is dominated by carbon and nitrogen assimilation. Other electron demanding processes, such as phosphor and sulfur assimilation, were neglected. The calculated electron demand thus constitutes a lower boundary. Simultaneously, the alternative electron flux r_{AEF} increased by 22% with nitrate

instead of ammonium as N-source (Table 2.2). The alternative electron flux is partly used for ATP regeneration. A higher rate thus indicates a higher energy demand of the cells grown on nitrate, e.g., for active ATP-dependent nitrate import into the cells.

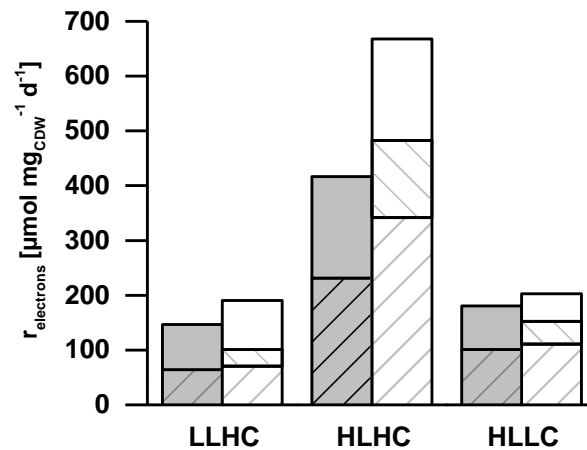


Figure 2.5: Cellular electron demand and electron supply in PCC6803 under different steady state conditions. Rates are given in $\mu\text{mol electrons mg}_{\text{CDW}}^{-1} \text{d}^{-1}$. PCC6803 was grown with ammonium (grey bars) or nitrate (white bars) as N-sources under LLHC (low light high carbon), HLHC (high light high carbon), and HLLC (high light low carbon) conditions. Growth conditions are described in the legend of Fig. 2.3. Photosystem II electron supply rates are derived from gross O_2 evolution rates ($r_{\text{O}_2, \text{gross}}$) and reflected by the entire column heights, whereas electron consumption rates for carbon (striped from lower left to upper right) and nitrate (striped from upper left to lower right) assimilation are shown as shares of the overall supply rates. Mean values and standard deviations were calculated for three different measurement days. See Materials and Methods for details on the measurements.

In conclusion, the supply of nitrate as an additional electron sink unexpectedly resulted in an increased photosynthetic efficiency enabling an increase in photosynthetic electron supply. This was contrary to the hypothesized decrease in carbon assimilation and biomass formation under light limited conditions.

Effect of an additional electron sink under carbon limitation

In strong contrast to the LLHC condition, the HLLC condition does not involve a limitation by light (source), but by CO_2 (sink). Under such C limitation, the cells have to balance their metabolism by reducing light harvesting and photosynthetic capacities and by the dissipation of excess energy. The additional electron demand for nitrate reduction can thus be covered by a higher but still submaximal PSII efficiency and electron supply without further negative effects on biomass formation. Nitrate reduction and biomass formation thus are not expected to compete for energy.

As expected, the growth rate under HLLC conditions was not affected by the additional electron demand for nitrate assimilation ($\mu = 0.77$ and 0.74 d^{-1} with ammonium and nitrate, respectively, Table 2.1). Electron balancing indicated that reduction of nitrate consumed 20% of the PSII-derived electrons (Table 2.2), which had to be provided in addition to the electrons required for C fixation. The cells met this additional electron demand by a 31% higher effective quantum efficiency at PSII ($Y(\text{PSII})$). This resulted in a strong increase of r_F by 59% but only a moderate enhancement of r_O by 12% (Table 2.1). Consequently, an increase of the alternative electron flux by a factor of 2.5 was observed under nitrate instead of ammonium supply (Table 2.2). It should be highlighted that nitrate instead of ammonium assimilation was not reflected by an increase in the quantum absorption rate (Q_{phar} , Table 2.1), but only by an increased quantum yield $Y(\text{PSII})$.

In summary, the results under HLLC conditions met the expectation that an additional electron sink can be covered by the surplus light and thus energy available, without affecting carbon assimilation and cell growth. The cells did not show increased absorption but an increased quantum yield at PSII.

Effect of an additional electron sink under excess sink and source availability

Under HLHC conditions, the cells can be expected to maximize their carbon fixation capacity and thus growth. Following the hypothesis of a sink-limited photosynthesis [164, 165], the introduction of an additional electron sink should result in increased activity of the light reaction to cover the additional electron demand, whereas growth should not be affected.

Surprisingly, the cultivation of PCC6803 under HLHC conditions with nitrate as N-source resulted in a 16% higher growth rate as compared to ammonium fed cells (Table 2.1). In contrast to LLHC and HLLC conditions, nitrate instead of ammonium supply resulted in a significant increase of both N- and C-assimilation rates (Fig. 2.4). Thereby, an enhancement of Q_{phar} by 17% was accompanied by a strong increase of $Y(\text{PSII})$ by 53% and of the photosynthesis rates r_O and r_F by 69 and 80%, respectively (Table 2.1).

The electron demand was doubled with nitrate instead of ammonium as N-source as a consequence of the increased N- and C-assimilation rates and the additional electron demand for nitrate reduction. This electron demand was covered by a strongly increased photosynthetic electron supply and was accompanied by an enhanced alternative electron flux (Table 2.2). The relative proportion of electrons required for nitrate assimilation (21%) under HLHC was comparable to those under LLHC and HLLC conditions. The C/N ratio in

biomass was similar under all conditions tested and did not significantly differ upon nitrate and ammonium supply (Table 2.1).

Overall, cells of PCC6803 under HLHC conditions responded in an unexpected manner to nitrate assimilation as an additional electron sink, i.e., by a distinctive stimulation of growth (and consequently C- and N- assimilation) and photosynthetic rates. This indicates that metabolic activity is not only regulated by general source (light) and sink availabilities, but also by the type of electron sinks.

Discussion

Nitrate assimilation constitutes a significant electron sink in PCC6803

In the present study, the physiological acclimation of the model organism PCC6803 to an additional electron sink was investigated at different source/sink ratios. The availability of source (light) and sink (CO₂) was modulated to force the cells into differently balanced metabolic states. The assimilation of nitrate was employed as an additional electron sink and compared with cultures grown on ammonium as N-source. In contrast to other studies, in which ammonium was demonstrated to have negative and toxic effects in cyanobacteria by causing photodamage at PSII or interfering with the proton gradient in the thylakoid membrane [212-216], no negative effect of ammonium up to 50 mM on the growth pattern and phenotype of PCC6803 in shaking flask batch cultivations was observed (see Supplemental Information 2, Fig. S2). Nitrate assimilation consumed 16-21% of the photosynthetically produced electrons (based on $r_{O_2, gross}$ and the C/N content of biomass) under all experimental conditions. This corresponds to electron sink rates of 30 ± 4 , 141 ± 24 , and 41 ± 6 $\mu\text{mol electrons mg}_{CDW}^{-1} \text{d}^{-1}$ or, in biotechnological terms, 21, 98, and 29 U g_{CDW}^{-1} under LLHC, HLHC, HLLC conditions, respectively. These rates are in the range of or exceed most published electron consumption rates of heterologous systems in cyanobacteria [83, 84, 86, 169, 202-205]. To our knowledge, higher electron withdrawal rates were only measured for an NADPH dependent alkane reduction mediated by an enoate reductase (123 and 246 U g_{CDW}^{-1} for the reaction and the electron consumption rates, respectively) [86]. Nitrate assimilation can, therefore, be considered a strong natural electron sink in PCC6803. Heterologous electron sinks have typically been introduced to establish a product formation concept. However, investigations on physiological responses to and cellular capacities for such biotransformations are largely missing so far [84, 202-204]. The cultivation and analytic setups developed in this study are suitable for this purpose. Such

studies will answer the question if the sink effects observed in this study are specific for the assimilation of different N-sources or more generally valid for electron sinks including productive recombinant reactions or pathways.

PCC6803 can easily cope with additional electron sinks

The physiological response of PCC6803 to an additional electron sink may depend on the actual source/sink ratio, to which the cells are exposed under different growth conditions. Source limitation resulted in slow growth combined with high photosynthetic efficiency. Sink limitation also resulted in slow growth with cells operating at low photosynthetic efficiency. Source-sink excess conditions resulted in fast growth combined with moderate photosynthetic efficiency. Thus, the light reaction obviously did not operate at maximum efficiency although the cells were not sink (carbon) limited. This indicates that other cellular processes limit growth rates. These observations are consistent with the source-sink balance hypothesis, stating that photosynthetically active cells balance light absorption efficiency and light reaction performance with other metabolic capacities (e.g., carbon concentration mechanism, Calvin-Benson cycle, anabolism) according to environmental source/sink ratios [165].

The cultivation of PCC6803 with nitrate as an additional electron sink generally resulted in increased effective quantum yields at PSII and light reaction rates irrespective of the sink/source availability (Table 2.1 and 2.2), whereas the absorptivity of the cells (a^*_{phy}) remained unaffected. Such an increase in the efficiency of the photosynthetic light reaction has previously been observed with either additional electron consuming reactions under HLLC-type conditions (200 $\mu\text{mol photons m}^{-2} \text{ s}^{-1}$ and ambient CO_2) [169] or the synthesis and excretion of sucrose under HLHC-type conditions (100 $\mu\text{mol photons m}^{-2} \text{ s}^{-1}$, 2% CO_2 enriched air) [168]. Enhanced light reaction efficiency can be expected under HLLC and HLHC conditions, since the photosynthetic activity was not limited by light and thus source availability. Instead, sink availability or other metabolic capacities such as carbon concentration mechanism, Calvin-Benson cycle, or anabolism can be limiting [164, 165]. The increase of $Y(\text{PSII})$ as a response to nitrate assimilation under LLHC conditions was unexpected. The light reaction of photosynthesis is commonly assumed to operate at maximum efficiency under conditions of low light and excess carbon availability. Moreover, the results obtained contradict the view that nitrate reduction is a metabolic burden and should be avoided under light-limited conditions [233]. It can be concluded from the

presented results that the cells did not run their light reaction at maximum efficiency under LLHC conditions with ammonium as N-source. The cells are thus not operating their light reaction at maximum capacity, possibly for adaptations to dynamic changes in the availability of resources (such as N-sources). This would mean that cells sacrifice their full metabolic potential for a higher robustness in a dynamic environment. The introduction of nitrate as an additional electron sink obviously released further photosynthetic potential. It can be hypothesized that this phenomenon is connected to the increase in alternative electron fluxes and thus a changed ATP/NADPH ratio (see below).

Another interesting observation was that the alternative electron flux increased in response to nitrate as an additional electron sink under all experimental conditions. This increase correlated linearly with the nitrate assimilation rate (Fig. 2.6). In principle, the electrons used for the stepwise reduction of nitrate to ammonium are derived from photosynthetic electron transport at the acceptor side of PSI. Therefore, nitrate reduction in cyanobacteria is light-dependent, and the requirement of eight electrons per molecule nitrate results in the evolution of 2 O₂ molecules at PSII as shown before [234]. Increased O₂ evolution with nitrate as N-source also was observed in the present study. The alternative electron flux, on the other hand, is calculated from the difference of fluorescence-based and O₂-based electron flux at PSII. Alternative electron flux is thought to comprise electrons that re-reduce O₂, e.g., Mehler and Mehler-like reactions. The Mehler-like reaction involves electron transfer via the flavodiiron proteins flv1/flv3 and flv2/flv4 to O₂ [162, 163, 235, 236]. The flv1/flv3-mediated O₂ reduction is an electron valve at the acceptor side of PSI. Thus, electrons derived from water splitting at PSII run through the entire photosynthetic electron transport chain (ETC) to end up on O₂ again. The flavodiiron proteins flv2 and flv4, on the other hand, are discussed to accept electrons from the electron accepting plastoquinone pocket (Q_B) of PSII [163, 236, 237]. The electron acceptor of flv2/flv4 is not identified, but there are indications that O₂ can be an electron acceptor at least under carbon limited conditions [161]. With O₂ as electron acceptor, such electron fluxes over the thylakoid membrane involve the generation of 4 protons per O₂ molecule formed on the thylakoid lumen side and the consumption of 4 protons per O₂ molecule consumed on the cytoplasmic side. Thereby, and by a possible flux through the ETC as in case of flv1/flv3-mediated O₂ reduction, such alternative electron flux contributes to ATP synthesis via the proton gradient over the thylakoid membrane. This means that, due to the strong electron consumption for

nitrate reduction at the expense of NADPH and the enhanced alternative electron flux, an increase of the ATP/NADPH ratio under conditions with nitrate supply is plausible. The Calvin-Benson cycle requires an ATP/NADPH ratio of 3:2. The linear photosynthetic electron transport does not fulfill this requirement. Therefore, insufficient ATP supply is often limiting carbon assimilation by the Calvin-Benson cycle [238]. Given the increase in alternative electron flux at PSII upon substitution of ammonium with nitrate, the described electron flux over the thylakoid membrane at PSII may, beside cyclic photophosphorylation [165], contribute to the flexible adjustment of the ATP/NADPH ratio. Continuing this argumentation, the ATP/NADPH ratio under ammonium supply would limit the Calvin-Benson cycle, even under source limited LLHC conditions, and nitrate supply would induce an optimized ATP/NADPH ratio. This could explain why the cells were able to supply the additionally required electrons for nitrate reduction under LLHC conditions by an increased photosynthesis rate with no negative effect on carbon fixation and growth. To confirm this hypothesis, it would be interesting to investigate on a systems level, including transcriptomic and proteomic analyses, how nitrate is capable to stimulate such alternative electron flux and ATP formation and if this phenomenon also is triggered by other artificially introduced electron sinks.

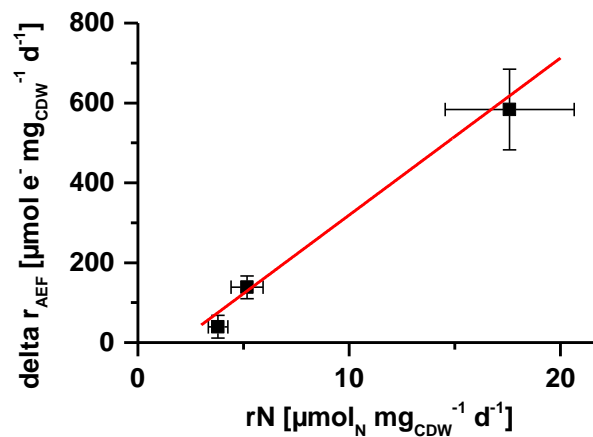


Figure 2.6: Increase of alternative electron flux (Δr_{AEF}) in dependence of the nitrate assimilation rate (r_N). Δr_{AEF} corresponds to the difference in alternative electron flux with nitrate and ammonium as N-source. See Table 2.2 for r_{AEF} 's with the different N-sources. Δr_{AEF} is plotted against the respective N assimilation rate (which corresponds to the increased electron demand for nitrate assimilation) under LLHC (low light high carbon), HLHC (high light high carbon), and HLLC (high light low carbon) conditions. The growth conditions are described in the legend Fig. 2.3. Mean values and standard deviations were calculated for three different measurement days. See Materials and Methods for details on the measurements.

An electron sink can stimulate light and dark reactions

Another unexpected result was that nitrate instead of ammonium supply under HLHC conditions led to increased C- and N-assimilation and finally biomass formation rates. This was surprising since the HLHC condition was the condition with most degrees of freedom for metabolic balancing expected to enable growth maximization. The cultures indeed showed high growth rates, but obviously did not exploit their full growth potential with ammonium as N-source. As cell growth was not limited by light or carbon supply, the metabolic capacity of the cells obviously differed with the two N-sources, with a non-optimum ATP/NADPH ratio as a possible factor limiting metabolic rates and growth in the presence of ammonium (see above). The further stimulation of biomass production and carbon uptake as a result of an additional electron sink also was observed for cyanobacterial strains engineered to synthesize and secrete butanediol [171], sucrose [72] or isoprene [79]. Product formation as an additional sink for electrons and also carbon was proposed to relieve a yet unspecified inherent metabolic limitation. The increase of biomass production upon provision of an additional electron sink is a novel observation but may be explained via the same line of argumentation. Cellular metabolism and particularly the activity of the Calvin-Benson cycle is regulated by the redox state of the cells. It can be hypothesized that electron withdrawal for nitrate reduction lowered the redox potential, e.g., the NAD(P)H/NAD(P) ratio and the oxidation state of the plastoquinone pool. Similar to vascular plants and algae [239], the plastoquinone pool is an important source for redox signals in cyanobacteria with direct impact on the establishment of a certain photo-acclimation state [240, 241]. Accordingly, a more oxidized plastoquinone pool rapidly initiates the transcription of PSII genes and finally increases O₂ evolution at PSII. Thus, the observed increase in rates for the light reaction as well as the dark reaction upon nitrate supply in HLHC conditions may not only be due to the electron demand for nitrate reduction or a nitrogen source specific regulation mechanism, but also may reflect a new photo-acclimation state in response to a change in the redox state of the plastoquinone pool.

Conclusion

Overall, the presented data demonstrated a remarkable potential of PCC6803 to cope with additional electron withdrawal. The results indicate that electron sinks can be beneficial for overall cellular performance. Even a high electron demand can be covered by exploiting the inherently available potential of the non-limiting light reaction. Astonishingly, this also was

the case under light limiting conditions indicating that the capacity of the light reaction is not necessarily completely exploited under low light conditions. Moreover, an experimental setup was developed in this study, which is suitable to unravel changes in electron demand and electron supply in a quantitative manner. We are convinced that this setup is also applicable to production strains with an inherently high or elevated energy and electron demand.

Acknowledgements

The authors thank Prof. Stan Harpole and Petra Hoffmann from the Department for Physiological Diversity at UFZ and the German Centre for Integrative Biodiversity Research (iDiv) in Leipzig for analyzing the C/N samples.

Chapter 3: Heterologous lactate synthesis in *Synechocystis* sp. PCC 6803 causes a condition-dependent increase of photosynthesis rates

Marcel Grund, Torsten Jakob, Jörg Toepel, Andreas Schmid, Christian Wilhelm, Bruno Bühler

This chapter was submitted as a research article.

Marcel Grund performed all experiments and wrote the manuscript. Torsten Jakob and Marcel Grund measured the light induction curves and photosynthetic quotient. Jörg Toepel, Andreas Schmid, Christian Wilhelm and Bruno Bühler coordinated the project and corrected the manuscript.

Abstract

Cyanobacteria are promising hosts for the heterologous synthesis of carbon-based products directly from CO₂ and the direct harvest of electrons derived from photosynthetic water oxidation for biotransformations. Interestingly, many metabolic engineering studies observed that heterologous pathways stimulated photosynthetic activity, for example O₂ evolution rates, quantum efficiencies, and carbon fixation rates. Such effects are in literature widely discussed as carbon sink effect, but there is no clear definition of the carbon sink effect and the understanding of underlying mechanisms is poor. Such an understanding is however essential for a more rational engineering of cyanobacteria. We investigate the physiological response of *Synechocystis* sp. PCC 6803 SAA023 to lactate synthesis via a heterologous lactate dehydrogenase in comparison to a wildtype strain. Steady metabolic states were established via continuous cultivation involving excess supply of CO₂ and light, light limitation, or carbon limitation. Interestingly, only under carbon limitation, lactate synthesis caused a distinct carbon sink effect, i.e., increased O₂ evolution and quantum efficiency of Photosystem II, and an increased carbon fixation rate. The partitioning of carbon to lactate is not exclusively determined by the lactate dehydrogenase activity, but also by the metabolic state of the cell, i.e., its adaption to distinct light and carbon availabilities. Lactate as carbon sink lead to growth impairment if cellular metabolism was light limited or if the maximum carbon fixation capacity was reached. Furthermore, it is hypothesized that a carbon sink can stimulate carbon fixation by changing the cellular ATP/NAD(P)H balancing.

This study emphasizes the potential to unleash yield and product formation rate improvement potentials by selecting appropriate growth/reaction conditions as well as by engineering the cellular redox and energy metabolism.

Introduction

Cyanobacteria have the potential to contribute to a sustainable and fossil resource-free bio-economy. Similar to plants, cyanobacteria are capable of utilizing CO₂ and light as sources for carbon and energy, respectively. Regarding biotechnological applications, cyanobacteria exhibit, in comparison to higher plants, distinct advantages such as faster growth, higher yearly area based carbon fixation [195], genetic accessibility [185, 194] and reduced competition with agricultural land use [37].

Cyanobacteria have been engineered to synthesize a variety of molecules (reviewed by [173, 242, 243]). Metabolic engineering allowed the synthesis of hydrocarbons [79, 172, 244, 245], fatty acids [246], organic acids [73, 134, 247], alcohols [69, 71] as well as sugars [72, 248] from CO₂. Most of these studies focused on the optimization of the carbon partitioning into the product and the final product titer. One approach is the engineering of the Calvin-Benson cycle to increase the carbon fixation rate and thereby the product formation rate [249, 250]. However, strain and process development are not yet as advanced as they are for heterotrophic organisms, for which more detailed physiological knowledge and development rules are available [100, 103, 131].

Two aspects have to be considered for productive photo-biotechnology. First, rational engineering of microorganisms requires a detailed understanding of basic modes and quantitative limits of the cellular metabolic fluxes [131, 251, 252]. Second, an integrated approach covering strain, reaction, and process engineering should be followed [101, 253]. The basis for both is an in-depth characterization and understanding of whole-cell biocatalysts under relevant reaction and process conditions. So far, research towards the application of cyanobacteria focused much more on metabolic engineering strategies than on quantitative physiology. However, the latter is required to answer two key questions: Which are the factors determining carbon fixation and product formation rates? How can we influence the carbon partitioning into the product? The systematic investigation of factors influencing cyanobacterial growth and product formation [148-150, 254, 255] and of the quantitative characterization of metabolism [152, 154, 256] just has been addressed recently.

One open, yet widely discussed aspect is the so-called carbon sink effect. In some cases, cyanobacteria engineered for product formation from assimilated CO₂ showed increased O₂ evolution rates and improved effective quantum yields of photosystem II (PSII) [70, 72, 168-

170]. In a few cases, even an enhanced carbon fixation rate in comparison to the respective wild type strain was observed [65, 70-72, 170-172]. This was explained by the relief of a general electron sink limitation of the light reactions, of which the capacity under full sunlight is much higher than that of the electron consuming dark reactions, i.e., C-fixation [165]. Under high light conditions, the efficiency of the light reactions is down-regulated to prevent cell damage. Therefore, it is assumed that the addition of alternate electron consuming pathways can circumvent such downregulation and lead to enhanced photosynthetic efficiency and rates. Whereas photosynthetic water oxidation appears to be limited by C-fixation, the latter in turn depends on appropriate ATP supply. The linear electron flux (LEF) does not supply the Calvin-Benson cycle with sufficient ATP in relation to the NADPH generated [167]. Cells can modify the ATP/NADPH ratio via alternative electron fluxes (AEF) contributing to ATP but not to NADPH regeneration [158, 159, 167, 235]. Beside the cyclic electron flux around PSI, AEF also comprise non-cyclic electron fluxes, where electrons from water splitting are transferred e.g., to O₂ instead of NADP⁺. It is discussed that heterologous sinks may contribute to cellular ATP and NADPH balancing, thereby enabling enhanced photosynthesis and carbon fixation rates [144, 170, 256]. As pointed out by Angermayr et al. [173], a detailed systematic and quantitative investigation of the carbon sink effect in cyanobacteria is needed.

This study investigates the carbon sink effect in the model cyanobacterium *Synechocystis* sp. PCC 6803, by comparing the wild type with the lactate producing SAA023 strain [134, 135]. The SAA023 strain forms lactate from pyruvate via a heterologous lactate dehydrogenase depending on NAD(P)H as cofactor. Such alternative carbon withdrawal changes the cellular ATP/NAD(P)H demand. Whereas biomass and lactate feature a similar degree of reduction, biomass formation requires more ATP than lactate formation, as it is illustrated by the ratio of ATP and NADPH demands for biomass (2.13) and lactate formation (1.17) [144]. We combined a continuous cultivation approach, enabling reproducible and well-defined metabolic states, with a comprehensive quantification of cellular physiology in terms of the PSII rate, LEF and AEF, and carbon fluxes into biomass and product.

Materials and Methods

Bacterial strains

Synechocystis sp. PCC 6803 (originating from the Bhaya Lab, Stanford) and the lactate producing strain SAA023 harboring a lactate dehydrogenase were provided by Prof. Hellingwerf and Prof. dos Brancos from the University of Amsterdam, see details in [134, 135]. The strains were maintained as cryo-culture at -80°C in BG11 medium supplemented with 20% DMSO and freshly cultivated prior experiments.

Growth conditions

PCC6803 was cultivated as described before [256]. In short, BG11 [221] supplemented with 1.5% agar and 0.03% sodium thiosulfate was used for agar plate cultivation, and YBG11 [150] for liquid cultivations. YBG11 was supplemented with 50 mM HEPES for shaking flask cultivations and 2 mM HEPES for bioreactor cultivations, respectively. The medium was adjusted with 10 M NaOH to a pH of 8.0. Standard cultivation conditions were 20 $\mu\text{mol photons m}^{-2} \text{s}^{-1}$, 30°C and 75% relative humidity (rH) in a plate incubator (poly klima GmbH, Freising, Germany) for agar plates, and 140 rpm, 30°C, 50 $\mu\text{mol photons m}^{-2} \text{s}^{-1}$ under 75% rH for shaking flask experiments and for bioreactor precultures (Multitron, INFORS AG, Bottmingen, Switzerland).

Continuous cultivations were performed in flat-panel airlift bioreactors (Labfors 5 Lux, INFORS AG, Bottmingen, Switzerland) as described in [256]. Standard parameters were set to pH 8.0, 30°C and 1.0 vvm aeration (pressurized air or synthetic air enriched with CO₂ when appropriate). Three different conditions were tested: i. light limitation (aeration with 1% CO₂ and low light intensity of 65 $\mu\text{mol photons m}^{-2} \text{s}^{-1}$ (LLHC)), ii. excess supply condition (aeration with 1% CO₂ and high light intensity of 250 $\mu\text{mol photons m}^{-2} \text{s}^{-1}$ (HLHC)), iii. carbon limitation (approx. 0.05% CO₂, considered as ambient, and high light intensity of 250 $\mu\text{mol photons m}^{-2} \text{s}^{-1}$ (HLLC)). The biomass concentration was kept constant by feeding fresh medium into the bioreactor with a rate equal to the growth rate at the respective conditions via a peristaltic pump (IPC-series, ISMATEC, Cole-Parmer GmbH, Wertheim, Germany). The filling level was kept constant by pumping culture through a fixed efflux tube at the top of the reactors. The growth rate was calculated from the dilution rate according to

$$D = \mu = \frac{\dot{V}}{V}$$

with a working volume of $V=1.8 \text{ L}$ and the feeding rate $\dot{V} \left[\frac{\text{L}}{\text{d}} \right]$.

Determination of cell dry weight (CDW), biomass concentration, C/N and Chl α content

Biomass, i.e. CDW-OD₇₅₀ correlations, CDW and Chl α content was determined as described in detail in [256]. CDW-OD₇₅₀ correlations and Chl α content were determined in triplicates, the C/N ratios in duplicate) for each measuring day (three days per condition and strain). OD₇₅₀ was measured at least four times per day.

Measurement of the effective quantum yield at PSII and of photosynthetic rates

The effective quantum yield and the photosynthetic rates were measured and calculated as described in [256]. A Multi-Color PAM [223] (Heinz Walz GmbH, Effeltrich, Germany) was used to determine the quantum yield of photosynthesis at PSII (Y(PSII)). The measurement light was set to 400 nm and white light was used as actinic light and for the saturation flash. A light induction curve (LIC) was recorded with increasing light intensities. The measurements were conducted at least 9 times per steady state (minimum 3 times per measuring day on three independent measuring days).

The following photosynthetic parameters were determined as described previously [217, 218, 230, 256]: the Chl α -specific absorption coefficient of the cells (a^*_{phy}), the cellular quantum absorption rate (Q_{phar}), the net O₂ evolution rate (r_{O}), as well as the maximum electron flux at PSII (r_{F}). r_{O} and r_{F} are given as O₂ evolution rates in mmol O₂ g_{CDW}⁻¹ d⁻¹. Q_{phar} is given as quantum uptake rate in mmol photons mg_{CDW}⁻¹ d⁻¹.

To determine Q_{phar} , the emission spectrum of the LED panel of the reactor (Supplemental information, Fig. S1) and specific *in vivo* chl α absorption spectra of the cells were measured [230]. Absorption spectra were recorded by means of a dual beam spectrophotometer (Zeiss M500, Carl Zeiss AG, Oberkochen, Germany). The emission spectrum of the light source was determined using a spectroradiometer (Tristan 4.0, m-u-t GmbH, Wedel, Germany).

For all steady state experiments, the net O₂ evolution rate, r_{O} , was determined using a Clark-type electrode (MI-730, Microelectrodes Inc., Bedford, USA). For this purpose, LICs were recorded by determining O₂ evolution and respiration rates under light and dark conditions, respectively (Supplemental information, Fig. S5). Gross O₂ formation rates were calculated by correcting measured O₂ evolution rates for corresponding respiration rates. The maximum electron flux through PSII, r_{F} , expressed as an O₂ evolution rate, was estimated based on the measured Y(PSII) at the applied cultivation light intensity (see above). Given Q_{phar} and r_{O} values represent averages of measurements taken on three different days.

Quantification of lactate and lactate production rate

Lactate was quantified in the supernatant of the cell suspension. For that, approx. 0.5 to 1.0 ml of cell suspension were centrifuged for 5 min at 17,000 *g* and 4°C (Heraeus Fresco 17, Thermo Scientific, Waltham, USA). The supernatant was stored at -20°C until further analysis. Lactate concentration was determined either by HPLC (Ultimate 3000 Series, Dionex, Thermo Scientific) equipped with an RI detector (Refractomax 520, Thermo Scientific) or an assay kit according to the suppliers instructions (MAK065, Sigma-Aldrich). For the quantification via HPLC, a HyperREZ XP Carbohydrate H⁺ column was used with 5% sulfuric acid as mobile phase at 40°C and a flow rate of 1.2 ml min⁻¹. The lactate production rate is calculated based on the lactate concentration in the supernatant, the biomass concentration and the dilution rate with the formula

$$r_{C,lac} = c(lac) * D * X^{-1}$$

with: D, dilution rate = growth rate [d⁻¹]; c(lac), C-mol based lactate concentration in the supernatant [mmol C l⁻¹] and X, biomass concentration [g l⁻¹] in the steady states. The rate is given as mmol C g_{CDW}⁻¹ d⁻¹.

Calculation of carbon fixation rates and carbon partitioning

The carbon fixation rate was calculated as a mean of three independent measuring days. For that, the biomass production rate r_X [g l⁻¹ d⁻¹] was calculated with the formula

$$r_X = D * X$$

with: D, dilution rate = growth rate [d⁻¹] and X, biomass concentration during the steady states [g l⁻¹].

The biomass-based carbon fixation rate $r_{C,X}$ can be derived by multiplying the biomass production rate and the relative carbon content, rel_C [%], based on C/N measurements:

$$r_{C,X} = r_X * rel_C$$

The specific carbon fixation rate is calculated as the sum of the biomass-based carbon fixation rate and the lactate formation rate:

$$r_C = r_{C,X} + r_{C,lac}$$

All carbon-based rates are given in mmol C g_{CDW}⁻¹ d⁻¹.

Results

Effect of lactate formation as a carbon sink on cellular physiology of PCC6803 in batch cultivation

In a first step, a *Synechocystis* sp. PCC 6803 wild-type strain and a respective strain engineered for lactate production, *Synechocystis* sp. PCC 6803 SAA023 (hereafter referred to as WT and SAA023, respectively) [134, 135], were characterized in order to investigate if lactate synthesis as a carbon (C) sink has an effect on the cellular physiology of PCC6803, i.e., on growth characteristics, effective quantum yield, and total carbon fixation rate. Growth and lactate formation patterns of WT and SAA023 at standard growth conditions (50 $\mu\text{mol photons m}^{-2} \text{s}^{-1}$, 30°C, pH 8.0, baffled shaking flasks) are depicted in Fig. 3.1. Exponential growth was observed at the beginning of the cultivation (0 – 70 hours) when the cell density was low and nutrients were available in excess. In this time range, cells displayed high effective quantum yield at PSII (Y(PSII); 0.59 ± 0.01 , Fig. 3.1A). After 71 hours of cultivation, a transition into a linear growth phase occurred due to limited light and/or carbon dioxide availability. Effective quantum yields decreased continuously with ongoing cultivation. The WT cultures did not accumulate any lactate.

In comparison to the WT, SAA023 showed a prolonged exponential growth phase (until 120 instead of 70 h, Fig. 3.1B). However, the exponential growth rate, calculated from 0 – 71.3 h (WT) and from 23.5 to 95 h (SAA023) of cultivation, was with $0.045 \pm 0.001 \text{ h}^{-1}$ almost 30% lower than for the WT ($0.064 \pm 0.002 \text{ h}^{-1}$). SAA023 reached a significantly higher OD_{750} after 220 h of cultivation and exhibited a 12% higher quantum yield during exponential growth. The decrease in effective quantum yield during linear growth was comparable for the two strains. After one week (169 h), the titer reached ($2.6 \pm 0.3 \text{ mM}$) was 3- [135] and 6.8-fold [134] higher than reported for the same strain before. After 220 h cultivation, a maximum lactate titer of $3.8 \pm 0.4 \text{ mM}$ was reached in SAA023.

The carbon fixation rate decreased steadily for both WT and SAA023 strains, when the cultures reached the linear growth phase (Fig. 3.1C). From this point on, the SAA023 strain showed a higher C-fixation rate compared to the WT, which in the initial but not in later growth stages may be attributed to lower biomass concentrations and the resulting higher light availability per cell. The partitioning of fixed carbon incorporated into lactate, however, decreased already during exponential growth and then continued to decrease in parallel to the biomass formation rate. The highest specific lactate formation rate in the initial phase of

the cultivation ($12.0 \text{ mmol C g}_{\text{CDW}}^{-1} \text{ d}^{-1}$) was almost 10-fold higher than described before by Angermayr and Hellingwerf [135] for the late exponential growth phase, but still did not reach the *in vitro* specific rate of $38.1 \text{ mmol C g}_{\text{CDW}}^{-1} \text{ d}^{-1}$ reported by the same authors. The additional carbon withdrawal by lactate formation obviously led to an extended higher total carbon fixation rate in the linear growth phase.

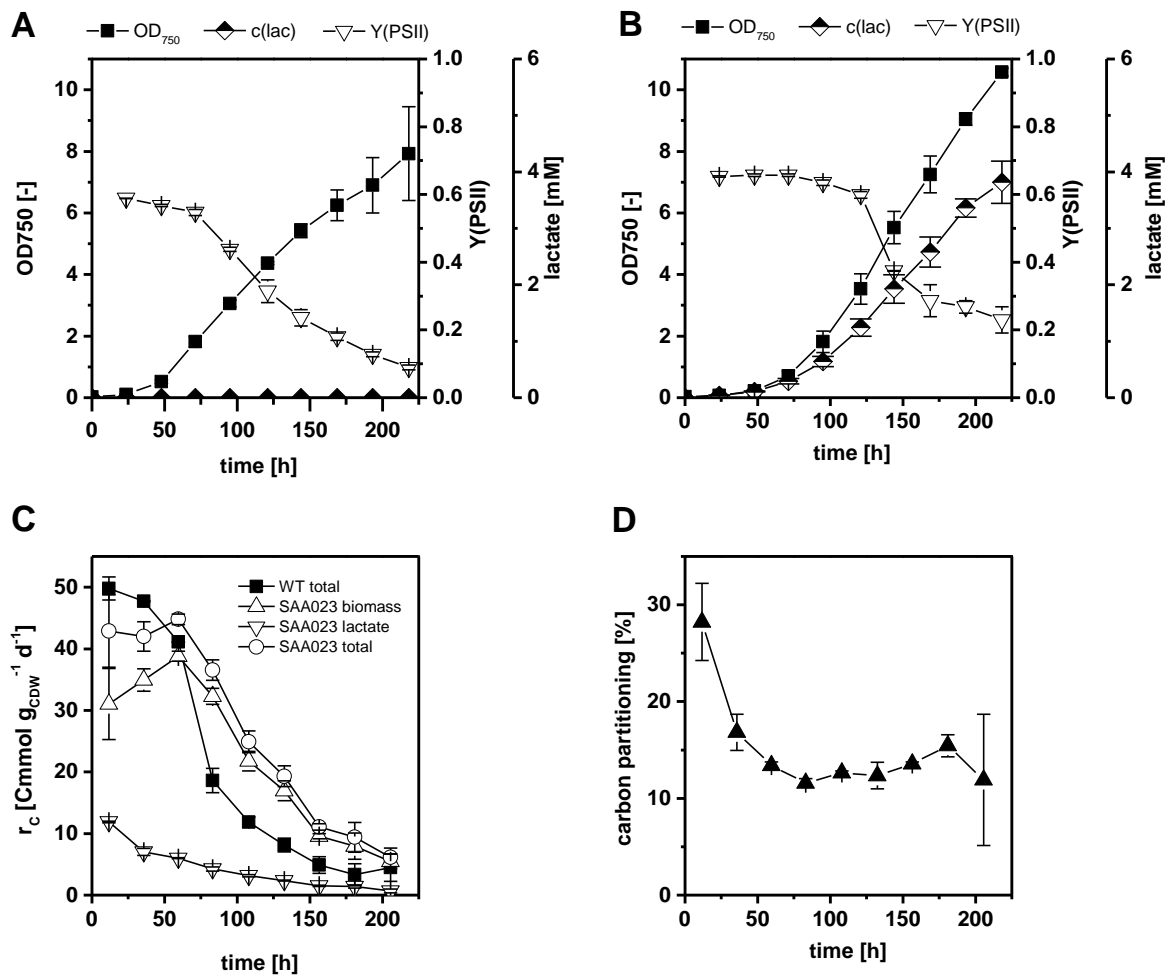


Figure 3.1: Growth and lactate formation characteristics of PCC6803 WT (A) and SAA023 (B, C, D) strains during batch cultivation. Panels A and B show the courses of cell density (OD₇₅₀), lactate concentration, and Y(PSII) (quantum yield at PSII). Panel C depicts the rates for total carbon fixation and its distribution into biomass and lactate production, whereas panel D gives the fraction of fixed carbon channeled into lactate in SAA023. Carbon partitioning is calculated based on the biomass and lactate formed between two sampling points. Cells were grown in YBG11 medium under standard growth conditions ($50 \mu\text{mol photons m}^{-2} \text{ s}^{-1}$, 30°C , pH 7.8) in baffled shaking flasks. Averages and standard deviations for duplicate experiments are given.

These variations in carbon fluxes are reflected in the carbon partitioning, i.e., the portion of total carbon used for lactate synthesis. A share of $13.0 \pm 1.4\%$ of the fixed carbon was channeled into lactate formation during the linear growth phase, which is more than twice

as much as reported before [134]. The carbon partitioning in the initial batch phase was even higher ($28.2 \pm 4.0\%$). In this stage, cells can be expected not to be limited by light and/or carbon. A growth phase dependent carbon partitioning was also observed by Angermayr and Hellingwerf (2013); in this case, it varied between 8 and 20% [135]. The increased carbon partitioning and the above mentioned increased lactate titer in comparison to earlier studies might be a consequence of the higher light intensity applied here (i.e., 50 instead of 30 - 40 $\mu\text{mol photons m}^{-2} \text{s}^{-1}$) and a better CO_2 mass transfer due to the use of baffled flasks [257, 258].

In summary, the physiological response of PCC6803 to lactate synthesis can be considered exemplary for a carbon sink effect: enhanced quantum yield, improved biomass formation, and increased total carbon fixation in the linear growth phase were observed. The reduced exponential growth rate of the lactate producer can be explained by a competition of biomass and lactate formation for the fixed carbon. The growth phase dependent carbon partitioning indicates that PCC6803 responds highly dynamic to a carbon sink (lactate synthesis) in dependence to the changing conditions during batch cultivation. The source-sink balance (light availability vs. metabolic sink capacity) of the cells seems to be the main factor influencing the cellular response. This was further investigated systematically and quantitatively under different steady state conditions as reported below.

Establishment of light or carbon limited steady metabolic states in continuous cultivation setups

In order to investigate the carbon sink effect of lactate synthesis in a systematic and quantitative way, we determined carbon fixation and lactate formation rates as well as light reaction efficiency and biomass formation of PCC6803 under steady state conditions under different light and carbon availabilities. For this purpose, cells were grown in bioreactors in turbidostat mode as described previously [256]. Three different metabolic states were established and tested: i. light limitation, i.e., low light and high carbon availability (LLHC, 1% CO_2 , 65 $\mu\text{mol photons m}^{-2} \text{s}^{-1}$), ii. carbon limitation, i.e., high light and low carbon availability (HLLC, ambient-like CO_2 ($\sim 0.05\%$), 250 $\mu\text{mol photons m}^{-2} \text{s}^{-1}$), and iii. unlimited in carbon and light supply, i.e., high light and high carbon availability (HLHC, 1% CO_2 , 250 $\mu\text{mol photons m}^{-2} \text{s}^{-1}$). Under carbon and light excess conditions (HLHC), the growth rate is expected to be maximal. The growth rate is determined either by the capacity of metabolic pathways, availability of nutrients besides CO_2 , or molecular processes [164]. A

behavior according or between two scenarios is plausible in such a case: 1. Carbon fixation is not the growth limiting module. Thus, the biomass formation rate should remain constant and lactate should be synthesized additionally. This would result in increased rates for carbon fixation and light reactions. 2. The carbon fixation rate is growth limiting. Here, the cells would not be able to fix more carbon in total and consequently, the synthesis of lactate would compete with biomass formation for metabolically available carbon and energy resulting in a reduced growth rate. Under LLHC conditions light- and thus energy limitation was established and cells are expected to acclimate for optimal photon uptake and efficient quantum usage. An additional C-sink consequently should result in reduced growth, as no additional energy (ATP) and/or electrons (NADPH) can be made available by the light reactions. HLLC conditions lead to carbon limitation, and the available carbon is expected to be distributed between biomass and lactate formation. The total carbon fixation rate should remain unaffected.

As expected, the highest growth rate of the WT was found under HLHC with 2.4 d^{-1} (Table 3.1). In comparison, light (LLHC) and carbon (HLLC) limitation resulted in a 66% and 53% reduced growth rate, respectively. The specific chlorophyll *a* ($\text{Chl}a$ [$\text{mg}_{\text{chl}a} \text{g}_{\text{CDW}}^{-1}$]) content was approximately doubled for cells under LL in comparison to HL conditions (Table 3.1), indicating that the cells maximized their light-harvesting capacity. Accordingly, the highest effective quantum yield $Y(\text{PSII})$ (0.56 ± 0.01) was measured under light limitation (Table 3.1). Under HLLC conditions, the cells are limited by the availability of metabolic sinks which also limited the photosynthetic capacity and strongly reduced $Y(\text{PSII})$ by 25% compared to the unlimited HLHC state.

All in all, the physiological parameters indicate that all applied growth conditions forced the cells into different metabolic states. The following sections describe the effects of carbon withdrawal mediated by a lactate dehydrogenase on the physiology of PCC6803 under the three selected growth conditions.

Table 3.1: Basic physiological parameters of the cyanobacterium *Synechocystis* sp. PCC 6803 WT and the lactate producer SAA023 in the investigated stable metabolic states.

	Light limitation (LLHC)		Excess supply (HLHC)		Carbon limitation (HLLC)	
	WT	SAA023	WT	SAA023	WT	SAA023
D = μ [d ⁻¹]	0.82	0.67	2.41	1.86	1.13	1.20
c(Chl <i>a</i>) [mg _{chl<i>a</i>} l ⁻¹]	1.79 ± 0.02	2.17 ± 0.16	1.13 ± 0.14	1.28 ± 0.10	1.13 ± 0.14	1.18 ± 0.02
Chl <i>a</i> _{CDW} [mg _{chl<i>a</i>} g _{CDW} ⁻¹]	19.9 ± 0.7	19.4 ± 3.0	11.0 ± 1.8	10.8 ± 1.4	8.0 ± 1.2	8.7 ± 0.5
Y(PSII) [-]	0.56 ± 0.01	0.58 ± 0.01	0.44 ± 0.02	0.53 ± 0.01	0.33 ± 0.05	0.41 ± 0.02
a* _{phy} [m ² g _{chl<i>a</i>} ⁻¹]	20.0 ± 0.3	17.7 ± 0.6	21.6 ± 2.1	20.0 ± 1.0	25.8 ± 1.4	24.6 ± 0.1
Q _{phar} [mmol quanta mg _{CDW} ⁻¹ d ⁻¹]	1.63 ± 0.07	1.34 ± 0.26	4.25 ± 1.13	3.55 ± 0.66	3.29 ± 0.76	3.38 ± 0.25
r _O [mmol O ₂ g _{CDW} ⁻¹ d ⁻¹]	40.4 ± 5.0	32.7 ± 15.2	74.3 ± 21.1	72.6 ± 20.2	57.9 ± 17.4	62.8 ± 14.9
r _{O,gross} [mmol O ₂ g _{CDW} ⁻¹ d ⁻¹]	53.1 ± 2.2	50.0 ± 9.1	91.5 ± 16.1	91.8 ± 15.3	65.6 ± 14.4	74.8 ± 11.1
r _F [mmol O ₂ g _{CDW} ⁻¹ d ⁻¹]	114.8 ± 5.0	97.5 ± 17.9	232.8 ± 53.6	234.9 ± 42.8	134.4 ± 28.2	172.4 ± 19.2
r _{resp} [mmol O ₂ g _{CDW} ⁻¹ d ⁻¹]	12.7 ± 2.8	17.2 ± 6.1	17.2 ± 5.0	19.1 ± 4.8	7.6 ± 3.0	12.0 ± 3.9
C:N [mol(C) mol(N) ⁻¹]	4.92 ± 0.03	5.44 ± 0.17	5.13 ± 0.08	5.42 ± 0.20	5.94 ± 0.50	5.50 ± 0.11

Mean values and standard deviations correspond to 3-12 samples (depending on the parameter, see Materials and Methods section) taken during at least 3 different days for the same metabolic state. Three conditions were investigated: Light limitation (1% CO₂, 65 μmol photons m⁻² s⁻¹; LLHC); excess condition (1% CO₂, 250 μmol photons m⁻² s⁻¹, HLHC), carbon limitation (ambient CO₂, 250 μmol photons m⁻² s⁻¹, HLLC); D, dilution rate equaling the specific growth rate μ in the respective steady state; X, biomass concentration; c(Chl*a*), volumetric chlorophyll *a* concentration; Chl*a*_{CDW}; biomass specific Chl*a* concentration; Y(PSII), effective quantum yield at PSII; a*_{phy}, Chl*a* normalized absorption coefficient of the cells; Q_{phar}, rate of quantum uptake; r_O, net O₂ evolution rate; r_{O,gross}, gross O₂ evolution rate; r_F, fluorescence-based electron flux at PSII expressed as O₂ evolution at PSII; r_{resp}, respiration rate; C:N, molar ratio of carbon and nitrogen in biomass.

The effect of lactate formation under light limitation

Under light limitation (LLHC), lactate formation induced growth impairment as expected, indicating that lactate and biomass formation compete for the available energy. The growth rate decreased by 18% in comparison to the WT (Table 3.1). The total carbon fixation rate (r_c) was not affected by the carbon sink and, in SAA023, was split up between biomass ($r_{c,x}$, Fig. 3.2, and Table 3.2) and lactate formation at a rate of $4.9 \pm 0.2 \text{ mmol C g}_{\text{CDW}}^{-1} \text{ d}^{-1}$. This corresponds to a carbon partitioning towards lactate of $15.7 \pm 0.4\%$ (Fig. 3.2 and Table 3.2), which is comparable to that found in the linear growth phase during batch cultivation (Fig. 3.1 and 3.2).

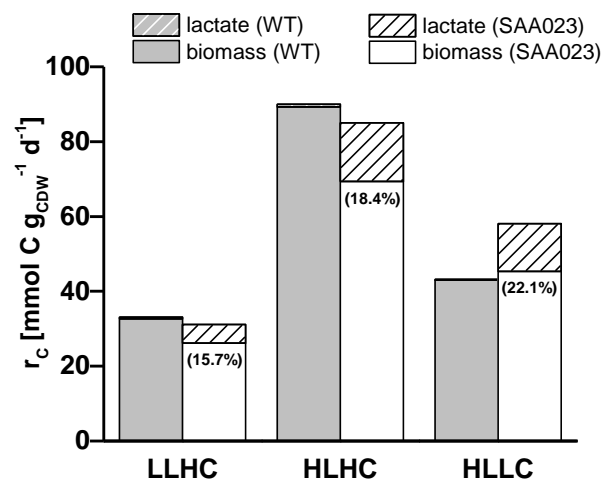


Figure 3.2: Carbon fixation rates in WT PCC6803 and lactate producing SAA023 strains under different growth conditions. For strain SAA023 the relative carbon partitioning into lactate formation is depicted by the values given in brackets. Cells were grown under excess condition (1% CO₂, 250 μmol photons m⁻² s⁻¹, HLHC), light limitation (1% CO₂, 65 μmol photons m⁻² s⁻¹; LLHC) and carbon limitation (ambient CO₂, 250 μmol photons m⁻² s⁻¹, HLLC).

To gain a deeper understanding on physiological changes in PCC6803 upon lactate formation, different photo-physiological parameters were investigated (Table 3.1). Thereby, $r_{\text{O}_2, \text{gross}}$ represents the measured net O₂ evolution rate corrected for the respective respiration rate, whereas r_F is calculated based on the fluorescence yield at PSII and Q_{phar} and represents the O₂ evolution at PSII not diminished by alternative electron fluxes (AEF) ($r_{\text{AEF}} = r_F - r_{\text{gross}}$). Such AEF do not contribute to NADPH regeneration but do contribute to the formation of the proton gradient over the thylakoid membrane and thus ATP regeneration. Under light limitation, SAA023 showed a 18% lower Q_{phar} than the WT, while both strains showed a similar $Y(\text{PSII})$ (Table 3.1). Whereas $r_{\text{O}_2, \text{gross}}$ was similar, r_F and thus r_{AEF} (given in mmol electrons g_{CDW}⁻¹ d⁻¹ in Fig. 3.3) were reduced by 15 and 23%, respectively, in SAA023 compared to the WT.

In summary, carbon fixation was limited by light availability, and lactate formation competed with biomass formation for the fixed carbon, resulting in reduced growth of the lactate producer SAA023. Also, photon uptake and PSII rates were slightly reduced in SAA023 compared to the WT cells. PCC6803 could not improve light harvesting and photosynthetic efficiency to enhance carbon fixation and to cover the carbon withdrawal for lactate formation.

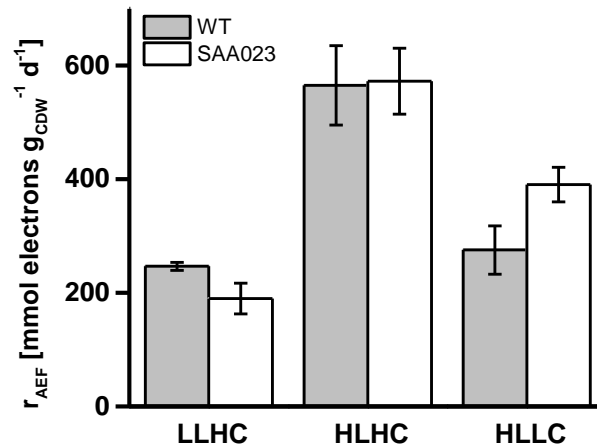


Figure 3.3: Alternative electron flux r_{AEF} in wildtype (WT, grey bars) and lactate producing (SAA023, white bars) PCC6803 strain under different growth conditions. Cells were grown in a continuous turbidostat mode under excess conditions (1% CO₂, 250 $\mu\text{mol photons m}^{-2} \text{s}^{-1}$, HLHC), light limitation (1% CO₂, 65 $\mu\text{mol photons m}^{-2} \text{s}^{-1}$; LLHC) and carbon limitation (ambient CO₂, 250 $\mu\text{mol photons m}^{-2} \text{s}^{-1}$, HLLC).

Table 3.2: Carbon fixation rates and carbon partitioning into lactate of PCC6803 WT and SAA023 when grown in the selected growth conditions.

	Light limitation (LLHC)		Excess supply (HLHC)		Carbon limitation (HLLC)	
	WT	SAA023	WT	SAA023	WT	SAA023
$r_{C,X}$ [mmol C g _{CDW} ⁻¹ d ⁻¹]	32.7 ± 3.1	26.2 ± 0.7	89.3 ± 4.8	69.4 ± 3.0	43.0 ± 5.1	45.3 ± 2.2
r_{LAC} [mmol C g _{CDW} ⁻¹ d ⁻¹]	0.4 ± 0.1	4.9 ± 0.2	0.7 ± 0.1	15.6 ± 0.2	0.2 ± 0.1	12.8 ± 0.4
r_C [mmol C g _{CDW} ⁻¹ d ⁻¹]	33.1 ± 3.1	31.1 ± 0.7	89.9 ± 4.8	85.0 ± 3.2	43.2 ± 5.2	58.2 ± 2.3
CP [%]	1.2 ± 0.2	15.7 ± 0.4	0.8 ± 0.1	18.4 ± 1.6	0.5 ± 0.1	22.1 ± 0.7

Three conditions were investigated: Light limitation (1% CO₂, 65 $\mu\text{mol photons m}^{-2} \text{s}^{-1}$; LLHC); excess condition (1% CO₂, 250 $\mu\text{mol photons m}^{-2} \text{s}^{-1}$, HLHC), carbon limitation (ambient CO₂, 250 $\mu\text{mol photons m}^{-2} \text{s}^{-1}$, HLLC); $r_{C,X}$, carbon flux towards biomass formation; $r_{C,LAC}$, carbon flux towards lactate formation; r_C , total carbon fixation rate; CP, carbon partitioning, percentage of total fixed carbon channeled into lactate.

The effect of lactate formation under excess conditions

As discussed before, a behavior according or between two scenarios can be expected upon lactate formation with excess light and carbon availability (HLHC): 1. Impaired biomass formation in case the carbon assimilation operates at its maximum or 2. Increased total carbon fixation enables a non-impaired growth rate and promotes additional lactate formation.

Our experiments show that biomass formation rates of SAA023 were decreased by 23% in comparison to the WT, while the total carbon fixation rates were similar (Fig. 3.2 and Table 3.2), following the sketched scenario 1. Similar to the LLHC condition, the quantum uptake rate Q_{phar} was 18% lower in SAA023 than in the WT. In contrast to LLHC, the effective quantum efficiency $Y(\text{PSII})$ was increased by 20% in SAA023 compared to the WT (Table 3.1). As the improved $Y(\text{PSII})$ compensated the reduced Q_{phar} , r_F , as well as $r_{\text{O},\text{gross}}$ and thus r_{AEF} , remained similar (Table 3.1, Fig. 3.3). The C:N ratio of the biomass increased, but not as drastically as under light limitation.

The results emphasize that, with excess carbon and light supply, carbon fixation was not increased upon the introduction of lactate formation as carbon sink. The assimilated carbon was consequently distributed between biomass formation and lactate synthesis with a partitioning into lactate of $18.4 \pm 1.6\%$ (Fig. 3.2 and Table 3.2). In conclusion, the missing positive effect of lactate formation on the total carbon fixation rate was similar to LLHC, whereas, in contrast to light limitation, an improved quantum efficiency but no change in LEF and AEF were observed.

The effect of lactate formation under carbon limitation

For lactate synthesis-related carbon withdrawal under carbon-limited growth conditions (HLLC), a competition between lactate formation and biomass formation for assimilated carbon was expected, which would lead to a reduced growth rate.

Interestingly, the growth rate of SAA023 was similar to that of the WT (Table 3.1), and the overall carbon fixation rate increased compared to the WT by almost 35% (Fig. 3.2 and Table 3.2). As much as $22.1 \pm 0.7\%$ of the fixed carbon was channeled into lactate formation without compromising growth. This represents the highest carbon partitioning into lactate among the three tested conditions. The cellular Chl a content was similar, whereas $Y(\text{PSII})$ increased by 24% (Fig. 3.2 and Table 3.2). Despite a slightly reduced Q_{phar} , this enhanced

Y(PSII) resulted in an increase in $r_{O_2, gross}$ and especially in r_F and r_{AEF} (Table 3.1 and Fig. 3.3), enabling increased carbon fixation.

Under carbon limitation, PCC6803 unexpectedly was able to enhance the carbon fixation rate to enable lactate synthesis without decreasing the growth rate. This was enabled by increased photosynthetic efficiency and light reaction rates. It remains open, how carbon assimilation was increased under carbon limitation.

Discussion

Lactate synthesis as a C-sink and its impact on cellular energy metabolism

The degree of reduction (DoR) of cyanobacterial biomass is estimated to be between 4.0 [134] and 4.16 [259], which is similar to that of lactate with a DoR of 4.0. Consequently, on a C-mol basis, the same amount of electrons has to be spent for lactate and biomass formation from CO₂. Lactate synthesis thus does not constitute an additional electron sink. Lactate synthesis, however, requires less ATP per fixed carbon compared to biomass formation, which involves ATP-intensive processes such as protein biosynthesis, DNA replication, cell division, and cellular maintenance. Compared to glyceraldehyde-3-phosphate formation, lactate synthesis from 3-phosphoglycerate even saves two ATP equivalents [142]. In this way, cellular ATP and NAD(P)H requirements change disproportionally in dependence of the carbon partitioning between biomass and lactate formation. Consequently, the presence of the heterologous lactate dehydrogenase can lead to/ enable a rebalancing of cellular ATP and NAD(P)H demands as a response to resource availabilities. The reduction of the overall ATP demand per fixed C upon lactate formation can be considered a cause for the observed reduction in energy generating AEF under light limitation, whereas LEF and carbon fixation rate remained unaffected (Table 3.1 and 3.2, Fig. 3.3). A similar reduction of AEF upon lactate synthesis was not observed under high light conditions. This can be attributed to the excess availability of light which induces AEF as protection system, especially the Mehler-like reactions via flavodiiron proteins [159]. Non-cyclic AEF through flv1/flv3 or flv2/flv4 or cyclic AEF around PSI contribute differently to proton gradient and thus ATP formation. Thus, similar AEF can lead to different ATP regeneration. Under excess light but limited carbon conditions, AEF even increased upon lactate formation. This may be a result of the higher carbon uptake rate at low carbon concentrations functioning as ATP sink [260]. A quantitative differentiation between non-

cyclic and cyclic AEF would give further insights into cellular measures to balance ATP and NAD(P)H regeneration.

Lactate formation rate and carbon partitioning are determined by the metabolic state

The capacity for lactate synthesis from pyruvate via the recombinant lactate dehydrogenase has been proposed to be the main limitation in the SAA023 strain [135]. This conclusion was based on the observed enhancement of the lactate formation rate via improved *ldh* gene expression achieved via codon and promoter optimization and multiple cassettes as well as by optimization of the fluxes towards the precursor pyruvate [134, 135]. However, lactate formation rate and carbon partitioning were reported to vary over the course of batch cultivation. This is similar to the observations in the present study and indicates the importance of the metabolic state of the cell and the respective intracellular NAD(P)H, ATP, and precursor availabilities for lactate synthesis [135]. The carbon partitioning varied between 8 and 20%, which is comparable to the carbon partitioning between 12 and 28% observed here during batch cultivation (Fig. 1D).

Similar changes in carbon partitioning were observed for other carbon sinks. The carbon partitioning towards 2,3-butandiol formation during the first days of batch cultivation varied by a factor of up to 4 [171]. An ethylene producer showed a dependency of the carbon partitioning on the cell density and consequently the light availability [75]. This indicates that product formation depends on both light and carbon availability and the respective metabolic state, which the cells adjust. This was confirmed by our experiments under controlled steady state conditions, with carbon partitioning towards lactate of 15.7% (LLHC), 18.4% (HLHC), and 22.1% (HLLC). The specific lactate formation rates varied even more depending on the conditions applied and were 3.9- (LLHC), 10.2- (HLLC), and 12.4-fold (HLHC) higher than the $1.26 \text{ mmol C g}_{\text{CDW}}^{-1} \text{ d}^{-1}$ reported by Angermayr and Hellingwerf (Fig. 3.2 and Table 3.2), but still lower than the *in vitro* lactate formation rate ($38.1 \text{ mmol C g}_{\text{CDW}}^{-1} \text{ d}^{-1}$) determined with cell extracts [135]. The interdependency of the differing overall NAD(P)H/ATP demand for biomass and lactate formation on the one hand and the different metabolic states, on the other hand, represent possible reasons for these variations. The cells might adjust the distribution of energy and electrons between biomass and lactate formation in a way to achieve an optimal sink-source balance. In conclusion, the lactate production rate and the carbon partitioning depend on environmental conditions.

High light and low carbon conditions, as found during a sunny day, appear to be optimal for carbon partitioning towards lactate.

Lactate synthesis-mediated ATP/NAD(P)H balancing may promote photosynthesis

The so-called carbon sink effect comprises the physiological responses to a heterologous carbon sink, i.e., enhanced O₂ evolution, quantum yield, and, in some cases, carbon fixation. Until recently, only a few studies investigated the physiological response of a cyanobacterial cell to an additional carbon and/or electron sink. The investigation of the effect of sucrose synthesis on the photophysiology of *Synechococcus elongatus* PCC 7942 represents an example [168] showing that induction of a sucrose production pathway can relieve the sink limitation of photosynthesis, as indicated by enhanced O₂ evolution and relative PSII rates as well as improved effective quantum yields. Our recent study on the physiological response of *Synechocystis* sp. PCC 6803 to differing electron demands caused by supplying N-sources differing in reduction degree [256] demonstrated, beside a dependency on environmental conditions, that an N-source related electron sink resulted in enhanced PSII rates and LEF, even when light was limiting.

The carbon sink effect is typically explained by the potential of a carbon sink to unleash a general sink limitation of the photosynthetic light reaction [164, 165] due to limited electron acceptor availability or limited capacities to further process reduced acceptors such as carbon fixation products [168, 171]. The provision of additional electron or metabolic sinks may consequently unleash the unused light reaction potential and even increase carbon fixation rates. Furthermore, carbon and/or electron sinks are discussed to promote the balancing of ATP/NAD(P)H regeneration and demand [144, 170, 256]. For the adjustment of appropriate ATP and NAD(P)H supplies, the ratios of LEF to AEF play a crucial role. Photosynthetic electron fluxes do not a priori provide ATP and NAD(P)H in the optimal ratio required for Calvin-Benson cycle activity [167]. Accordingly, carbon and/or electron sinks are proposed to adjust the cellular ATP/NAD(P)H demand to the NAD(P)H side and thereby enhance photosynthesis and carbon fixation rates [170, 256]. Examples include enhanced carbon fixation as a response to isopropanol synthesis [170] and to enhanced electron withdrawal with nitrate instead of ammonium as N-source [256]. Interestingly, the AEF and PSII rates of all tested conditions/strains of the latter and the present study showed linear interdependencies with similar slopes (0.70 and 0.68 $r_{\text{AEF}} r_{\text{PSII}}^{-1}$, respectively, Fig. 3.4B), indicating an underlying interdependency of the AEF and the PSII rate. This interdependency

may constrain the electron flux distribution along these pathways and thus the balancing of NAD(P)H and ATP supply. Such constrained balancing obviously depends on the environmental conditions in terms of source-sink availability and may be restricted by factors such as light limitation (source limitation), the maximum inherent carbon fixation capacity, carbon availability (sink limitation), or other regulatory circuits including, e.g., responses to light stress.

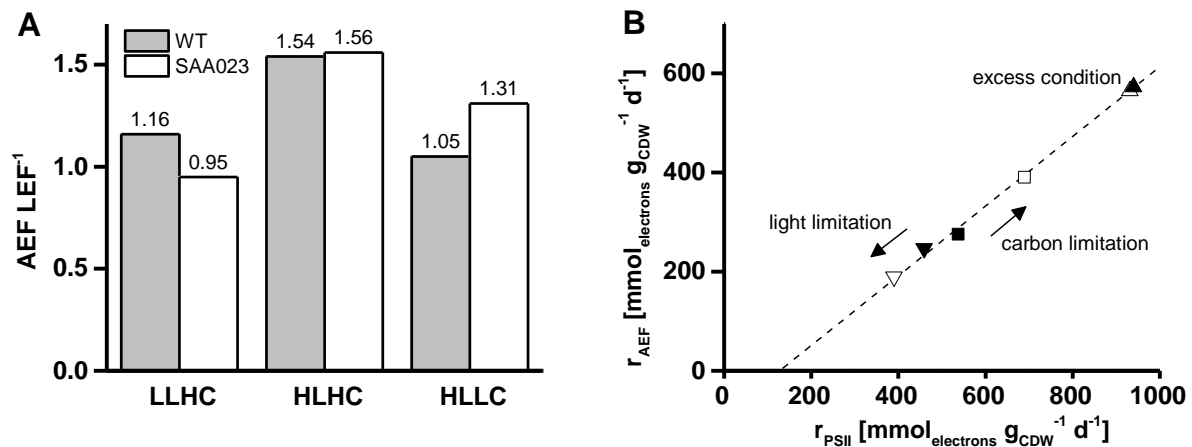


Figure 3.4: Changes in photosynthetic electron fluxes in the different metabolic states with (closed symbols) and without (open symbols) lactate formation. Panels A and B show the ratio of non-circular alternative over linear electron fluxes (AEF/LEF) in the different states and the AEF in dependency of the PSII rate, respectively.

Under carbon limitation, we observed a prominent carbon sink effect, comprising increased PSII, O₂ evolution, and carbon fixation rates. Remarkably, these effects came along with a 34% increase of AEF (Fig. 3.3) and a 24% higher ratio of AEF over LEF (Fig. 3.4A). This supports the hypothesis that a beneficially balanced ATP/NAD(P)H ratio enables the cells to exploit the excess light availability to increase the PSII rate and to finally enhance carbon fixation rates (Fig. 3.4B). Elevated ATP generation, as indicated by the increase of AEF, might enable a boost of the ATP dependent CCM, which was shown to be upregulated under excess light and limited carbon conditions [260, 261]. The resulting increased total carbon fixation rate enabled lactate synthesis with the highest carbon partitioning among all tested conditions (Tables 3.1 and 3.2, Fig. 3.3) while the growth rate was similar as that of the WT. Thus, the high energy demand for biomass formation (which did not substantially increase) may limit carbon fixation in the absence of a heterologous carbon/electron sink. Interestingly, similar physiological effects were observed in a previous study with PCC6803 as a response to differing electron sink availability [256]. Higher electron demand resulted in

growth stimulation, but only under excess light and CO₂ availability and not, as here, under carbon limitation.

In contrast, lactate synthesis as a C-sink did not result in increased carbon fixation under light and carbon excess conditions. This was unexpected as, under excess conditions, the cells should have the highest degree of freedom to adjust to the additional (carbon) sink. Following the argumentation line that a beneficially balanced ATP/NAD(P)H ratio promotes enhanced carbon fixation and an electron flux rearrangement should be consistent with the linear interdependency of PSII rate and AEF, an increase in carbon fixation rate upon lactate formation may have been prevented as carbon fixation had reached a maximum rate with an already optimal ATP/NAD(P)H balancing. Based on the higher biomass formation rate of the WT compared to SAA023 under this condition, it can be concluded that growth was not limited by metabolic constraints of biomass formation [164], but a limitation by the mere carbon fixation capacity may be a possible explanation. In our earlier study, we observed similar maximum carbon fixation rates for a different PCC6803 wild-type strain under light and CO₂ excess conditions [256]. Zavrel et al. demonstrated that the growth rate of a PCC6803 wild-type strain could not be increased by providing more light than approx. 220 $\mu\text{mol photons m}^{-2} \text{ s}^{-1}$ and more than 1.7% CO₂ (at 32°C and 220 $\mu\text{mol photons m}^{-2} \text{ s}^{-1}$) [154]. Consequently, the maximal carbon fixation rates observed in this study may constitute a maximum for wild-type PCC6803.

Under light limitation, it could be expected that the PSII rate remains similar and that lactate formation, possibly involving decreased biomass formation, leads to an increased LEF and carbon fixation due to the reduced energy demand for lactate compared to biomass formation. Instead, LEF and carbon fixation rate were similar, whereas PSII rate and AEF decreased (Tables 3.1 and 3.2, Fig. 3.4). Whereas this supports the above-mentioned assumption that lactate synthesis required less ATP in comparison to biomass formation, such reduced energetic costs though did not enable the cells to optimize the ATP/NAD(P)H balancing and thereby the carbon fixation rate. In contrast to this observation, an increase in carbon fixation-independent electron sink availability was shown to enhance the light reaction [256]. This is obviously not the case for a carbon-based product with a DoR similar to biomass. Interestingly, the linear interdependence of PSII rate and AEF remained fulfilled (Fig. 3.4B), which would not have been the case for an unaffected PSII rate involving a

reduced AEF and an increased LEF. The exact nature of and reasons for the apparent linear interdependency of PSII rate and AEF remain to be investigated.

In conclusion, the obtained results indicate that, in a certain range of environmental conditions, lactate synthesis-mediated ATP/NAD(P)H balancing can promote photosynthetic electron transfer and carbon fixation rates, supporting the hypothesis of a metabolically favorable ATP/NAD(P)H balancing as underlying mechanism causing all the effects referred to as the carbon sink effect. In other words, the carbon sink effect is the physiological response of a phototrophic cell to alternative carbon and/or electron sinks with the potential to beneficially shift the cellular ATP/NAD(P)H demand. It would be interesting to investigate other heterologous pathways differing in ATP and NAD(P)H demands in order to more closely define the mechanism and operational space of such ATP/NAD(P)H balancing, as it has been done *in silico* for ethanol, propane, and ethylene formation [144].

Conclusions

The results of this study confirm that an additional carbon sink can stimulate quantum efficiency at PSII, photosynthetic water oxidation, and carbon fixation within PCC6803. These effects were found to heavily depend on the environmental/growth conditions. Three different cellular responses to lactate as a carbon sink could be observed: i: impaired growth under light limitation due to competition for the fixed carbon among lactate and biomass formation; ii: impaired growth under excess supply of carbon dioxide and light due to the same competition indicating a limitation by the maximum carbon fixation capacity, and iii: stimulated growth under carbon limitation and simultaneous lactate formation with the highest carbon partitioning observed under all conditions tested. This was enabled by enhanced carbon fixation and PSII activity. The observed rearrangement of photosynthetic electron fluxes (LEF/AEF) appears to be an important cellular regulating screw to balance ATP and NAD(P)H regeneration. Thereby, the lower ATP demand for lactate than for biomass formation most likely played a crucial role and finally led to the observed carbon sink effect. The condition-dependent physiological responses demonstrate that the metabolic capabilities of cyanobacteria depend on the cellular sink/source regime and the respective cellular steady state. Furthermore, this study emphasizes the importance of a systematic and quantitative characterization of phototrophic cells and their responses to (genetic) perturbations in order to enable an efficient design of phototrophic biocatalysts and respective bioprocesses.

Acknowledgements

We thank Prof. Klaas Hellingwerf, Prof. Branco dos Santos and Davide Montesarchio for providing the strains *Synechocystis* sp. PCC 6803 WT (Stanford) and *Synechocystis* sp. PCC 6803 SAA023. We thank Kristin Lindstaedt for support with the lactate quantification assays. We thank Prof. Stan Harpole and Petra Hoffmann from the Department for Physiological Diversity at UFZ and the German Centre for Integrative Biodiversity Research (iDiv) in Leipzig for analyzing the C/N samples.

Chapter 4: Accessing the efficiency of the hydroxylation of cyclohexane to cyclohexanol in a continuous photo-biotransformation

Marcel Grund, Marco Schmidt, Jörg Toepel, Andreas Schmid, Rohan Karande, Bruno Bühler

Marcel Grund developed the process setup, performed all biotransformations in reactor scale, and wrote the manuscript. Marco Schmidt performed the whole-cell activity assays under supervision of Jörg Toepel and Marcel Grund. Andreas Schmid, Rohan Karande and Bruno Bühler coordinated the project and corrected the manuscript.

Abstract

Photo-biotechnology aims at the rational exploitation of the capability of phototrophic cells to harness electrons from water splitting and to fix carbon from carbon dioxide for the production of chemicals and energy carriers. Approaches and rationales to achieve relevant reaction rates and carbon partitioning have been established for product synthesis from CO₂. The direct coupling of electron demanding reactions to the photosynthetic electron chain, on the other hand, gained attention only recently. Further understanding of the physiological responses to biocatalytic electron withdrawal and the quantitative capabilities to cope with that additional electron demand will be essential to make progress. Here, we demonstrate that the specific whole cell-activity for cyclohexane hydroxylation catalyzed by a cytochrome P450 monooxygenase (CYP450) in a recombinant *Synechocystis* sp. PCC 6803 ranges from 0.1 to 79 U g_{CDW}⁻¹ depending on the growth and reaction conditions applied. To further characterize cellular responses to oxygenase catalysis and environmental conditions, especially the photosynthetic electron fluxes, we developed a strategy to conduct the biotransformation in a continuous bioreactor system at a 0.5 L scale. The specific biocatalytic oxygenation rate depended directly on the incident light intensity (up to 80 μmol photons m⁻² s⁻¹). The oxygenation rate could be kept constant for several hours under optimized cultivation and reaction conditions. Photon/electron balancing revealed that the cells were capable to increase the PSII rate by 20% and the linear electron flux by a factor of 1.9 to meet the additional CYP450-related electron demand of 18 μmol electrons g_{CDW}⁻¹ d⁻¹. The oxygenation reaction consumed approx. 17% of the linear electron flux, which, however, corresponded to only 2.2% of the absorbed quanta. These results highlight the high potential of *Synechocystis* sp. PCC 6803 to utilize water and light as electron- and energy sources, respectively, to efficiently drive electron-dependent biotransformations.

Introduction

Cyanobacteria can be engineered as cell factories with high shares of the fixed carbon channeled into the product of interest [173, 243, 262]. Examples include the synthesis of sucrose [72], lactate [74, 134], ethanol [65, 249], 1,2-butanediol [70], isoprene [79] and ethylene [75]. Examples for the direct use of photosynthesis-derived electrons for oxidoreductase-catalyzed biotransformations, on the other hand, are scarce, even though the potential is well recognized [82, 263]. Substantial activities have been reported for cyclohexane hydroxylation by means of a cytochrome P450 monooxygenase (CYP450) [85] and enantioselective C=C bond reduction in cyclic α -keto alkenes via an enoate reductase [86].

The few studies on light-driven redox biocatalysis published so far focused on the proof of concept and the optimization of reaction rates and final titers by metabolic and reaction engineering. Important aspects such as the general physiological response to biotransformation mediated electron withdrawal were not yet addressed. However, it is important to understand to what extent photosynthetically derived electrons can be channeled into the reaction of choice, and furthermore, which factors might determine this. Nielsen et al. [264] calculated the share of photosynthesis-derived electrons exploited for the formation of diverse products directly from CO₂, showing that the synthesis of 2,3-butanediol by metabolically engineered *Synechococcus* sp. PCC 7942 exploited, due to the high carbon partitioning, up to 87.2% of photosynthetically derived electrons [70, 264]. This estimate is based on the calculated minimum number of electrons required to form both, biomass and the product. In earlier studies, we demonstrated that *Synechocystis* sp. PCC 6803 can increase under certain conditions photosynthesis rates to cover the demand of additional electron and carbon sinks, i.e. mediated by varying reduction grade of the N-source and a lactate synthesis pathway, respectively [256, 265].

Characterization of the *in vivo* physiological responses to a biotransformation has not yet been demonstrated. Berepiki and co-authors showed that expression of the mammalian cytochrome P450 CYP1A1 in *Synechococcus* PCC 7002 resulted in increased maximum electron transport rates and enhanced effective quantum efficiency at PSII [169]. A further in depth analysis would allow gaining insights into the impact of product formation on cellular physiology. For that, the measurement of fundamental *in vivo* rates, such as the photon uptake, LEF, and PSII rates is essential. Those rates and growth parameters such as effective

quantum yield at PSII and biomass formation rates were not yet measured and combined during a phototrophic whole-cell catalysis, mainly simply due to the lack of suitable reaction and reactor formats. Biotransformations at the proof of concept stage are typically conducted in small scale, i.e., reaction tubes or shaking flask scale, which limits cell material for an in-depth and comprehensive physiological investigation. Additionally, a stable reaction at significant rates for a sufficient period of time is required to enable the characterization of the cellular response to the additional electron sink. As demonstrated before, stable metabolic states are essential to reveal physiological responses to additional sinks [256, 265].

In this study, we aim at a systematic and quantitative investigation of the physiological responses of a biocatalytically active *Synechocystis* sp. PCC 6803 to an electron demanding biotransformation. The conversion of cyclohexane to cyclohexanol mediated by an engineered *Synechocystis* sp. PCC 6803 harboring a cytochrome P450 monooxygenase, originating from *Acidovorax* sp. CHX100, (hereafter PCC6803_CYP) was selected as a model reaction system [85]. A continuous bioreactor setup and process conditions were established which allowed running the reaction at a high and stable rate. An in-depth physiological investigation of the electron sink effects was carried out with the aim to answer the following questions: how does the cell respond to the biocatalytic electron withdrawal and how does it cover the additional biotransformation-related electron demand? To answer those questions, we adapted a photon and electron balancing approach in order to assess the physiological response of PCC6803_CYP to the reaction-related electron withdrawal and consequently assess the reaction efficiency on an electron/photon level. This approach has been applied before to elucidate physiological responses to environmental changes/conditions and additional sinks in algae and cyanobacteria in a quantitative and systematic manner [217, 218, 256, 265]. The results confirmed on the one hand the light dependency of the P450 mediated hydroxylation of cyclohexane in a continuous cultivation setup and that photosynthesis is highly flexible in terms of covering additional electron demands, but demonstrates on the other hand that the cellular capability to provide electrons for a biocatalytic reaction is highly dependent on the carbon and light availabilities to which the cell is adapted to.

Materials and Methods

Bacterial strain

A recombinant *Synechocystis* sp. PCC 6803 strain harboring the plasmid pAH050 encoding a cytochrome P450 monooxygenase from *Acidovorax* sp. CHX100 (hereafter referred to as PCC6803_CYP) was used in all experiments [85]. The strain was maintained as cryo-culture at -80°C. An aliquot was resuspended in 20 ml YBG11 [150] at pH 8 in a 100 ml baffled shaking flask and grown as preculture for 4-5 days. The preculture was used as inoculum for the bioreactor experiments.

Whole-cell activity assay

Assayed cells were derived from continuous cultivations in a flat panel photo-bioreactor under four different conditions at 30°C, 20 ml min⁻¹ aeration, and different sink (CO₂) and source (light) availabilities: 88 μmol photons m⁻² s⁻¹ and ambient CO₂ (medium light – low carbon, MLLC_{cultivation}), 88 μmol photons m⁻² s⁻¹ and 2.5% CO₂ (medium light – high carbon, MLHC_{cultivation}), 151 μmol photons m⁻² s⁻¹ and ambient CO₂ (high light – low carbon, HLLC_{cultivation}), and 151 μmol photons m⁻² s⁻¹ and 2.5% CO₂ (high light – high carbon, HLHC_{cultivation}). A dimmable LED panel was used as light source for cultivation as well as activity assays (Celldog GmbH, Berlin, Germany). Four different conditions also were applied for the activity assays, in order to test the differently adapted cells under different sink and source availabilities during the reaction: 63 μmol photons m⁻² s⁻¹ and ambient CO₂ (low light – low carbon, LLLC_{assay}), 63 μmol photons m⁻² s⁻¹ and 50 mM NaHCO₃ (low light – high carbon, LLHC_{assay}), 250 μmol photons m⁻² s⁻¹ and ambient CO₂ (high light – low carbon, HLLC_{assay}), and 250 μmol photons m⁻² s⁻¹ and 50 mM NaHCO₃ (high light – high carbon, HLHC_{assay}).

Fully adapted cells from steady states were sampled, centrifuged at 7000 g and 20°C for 7 min (Heraeus Fresco 17, Thermo Scientific, Waltham, USA), resuspended in YBG11 optionally supplemented with 50 mM NaHCO₃ to an OD₇₅₀ between 4.0 and 4.5, and transferred into Pyrex tubes. Then, whole-cell activity assays were conducted as described before [85]. In short, the cells were adapted to the respective assay condition for 10 mins at 30°C (Multitron, INFORS AG, Bottmingen, Switzerland). Reactions were started by addition of 1.25 μl cyclohexane and stopped after 10 min by adding 1 ml ice-cold diethylether containing 0.2 mM n-decane as internal standard and immediate vortexing for 1 min followed by phase separation at 3214g and 4°C for 2 min (5810R centrifuge, rotor

FA-45-6-30, Eppendorf AG, Hamburg, Germany). The upper organic phase was transferred into an Eppendorf cup, dried over sodium sulfate and subjected to GC analysis.

Bioreactor setup and conditions for cultivation and biotransformation

Experiments were carried out in 525 ml flat panel bioreactors (PSI Photon Systems Instruments, Drasov, Czech Republic). Temperature was kept constant at $30.0 \pm 0.5^\circ\text{C}$ and the culture was mixed via a magnetic stirrer. The reactor was aerated with a gas mixture as specified in the main text. A gas mixer (PCU-10, Vögtlin Instruments AG – flow technology, Aesch, Switzerland) was used to adjust aeration rate and gas mixture (pressurized air, synthetic air, or nitrogen). The gas mixture was humidified in a bubbling bottle and channeled into a separate medium loop in which a segmented flow was generated, i.e., a sequence of gaseous and liquid (medium) segments. This enabled efficient mass transfer for cyclohexane supply via the gas phase and for the removal of photosynthetically produced O_2 from the medium. Off-gas and medium outflow were guided through a tube on top of the reactor. The headspace was kept minimal. Fresh medium supply and medium loop were operated using a peristaltic tube pump (IPC-series, ISMATEC, Cole-Parmer GmbH, Wertheim, Germany). Fluorescent lamps were used to provide light of which the intensity was adjusted via the distance between light source and reactor.

Quantification of cyclohexanol and calculation of biocatalytic activity

Cyclohexanol concentrations were measured as described before [85, 266, 267]. Briefly, cultivation broth was sampled from the reactor vessel. The reaction was stopped by addition of pre-cooled diethylether supplemented with 0.2 mM n-decane as internal standard. After 1 min of extraction via vortexing, the ether phase was separated via centrifugation, dried over sodium sulphate, and transferred to a GC vial followed by GC analysis as described [85].

Quantification of cell dry weight (CDW) and chlorophyll a concentrations

Biomass concentrations were derived from OD_{750} measurements based on CDW- OD_{750} correlations determined for the conditions applied. For this purpose and chlorophyll *a* determination, samples were treated as described before [256].

Measurement of quantum efficiency

Quantum efficiency was measured as described [256] with the following modification: To ensure that the cyclohexane in the medium remained in the medium during measurement of the quantum yield, septum-sealed cuvettes were used for fluorescence measurements.

Samples from the bioreactor were taken by syringe and transferred through the septum into the cuvette.

Determination of the O₂ evolution rate

O₂ evolution rates were determined by measuring the difference in volumetric fractions of O₂ in the in- and off-gas of the reactor via O₂ sensors (BCP-O2, BlueSens gas sensor GmbH, Herten, Germany). During cyclohexane hydroxylation, the O₂ evolution rate was corrected for the oxygenation-related stoichiometric O₂ demand.

Results

The influence of growth conditions on the specific whole-cell activity in an assay format

As a starting point, we evaluated if and to what extent the specific cyclohexane hydroxylation activity of the recombinant CYP450 containing *Synechocystis* strain PCC6803_CYP is influenced by the metabolic state of the cells, i.e., if the growth conditions have an impact on the whole-cell activity assayed under identical conditions optimized for maximum initial biocatalyst activities involving substrate excess. To this end, PCC 6803_CYP was cultivated in continuous mode with varying light (i.e., medium or high light [ML or HL] corresponding to 88 or 151 $\mu\text{mol photons m}^{-2} \text{s}^{-1}$, respectively) and carbon availabilities (i.e., low or high carbon [LC or HC] corresponding to 0.04 or 2.5% CO₂, respectively). Cells were sampled from respective steady states and prepared for whole-cell activity assays as described in the materials and methods section. For cells derived from each steady state, assay conditions were varied in the same as it was done for the cultivation. Low and high light conditions (LL and HL, 63 and 250 $\mu\text{mol photons m}^{-2} \text{s}^{-1}$) were set based on the demonstrated light dependency of the reaction up to 150 $\mu\text{mol photons m}^{-2} \text{s}^{-1}$ in the assay format [85].

Figure 4.1 demonstrates that initial specific cyclohexane hydroxylation activities (10 min reaction time) varied strongly with the conditions at which cells were cultivated, whereas the assay conditions had less influence. The highest activities were measured for cells cultivated at HC conditions. Maximal activities amounted to $77.1 \pm 4.4 \text{ U g}_{\text{CDW}}^{-1}$ for MLHC_{cultivation} and $79.0 \pm 3.8 \text{ U g}_{\text{CDW}}^{-1}$ for HLHC_{cultivation} adapted cells - with excess light and carbon availability in the assay (Figure 4.1, panels B and D). The by far lowest activities were measured for cells grown under HLLC condition (Figure 4.1C).

In general, two conclusions can be drawn from these results: 1. Cells adapted to 2.5% CO₂ (HC_{cultivation}) show higher activities compared to cells grown under low carbon availability, irrespective of the carbon and light availabilities during the activity assay. This might be caused by the generally higher electron fluxes in those cells to sustain high carbon fixation and biomass formation rates (0.43 d⁻¹ vs. 0.25 d⁻¹ under ML and 0.61 d⁻¹ vs 0.17 d⁻¹ under HL). 2. cells adapted to low CO₂ and thereby low metabolic sink availability show decreasing activity with increasing light intensity, possibly due to light inhibition, downregulation of light harvesting and photosynthesis in general, ROS generation, and phototoxicity.

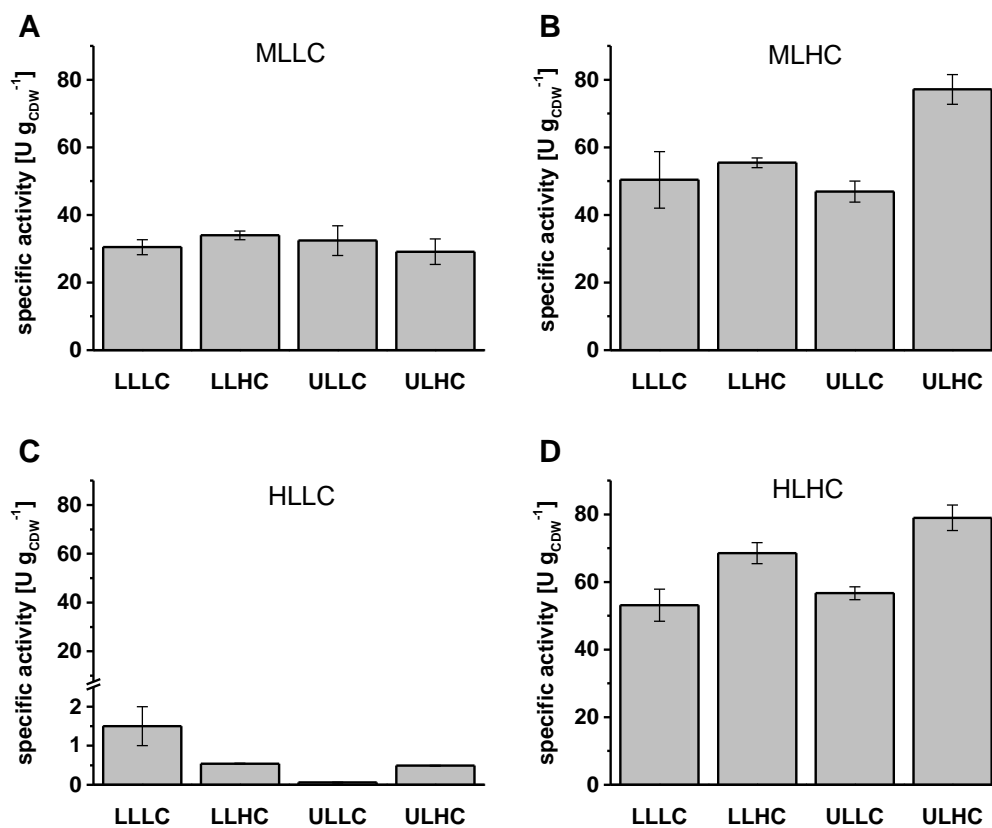


Figure 4.1: Whole-cell activity dependent on the growth condition of PCC6803_CYP. Assays were conducted with cells adapted to 88 μmol photons m⁻² s⁻¹ and 0.04% CO₂ (MLLC_{cultivation}, A) or 2.5% CO₂, (MLHC_{cultivation}, B), and 151 μmol photons m⁻² s⁻¹ and 0.04% CO₂ (HLLC_{cultivation}, C) or 2.5% CO₂ (HLHC_{cultivation}, D). Assay conditions are LL: 88 μmol photons m⁻² s⁻¹; UL 250 μmol photons m⁻² s⁻¹; LC: YBG11 w/o supplementation of NaHCO₃; HC: YBG11 w/ supplementation of 50 mM NaHCO₃.

The adaption status of the cells regarding light and carbon availability strongly influences the whole-cell activity. Furthermore, the whole-cell activity also depends on light and carbon availability during the assay, at least the cells adapted to HC show higher activities under HC compared to LC assay conditions (Fig. 4.1). Interestingly, lower carbon (sink) availability in the assay in comparison to the cultivation condition did not result in increased whole-cell activities in any assay condition. This could have been expected as the electrons required for

the carbon fixation might instead have been used for the hydroxylation reaction. The impact of the combination of cultivation and assay condition in terms of carbon and light availability underlines the importance of a systematic approach to assess the physiological responses of PCC6803_CYP to the biotransformation under well-defined conditions and stable metabolic states.

Cyclohexane hydroxylation during continuous cultivation

The targeted physiological characterization requires i) a metabolically significant, but not necessarily maximal redox biocatalysis-related electron consumption rate and ii) a stable performance of a non-toxified biocatalyst growing under defined conditions. Maximal cyclohexane hydroxylation rates in whole-cell activity assays correspond to an electron consumption rate of up to $9.5 \text{ mmol g}^{-1} \text{ h}^{-1}$ being well significant considering the $6\text{-}28 \text{ mmol g}^{-1} \text{ h}^{-1}$ reported for the linear electron flux (LEF) in a wildtype of PCC6803 under different conditions [256]. The light dependency of the reaction rate [85] further emphasizes that cyclohexane hydroxylation as a C-fixation independent electron sink fulfills requirement i). For whole-cell activity assays aiming at the determination of initial reaction rates, a stable and high cyclohexane concentration was maintained during the 10 min reaction time by adding cyclohexane to an amount exceeding its solubility limit ($650 \text{ }\mu\text{M}$) and rapid mixing – conditions which are toxic for PCC6803 [85] and thus expected to cause instability on the long term. To meet requirement (ii), PCC6803_Cyp was cultivated in continuous mode in a bioreactor setup at 0.5 L scale, aiming at defined, non-toxic, and constant conditions.

To mitigate its toxic effects, cyclohexane was supplied via the gas phase in a segmented flow medium loop (see materials and methods), which limited cyclohexane mass transfer and thus toxicity. A coinciding reduction in whole-cell activity thereby was considered acceptable. The suitability of such a cultivation/ reaction setup and the light dependency of the reaction were evaluated in a first approach. Briefly, PCC6803_CYP was grown in batch mode to an OD_{750} of 0.45. At this point, a feed was started for a continuous mode of cultivation at this comparatively low cell concentration minimizing shading effects. A dilution rate (D) of 0.013 h^{-1} enabled steady state cultivation at this cell density (densitostat). Cells were induced 1 day before starting the biotransformation by substrate addition via the gas phase. Light and feed were switched off shortly before substrate addition (time point 0 h in Fig. 4.2A), for a control condition without energy source resulting in a low specific cyclohexane hydroxylation rate of $3.1 \pm 0.1 \text{ U g}_{\text{CDW}}^{-1}$. This rate corresponded to half the

background activity measured in an assay system before ($6.2 \pm 0.6 \text{ U g}_{\text{CDW}}^{-1}$, [85]). Such basal activity in the dark presumably was enabled by cofactor regeneration via the catabolism of storage compounds [85]. After 1.17 h, feed ($D = 0.013 \text{ h}^{-1}$) and light ($40 \mu\text{mol photons m}^{-2} \text{ s}^{-1}$) were switched on, and the light intensity was increased in regular time intervals to 80 and $150 \mu\text{mol photons m}^{-2} \text{ s}^{-1}$ (Fig. 2A). thereby the hydroxylation activity increased in a light intensity-dependent way as reported before for batch assays [85], reaching 9.6 and $18.3 \text{ U g}_{\text{CDW}}^{-1}$ at 40 and $80 \mu\text{mol photons m}^{-2} \text{ s}^{-1}$, respectively (Fig. 4.2B). A further increase in light intensity did not result in a further activity increase. As expected, hydroxylation activities were lower than those achieved under assay conditions (Figure 1), where the substrate was added in excess combined with intense mixing. Substrate mass transfer limitation presumably also was the reason why the maximum whole-cell activity already was reached at $80 \mu\text{mol photons m}^{-2} \text{ s}^{-1}$, whereas it further increased reaching a maximum at $150 \mu\text{mol photons m}^{-2} \text{ s}^{-1}$ under assay conditions [85].

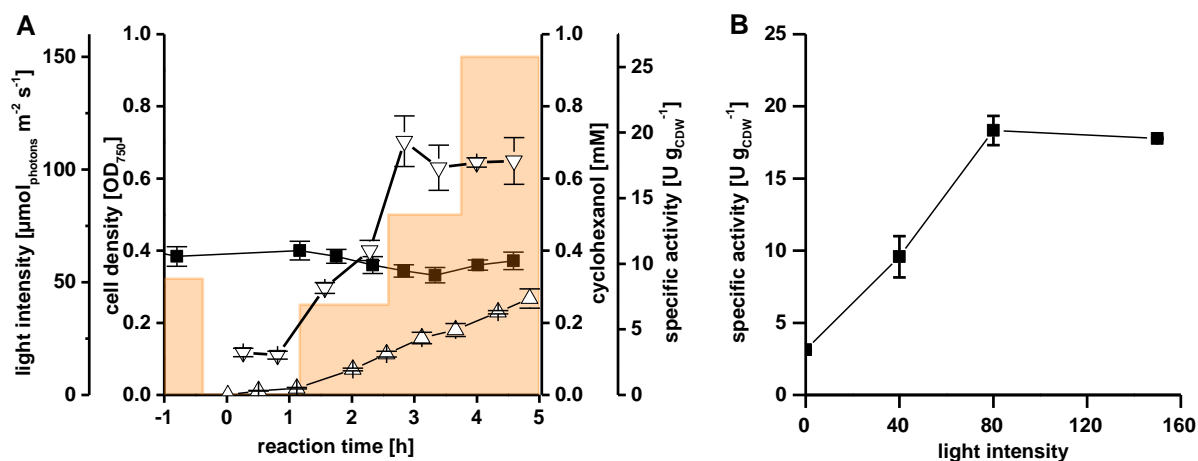


Figure 4.2: Light-dependent conversion of cyclohexane to cyclohexanol by the engineered PCC6803_CYP during continuous cultivation. Panel A shows the courses of cell and product concentration as well as of the light intensity and the hydroxylation activity. Panel B shows the specific activity in dependence of the light intensity. Cells were grown in YBG11 supplemented with 25 mM HEPES at 30°C. The culture was aerated at a rate of 3 ml min^{-1} of air via a segmented flow medium loop (see materials and methods section for details. The light intensity was varied as indicated.

Biomass concentration decreased upon biotransformation at low light intensities and stabilized and even increased when the light intensity was set to $150 \mu\text{mol photons m}^{-2} \text{ s}^{-1}$ (Fig 4.2A). This indicates that, at low light intensities, the cells cannot generate sufficient NADPH and ATP via photosynthesis to support both, stable growth and biotransformation. At higher light intensities, however, the growth rate was higher than the dilution rate,

indicating that the biotransformation-related electron withdrawal resulted in a sink effect, i.e., relieved the sink limitation of the photosynthetic light reaction [256]. Requirement ii. was thereby not fulfilled completely, as the cells were only at high light intensities able to maintain growth during the hydroxylation reaction.

Optimizing process parameters for continuous hydroxylation of cyclohexane

In the next step, the biomass concentration was increased in order to enable better physiological measurements, for example, increased O₂ differences in the in- and off-gas. Further, the growth conditions were improved to achieve better growth and fitness of PCC6803_CYP. PCC6803_CYP was cultivated at 75 μmol photons m⁻² s⁻¹ and carbon was supplied as NaHCO₃ (50 mM) directly with the feed to ensure that the cells are not carbon limited. With these modifications, the growth rate could be increased from 0.013 to 0.036 h⁻¹ and the carbon supply rate (18.7 mmol C d⁻¹) exceeded the carbon fixation rate (3.7 mmol C d⁻¹). As before, light and feed were switched off at the start of the biotransformation. Cyclohexane was supplied to start the reaction. Then, the following light intensities were applied stepwise: 75, 100, 125, 0, 50, and 75 μmol photons m⁻² s⁻¹ (see Fig. 4.3A). The “dark-activity” was with 0.9 ± 0.5 U g_{CDW}⁻¹ lower than in the first experiment, and the highest activity of 21.3 ± 2.3 U g_{CDW}⁻¹ was observed at 100 μmol photons m⁻² s⁻¹. Overall, the light dependency of the reaction could be validated, and the improved availability of carbon did not only result in an increased growth rate but also in increased specific activities (Fig. 4.3B).

PCC6803_CYP was able to maintain the growth rate while covering the additional electron demand for the conversion of cyclohexane to cyclohexanol at all applied light intensities except 50 μmol photons m⁻² s⁻¹ (Fig. 4.3A). Light and feed were turned off and on again to quantify rates in the dark and confirm the capability of the cells to instantly respond to light availability.

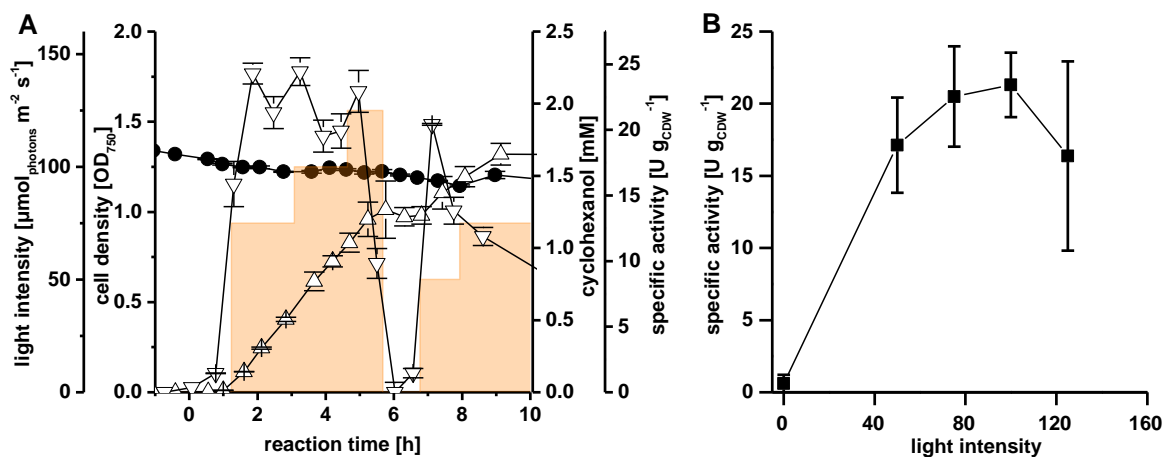


Figure 4.3: Light dependent conversion of cyclohexane to cyclohexanol by the engineered PCC6803_CYP under continuous growth mode (A) and the light dependent specific activities (B) in a bioreactor setup. Cells were grown in YBG11 supplemented with 25 mM HEPES and 50 mM NaHCO_3 at 30°C and 75 $\mu\text{mol photons m}^{-2} \text{s}^{-1}$ and an aeration of 3 ml min^{-1} with a 50% synthetic air and 50% nitrogen gas mixture. The light intensity was varied as indicated.

In summary, reaction conditions under carbon excess and light intensities between 80 and 100 $\mu\text{mol photons m}^{-2} \text{s}^{-1}$ seem suitable for an in-depth physiological investigation as the requirements i. and ii. were met.

Demonstrating the long term stability of the hydroxylation of cyclohexane under optimized process conditions

In the next step, the long-term stability of the cells during continuous cultivation and reaction were evaluated. PCC6803_CYP was grown at 30°C, 3 ml min^{-1} synthetic air-nitrogen mixture, and 90 $\mu\text{mol photons m}^{-2} \text{s}^{-1}$ in YBG11 supplemented with 50 mM carbonate. The light intensity was kept stable for constant growth and reaction conditions. After inoculation, cells were grown in batch mode up to an OD_{750} of approximately 1. At that point, the fresh medium feed was started to shift to the continuous mode of cultivation. The feed rate was estimated based on the batch growth rate and adjusted until the OD_{750} remained stable. A stable dilution rate was achieved at 0.036 h^{-1} . Cells were induced for 2 days before the reaction was started by supplying cyclohexane as described above.

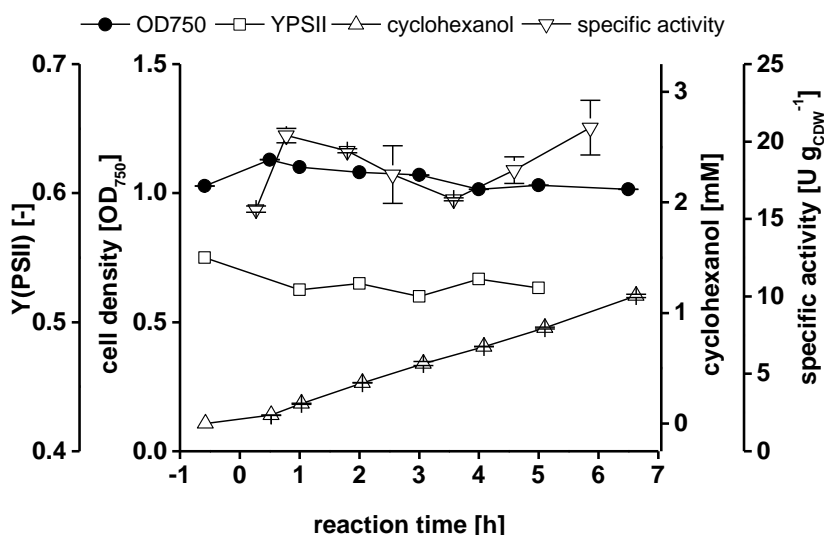


Figure 4.4: Stable biotransformation of cyclohexane to cyclohexanol mediated by PCC6803_CYP in a continuous growth mode in a bioreactor setup. PCC6803_CYP was grown in YBG11 supplemented with 25 mM HEPES and 50 mM NaHCO₃ at 30°C, 3 ml min⁻¹ synthetic air and nitrogen mixture and 90 μmol photons m⁻² s⁻¹.

The activity increased within the first 30 min to a specific rate of 21 U g_{CDW}⁻¹ and remained between 16 and 22 U g_{CDW}⁻¹ during the following 6.5 h. A cyclohexanol titer of 1.2 mM was reached, and the biomass concentration remained constant at an OD₇₅₀ of approx. 1 during the entire biotransformation phase, indicating that the cells can provide the required electrons for the reaction additionally to the electrons required for biomass formation. The measured activity and the stability of the reaction over several hours demonstrate the general suitability of the setup to investigate the physiological response of PCC6803 to an electron dependent biotransformation.

Assessing the reaction efficiency and the physiological response of PCC6803_CYP to the biotransformation

Finally, the physiological response of PCC6803_CYP to the biotransformation was characterized via photon and electron balancing. For this purpose, the number of absorbed quanta (Q_{phar}), the electrons derived by water-splitting at PSII (r_{PSII}), and the linear electron flux (r_{LEF}) were determined on the cellular source side. A slightly higher light intensity of 100 μmol photons m⁻² s⁻¹ was chosen to guarantee high activities. Two phases can be distinguished: the reference state before the reaction and the reaction phase.

The growth rate of PCC6803_CYP was 0.030 h⁻¹, which is slightly lower compared to the cultivation at 90 μmol photons m⁻² s⁻¹ (0.036 h⁻¹) and a similar biomass concentration (Fig. 4.5). The specific hydroxylation activity of 6.2 ± 0.1 U g_{CDW}⁻¹ was significantly lower than

in the previous experiment ($18.5 \pm 1.6 \text{ U g}_{\text{CDW}}^{-1}$), although all other process parameters were, except of the slightly increased light intensity, similar. Possible reasons for the low whole-cell activity include compromised cell fitness (which might be indicated by the reduced growth rate in comparison to the previous experiment) or underlying technical issues such as reduced cyclohexane supply via the gas phase.

The effective quantum yield increased from 0.56 ± 0.01 before the reaction to 0.61 ± 0.01 in the stationary reaction phase (2-6 h) (Fig. 4.5). The mean quantum uptake rate, Q_{phar} , increased only slightly after the start of the reaction (Fig. 4.6 and Table 4.2). The enhanced PSII and LEF rates in combination with a reduced specific activity resulted in quite low biotransformation efficiencies: $2.2 \pm 0.5\%$ of the absorbed quanta were utilized for the hydroxylation of cyclohexane, which corresponds to 180 ± 7 photons per cyclohexanol formed (Table 4.1).

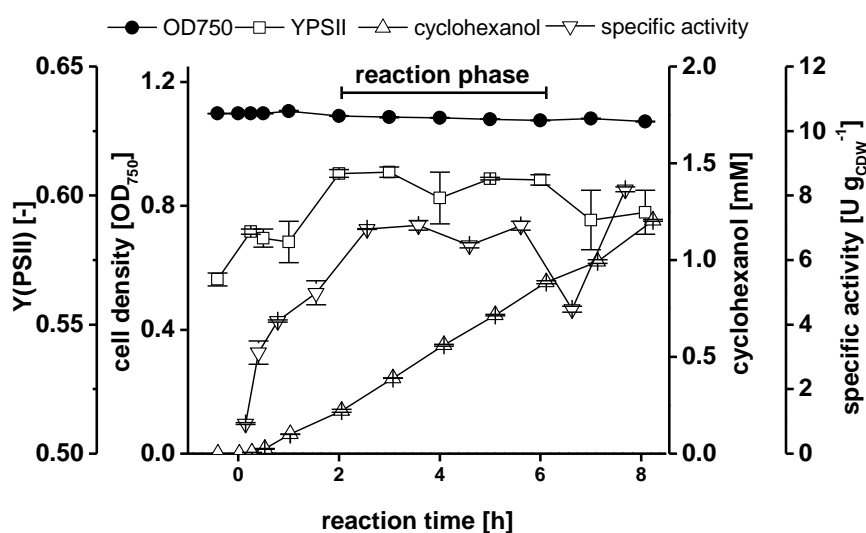


Figure 4.5: Biotransformation of cyclohexane to cyclohexanol mediated by PCC6803_CYP in a continuous growth mode in a bioreactor setup. PCC6803_CYP was grown in YBG11 supplemented with 25 mM HEPES and 50 mM NaHCO₃ at 30°C, 3 ml min⁻¹ synthetic air and 100 μmol photons m⁻² s⁻¹.

In accordance to the effective quantum yield, r_{PSII} was increased during the reaction phase. The net oxygen evolution rate derived electron flux increased from 108 ± 1 to 254 ± 11 mmol electrons $\text{g}_{\text{CDW}}^{-1} \text{d}^{-1}$ (Fig. 4.6 and Table 4.1). The increase by 146 mmol electrons $\text{g}_{\text{CDW}}^{-1} \text{d}^{-1}$ was 8.6 fold higher than the net electron demand for cyclohexane hydroxylation when considering a demand of 2 electrons per cyclohexanol formed (Table 4.1). Overall, $3.6 \pm 0.4\%$ of the electrons generated in PSII and $7.1 \pm 1.0\%$ of the LEF

(LEF = net O₂ evolution rate + O₂ consumed by the monooxygenase activity, respiration rates were neglected and assumed to be constant) were exploited by the reaction.

Table 4.1: Physiological and reaction parameters for cultivation and biotransformation for *Synechocystis* sp. PCC6803 CYP under 100 μmol photons m⁻² s⁻¹.

Reaction time [h]	-72	-48	-24	0	1	2	3	4	5	6
μ [1 d ⁻¹]	0.720	0.720	0.720	0.720	0.720	0.720	0.720	0.720	0.720	0.720
Y(PSII)	0.548	0.56	0.577	0.568	0.582	0.609	0.609	0.599	0.607	0.606
chl _a [μg ml ⁻¹]	3.68	3.57	3.52	3.41	3.37	3.37	3.30	3.51	3.67	3.61
biomass concentration [g l ⁻¹]	0.175	0.178	0.178	0.180	0.167	0.167	0.167	0.167	0.167	0.167
spec. CDW [mg mg _{chl_a} ⁻¹]	47.5	49.8	50.6	52.7	49.5	49.6	50.6	47.5	45.5	46.3
Carbon fixation rate [mmol _{electrons} g _{CDW} ⁻¹ d ⁻¹]	108	109	108	111	105	108	108	108	108	108
Qphar [mmol _{photons} g _{CDW} ⁻¹ d ⁻¹]	1337	1574	1509	1477	1573	1546	1488	1631	1734	1699
rPSII [mmol _{electrons} g _{CDW} ⁻¹ d ⁻¹]	358	444	446	442	489	503	494	500	516	514
Net oxygen evolution rate ^a [mmol _{O₂} g _{CDW} ⁻¹ d ⁻¹]	29.7	30.0	30.2	32.8	68.5	58.2	56.0	53.6	51.5	51.9
Net oxygen evolution rate ^a [mmol _{electrons} g _{CDW} ⁻¹ d ⁻¹]	119	120	121	131	274	233	224	214	206	207
cyclohexanol production rate [μmol g _{CDW} ⁻¹ min ⁻¹]	0.0	0.0	0.0	0.0	4.6	6.0	7.0	6.8	6.8	5.8
reaction rate [mmol _{electrons} g _{CDW} ⁻¹ d ⁻¹]	0	0	0	0	13	17	20	19	19	17
LEF ^b [mmol _{electrons} g _{CDW} ⁻¹ d ⁻¹]	119	120	121	131	300	267	264	253	245	241

a. net O₂ evolution rate is derived from the difference in the in- and off-gas, b. the overall LEF was corrected for the O₂ required for the hydroxylation of cyclohexane. Respiration was neglected and assumed to be similar before and during the reaction.

The causes for the unproportional increase of the LEF and the low activity remain unclear. However, the measured activity of $6.2 \pm 0.1 \text{ U g}_{\text{CDW}}^{-1}$ represents a decent rate in comparison to other model reactions and can be considered a representative model system for the characterization of physiological responses to biocatalytically induced electron withdrawal. The low usage of photosynthetically generated electrons for the hydroxylation demonstrates the potential of photosynthetically derived electrons for biocatalysis.

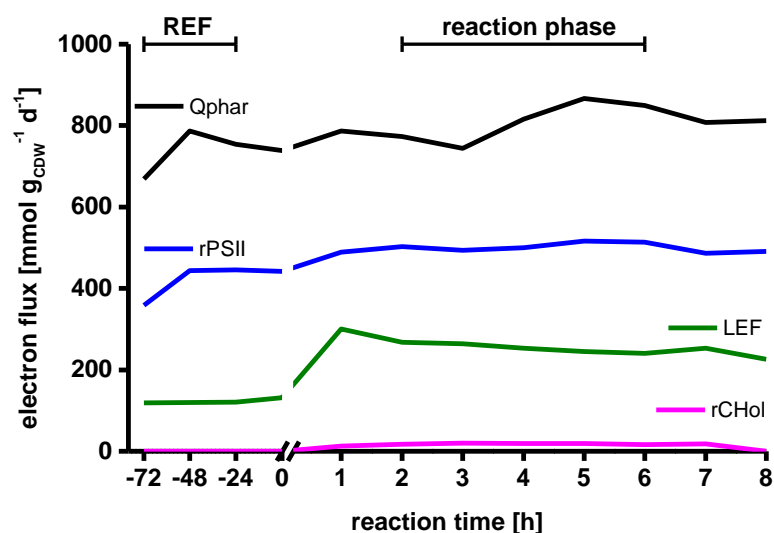


Figure 4.6: Electron fluxes in PCC6803_CYP before and during the biotransformation of cyclohexane to cyclohexanol. Rates were calculated hourly. PCC_CYP was grown in YBG11 supplemented with 25 mM HEPES and 50 mM NaHCO_3 at 30°C , 3 ml min^{-1} synthetic and $100 \mu\text{mol photons m}^{-2} \text{ s}^{-1}$.

Table 4.2: Impact of the biotransformation of cyclohexane to cyclohexanol on the physiology of PCC6803_CYP.

state	Q_{phar} [mmol quanta $\text{g}_{\text{CDW}}^{-1} \text{ d}^{-1}$]	PSII rate [mmol electrons $\text{g}_{\text{CDW}}^{-1} \text{ d}^{-1}$]	LEF [mmol electrons $\text{g}_{\text{CDW}}^{-1} \text{ d}^{-1}$]	Reaction rate [mmol electrons $\text{g}_{\text{CDW}}^{-1} \text{ d}^{-1}$]	% e BT^a/LEF^b	% e $\text{BT}^a/\text{PSII}^c$	% e $\text{BT}^a/Q_{\text{phar}}$	Quanta per CHol
reference	1474 ± 87	422 ± 37	108 ± 1	-	-	-	-	-
reaction*	1620 ± 92	506 ± 9	254 ± 11	18 ± 2	7.1 ± 1.0	3.6 ± 0.4	2.2 ± 0.5	180 ± 7

a. % e BT is the share of electrons used for the hydroxylation reaction of the calculated LEF in %; b. LEF = net O_2 evolution rate + O_2 consumed by the monooxygenase activity; c. PSII is the electron generation rate based on the fluorescence yield at PSII as described in the Materials and Methods section. Respiration rates were neglected and assumed to be constant; d. calculated for the stable reaction phase from 2-6 h from Figure 6.

Discussion

Cultivation and assay conditions can have a severe impact on initial whole-cell activity for the hydroxylation of cyclohexane to cyclohexanol in PCC6803_CYP

It was demonstrated before that environmental conditions, i.e., light and carbon availabilities, induce different physiological responses to additional electron and carbon sinks in *Synechocystis* sp. PCC 6803 [256, 265]. Consequently, steady metabolic states under constant environmental conditions were identified as a major requirement for the physiological characterization of phototrophic physiology and sink effects. The question rose if heterologous electron withdrawal activities also depend on and elicit differing physiological responses to environmental conditions, especially the growth conditions, but also the assay conditions. Indications for a growth phase-dependent whole-cell activity was observed for the regio-specific ω -hydroxylation of nonanoic acid methyl ester by a recombinant *Synechocystis* sp. PCC 6803 harboring an alkane monooxygenase system AlkBGT [136]. There, the activity varied depending on the time point and thus the cultivation stage, at which the cells were taken from an induced batch culture for whole-cell activity assays. In the present study, a growth condition-dependent activity was observed for the hydroxylation of cyclohexane in whole-cell assays (Figure 4.1). The maximum reaction rates were approx. 3.5 times higher than determined by Hoschek et al. for the same strain in shaking flask whole-cell activity assays [85]. An activity of ca. $23 \text{ U g}_{\text{CDW}}^{-1}$ was reached under illumination with $150 \mu\text{mol photons m}^{-2} \text{ s}^{-1}$ in YBG11 supplemented with 50 mM NaHCO_3 in the assay with cells grown in batch culture under $50 \mu\text{mol photons m}^{-2} \text{ s}^{-1}$ at ambient CO_2 conditions [85]. This is comparable to the conditions $\text{ULHC}_{\text{assay}}$ and $\text{MLLC}_{\text{cultivation}}$ applied in this study. Thus, the physiological state of the cells and assay conditions obviously have a severe impact on initial whole-cell activities (Fig. 4.1). In order to compare the true potential of engineered strains for the exploitation of photosynthesis-derived electrons for biotransformations, comparable analytical and assay conditions are required. Some reported recombinant strains might be able to achieve much higher whole-cell activities by selecting beneficial cultivation and reaction conditions.

Cyclohexane hydroxylation causes a distinct electron sink effect

Comprehensive and systematic investigations of physiological responses to additional sinks are rare. Abramson et al. investigated the photobiological response of *Synechococcus elongatus* PCC 7942 to sucrose synthesis and secretion, demonstrating that sucrose

secretion can lead to enhanced quantum efficiencies and PSII rates [168]. Berepiki et al. observed increased quantum efficiency and enhanced maximum ETR upon expression of the mammalian cytochrome P450 CYP1A1 in *Synechococcus* PCC 7002 [169]. We demonstrated in previous studies that an increased electron demand for biomass synthesis and lactate formation can result in increased PSII and LEF rates, improved quantum efficiencies, and stimulated carbon fixation rates in *Synechocystis* sp. PCC 6803 strains [256, 265]. These sink effects depended strongly on the process conditions, i.e., light and carbon availabilities, underlining the necessity of systematic and quantitative investigations.

Here, we set the basis for a systematic and quantitative investigation of photosynthesis-driven redox biocatalysis. With the selected reaction conditions, a specific reaction rate $18.5 \pm 1.6 \text{ U g}_{\text{CDW}}^{-1}$ was achieved during continuous cultivation (Figure 4). This was similar or significantly higher compared to other redox biotransformations in cyanobacteria [136, 169, 203, 204, 268], but less than the activity reported for an enoate reductase ($123 \text{ U g}_{\text{CDW}}^{-1}$) in a recombinant *Synechocystis* sp. PCC 6803 [86]. The whole-cell activity could, however, not be confirmed in a follow-up experiment, where a whole-cell activity of only $6.2 \pm 0.1 \text{ U g}_{\text{CDW}}^{-1}$ was observed under the same process conditions. The reduced activity might result from impaired cellular fitness, technical issues regarding cyclohexane supply via the gas phase, or intrinsic genetic instability of cyanobacteria, leading to mutations affecting growth and activity [141, 269]. The latter effect was observed in other long-term cultivations, where the lactate formation rate in recombinant *Synechocystis* sp. PCC 6803 decreased over time due to the accumulation of critical mutations (Personal communication Prof. Dos Santos and Prof. Hellingwerf, University of Amsterdam). Such variability or underlying technical issues require further investigations.

Even the low hydroxylation rate caused a clear (electron) sink effect, i.e., increased PSII and LEF rates, and improved quantum efficiencies. This combined stimulations enabled the cells to provide the electrons required for the hydroxylation without compromising growth (Fig. 4.5 and Table 4.2). The cells provided the electrons required for the reaction without further adaption and without compromising growth as long as sufficient light is available (Figure 4.3, 4.4, and 4.5). These results support the hypothesis that additional sinks can unleash the sink limitation of photosynthetic light reactions [164, 165]. Interestingly, the reaction rate depended directly on the incident light. This light dependency has been demonstrated

before [85], but not in continuous cultivations, underlining the plasticity and flexibility of the photosynthetic apparatus.

The quite low share of electrons exploited for the hydroxylation of cyclohexane resulted in a severe stimulation of the LEF. The redox balance in the reference condition before reaction start matched fairly well (Table 4.1). Assuming a similar C/N ratio of the biomass than determined in chapter 2, a rate of 154.8 ± 1.9 mmol electrons $g_{CDW}^{-1} d^{-1}$ would be required for biomass formation, which is slightly higher than the net oxygen evolution based LEF measured. The respiration rate was found at a level of approx. 53 mmol electrons $g_{CDW}^{-1} d^{-1}$ under similar light constrained growth ([256], chapter 1). After reaction start, however, a vast excess of photosynthetically derived electrons at a rate of 82.9 ± 3.4 mmol electrons $g_{CDW}^{-1} d^{-1}$ was measured based on the O_2 evolution rates under consideration of electrons and O_2 consumed for cyclohexane hydroxylation (Table 4.2). Assuming the measured O_2 evolution rate is correct and not compromised by a measurement or systematic error, the question arises where these electrons end up and why they are mobilized. The excess electrons were not used for accelerated growth as the biomass concentration remained constant during continuous cultivation. One may hypothesize that the excess electrons result in increased carbon fixation rates and metabolites are secreted into the supernatant as a kind of electron dissipation pathway. It was shown before that *Synechocystis* sp. PCC 6803 can apply metabolite overflow as a means to balance the cellular redox state [270]. Cyanobacteria also are known to form hydrogen as a valve to bind excess electrons [271, 272]. Furthermore, other “valve” or dissipation pathways, which are not predominantly used under known and regular conditions, might become active due to stress elicited by the biotransformation involving highly toxic compounds. This should be evaluated in future experiments by supernatant and off gas analyses during a biotransformation in combination with the investigation of underlying regulatory effects, for example, by applying omics analyses.

Another question is why the cells do not exploit those apparently feasible PSII rates/ LEFs for faster growth under the reference condition without ongoing biotransformation. It was demonstrated before that stimulation of carbon fixation rates and biomass formation is feasible if the ATP supply or regeneration rate can be optimized. Thus ATP supply might be limiting under the chosen conditions. Growth of *Synechocystis* sp. PCC 6803 on nitrate instead of ammonium as N-source resulted, under some conditions, in a beneficial shift in

the AEF over LEF ratio, indicating a stimulated ATP regeneration. While in some cases such a ratio change resulted in stimulated growth, this may have been prevented in other conditions due to metabolic and molecular constraints (chapter 2, [256]). This might also be the case for the hydroxylation. Furthermore, the hydroxylation caused a reduction of the AEF over LEF ratio, indicating that the AEF to LEF ratio might already be ideal under the respective conditions and a faster growth might not be achievable.

At this point, it cannot be excluded that the O₂ evolution rate measurements were compromised by technical issues. Since the gas sensors are determining the oxygen share in the given volume flow, multiple effects can lead to errors. One aspect to consider is the assumption made that the gas flow is saturated by cyclohexane during the reaction phase and that the reaction is not substantial enough to cause a decrease in the cyclohexane volume share in the off-gas flow. If this assumption would not hold true, for example, due to compromised cyclohexane supply as discussed before, and the off-gas flow would be reduced, the net oxygen evolution rate and consequently the LEF would be lower. Further, the galvanic cell used in the sensors may have been affected by organic compounds such as cyclohexane, even though this is not to be expected according to the sensor specifications. Such possible technical and cellular issues should be further investigated in order to validate the physiological responses of *Synechocystis* sp. PCC 6803 to the monooxygenase-based electron withdrawal.

The photon efficiency of cyclohexane hydroxylation by PCC6803_CYP

The reaction efficiency of a photo-biotechnological biotransformation could be quantitatively assessed in this study by applying an electron/photon balance. Such an approach has been applied before to analyze the physiological responses of phototrophic cells to environmental or biocatalytic perturbations [217, 218, 256, 265]. Nielsen et al. calculated the photon efficiency for a diverse set of carbon-based products based on available literature data for growth and product formation, but without knowledge on *in vivo* rates for absorbed photons and photosynthetically derived electrons [264]. The calculations demonstrated that the share of photosynthetically derived electrons used for the synthesis of carbon-based products can be as high as 87% as in the case for the synthesis of 2,3-butanediol. However, however, no conclusions can be drawn on the efficiency of the totally available photons since the respective photon absorption rates were not considered. Zavrel et al. characterized ethylene formation in a recombinant *Synechocystis* sp. PCC 6803

strain in a semi-continuous system combining model-based and *in vivo* data [255]. They found that the number of photons absorbed per synthesized ethylene molecule depends on the incident light intensity, and that increased pathway capacity improved the photon yield to an optimum of 100.2 ± 14.3 photons per molecule ethylene at $50 \mu\text{mol photons m}^{-2} \text{ s}^{-1}$ [255]. We showed in a previous study that 682 to 824 photons have to be absorbed depending on the carbon and light availabilities to form one molecule of lactate in a recombinant *Synechocystis* sp. PCC 6803 [265]. In general, a high photon flux is not necessarily beneficial for a product on photon yield, as, with increasing light intensity, a bigger share of photons has to be dissipated due to limiting metabolic sinks and the resulting photo-inhibitory effects [164, 165]. On the other hand, excess light represents an energy potential which could be unleashed by additional electron sinks in the form of electron demanding biocatalytic reactions.

The reaction efficiency of the cyclohexane hydroxylation, as it was assessed from photon absorption, PSII, and LEF rates, was surprisingly low: 180 ± 7 photons were absorbed for the synthesis of one cyclohexanol molecule. This corresponds to a productive photon usage of $2.2 \pm 0.5\%$ (yield on absorbed photons, Table 4.1). This is less efficient compared to ethylene synthesis, but more efficient compared to lactate formation [255, 265]. In those systems though, carbon fixation and precursor synthesis require more electrons per product molecule and additionally ATP.

While only a small fraction of the available light was exploited for cyclohexane hydroxylation, the apparent LEF increased significantly, which requires further investigations – ideally with a higher P450 activity *in vivo*. Overall, the electron flux going into the hydroxylation amounted to only 7.1% of the LEF leaving plenty of room for optimization (Table 4.1).

Conclusion

In this study, we developed a strategy to perform the hydroxylation of cyclohexane during continuous cultivation. This enabled the characterization of the physiological response of the model organism *Synechocystis* sp. PCC 6803 to a biocatalysis-related artificial electron sink. Initial investigations showed that the whole-cell cyclohexane hydroxylation activity strongly depends on cultivation and reaction conditions. Furthermore, photosynthesis was found to react in a highly flexible way and to be sink limited. The cells instantly were able to provide the electrons required for the hydroxylation. Finally, it was shown that photosynthesis-derived electrons fuel the P450 mediated reaction and that the reaction rate depends on the incident light intensity. Although the coupling of the P450 to the LEF appears to be quite inefficient, resulting in an inefficient use of photons for the biocatalytic reaction.

Further development of the setup will be required to ensure operation stability and reproducible reaction rates. Following this, further experiments will be required to elucidate the physiological response of PCC6803_CYP to the representative whole-cell activity of around $20 \text{ U g}_{\text{CDW}}^{-1}$ in the evaluation experiments. The approach described here constitutes a start point for the systematic evaluation of photosynthesis-driven biotransformation efficiency. It would furthermore be interesting to investigate the effect of changes in the light harvesting machinery such as the optimization of photon uptake via phycobilin engineering or targeted engineering of the electron transport chain on the reaction efficiency.

Chapter 5: General Discussion

The sink effect in *Synechocystis* sp. PCC 6803 depends on the environmental conditions and the character of the additional sink

Angermayr et al. addressed the need to systematically and quantitatively investigate the carbon sink effect in order to find underlying mechanisms and to gain knowledge for an efficient and straight forward strain development of photosynthetically active cells as whole-cell biocatalysts [173]. The reason for that call was the highly differing observations made by many researchers when a heterologous pathway for the synthesis of a product directly from CO₂ was introduced into photosynthetically active organisms. For some compounds, no stimulating effect of the respective introduced carbon sink on the carbon fixation rate, quantum efficiency, or the LEF and PSII rates, was observed. Others report a significant increase in one, a combination of, or all of them. All studies have in common that a comprehensive dataset is not given because accessing physiological parameters was not in the focus of the studies. The characterization of the dynamic photobiological response of *Synechococcus elongatus* to induced sucrose excretion represents one rare exception [168]. The authors observed increased electron transfer rates and increased quantum efficiency in comparison to the respective wildtype.

Lactate synthesis from CO₂ was selected in this study as a model carbon sink. It should be highlighted that previous studies on the same recombinant strain did not report any metabolic rate stimulation [135, 173]. Combining continuous cultivation with in-depth physiological characterization of the respective metabolic steady states confirmed these findings for light limited conditions: neither the carbon fixation rate, nor the quantum efficiency or LEF were increased upon lactate formation (Tab. 5.1). Under excess availability of light and CO₂, carbon fixation rates were not stimulated; the effective quantum efficiency was increased slightly. This, however, had no effect on the LEF due to a simultaneous reduction of the photon uptake rate. Lactate was formed in both conditions at the expense of biomass formation, as the carbon fixation rate did not increase.

An entirely different picture was gained under carbon limitation: lactate formation stimulated quantum efficiency, resulting in enhanced LEF and carbon fixation at a similar photon uptake rate. Similar responses, i.e., increased oxygen evolution (it has to be noted that this was measured in an assay at 800 $\mu\text{mol photons m}^{-2} \text{s}^{-1}$ and not under cultivation conditions) and enhanced carbon fixation rates were observed for the synthesis of isoprene from CO₂ under excess conditions (100 $\mu\text{mol photons m}^{-2} \text{s}^{-1}$, 5% CO₂) [79]. Sucrose secretion

was found to enhance carbon fixation rates and oxygen evolution rates during shaking flask cultivation at 65 $\mu\text{mol photons m}^{-2} \text{s}^{-1}$ and 2% CO_2 , but all parameters were measured at different light and presumably carbon availabilities in a diverse set of assays, compromising the view on the sink effects [72]. Both studies used *Synechococcus elongatus* sp. PCC 7942 as model cyanobacterium and can be considered operated under excess carbon, but varying light conditions. This additionally complicates a direct comparison with the results obtained in this thesis. However, the introduction of an isopropanol synthesis pathway in *Synechocystis* sp. PCC 6803 resulted in increased quantum efficiency, LEF, and carbon fixation rate under similar carbon limited conditions (100 $\mu\text{mol photons m}^{-2} \text{s}^{-1}$, ambient CO_2) [170] as in case of the carbon limited conditions applied in chapter 3 for lactate synthesis.

Table 5.1: Sink effects observed for the three model sinks investigated in this thesis.

sink	C-fixation rate			Y(PSII), Q_{phar} , LEF, AEF		
	Light limitation	Excess light and CO_2	Carbon limitation	Light limitation	Excess light and CO_2	Carbon limitation
Lactate as carbon sink	→	→	↑	→→→↓	↗↓→→	↗→↗↗
NO_3^- as electron sink	→	↑	→	↗→↗↗	↑↑↑↑	↗→↗↑
Hydroxylation of cyclohexane as electron sink		→			↑→↑↓	

Experimental data on the physiological responses of photosynthetically active cells to heterologous carbon sinks is scarce but exists. The physiological response to an additional electron sink, in contrast, is not yet described. The coupling of electron withdrawing enzymes to photosynthesis is still in an early research state, involving rather low reaction and thereby electron withdrawal rates. Many examples with decent rates and carbon partitioning exist for the synthesis of carbon-based products from CO_2 , but only a few examples can be found for the successful coupling of electron demanding enzymatic steps to photosynthetic water-splitting. The highest rates have been achieved in *Synechocystis* sp. PCC 6803 for enoate reductase-catalyzed C-C double bond reduction [86] and P450 monooxygenase-catalyzed cyclohexane hydroxylation [85]. The focus of respective biocatalysis studies so far was the maximization of the initial whole-cell activity and not the characterization of physiological parameters. Coupling the mammalian cytochrome P450 CYP1A1 to photosynthesis in *Synechococcus* sp. PCC 7002 is the only example, for which a stimulation of the quantum efficiency (0.0416 ± 0.002 in the WT versus 0.0436 ± 0.011 in the

recombinant strain) and the maximum ETR (357 electrons reaction center of PSII⁻¹ s⁻¹ in the WT versus 468 in the recombinant strain) has been reported [169]. The parameters accessed indicate physiological responses to a biocatalytic electron withdrawal, but the very low activity and the lack of other physiological rates such as O₂ evolution rates at the respective growth conditions limit the conclusions which can be drawn from the provided data. The physiological responses were even measurable for rather low activities of 0.031 U g_{CDW}⁻¹. In this thesis, two strategies were followed to investigate electron sink effects in *Synechocystis* sp. PCC 6803: variation of the electron demand via the supply of N-sources with differing degree of reduction under the same defined steady state conditions as applied for lactate synthesis on the one hand, and the above mentioned P450 monooxygenase-catalyzed cyclohexane hydroxylation with excess carbon and light availability on the other hand [85]. The additional electron demand was covered by enhanced quantum efficiency and an increased LEF, irrespective of the electron sink and the conditions applied. This increase of the quantum efficiency and LEF under all conditions, even under light limitation, supports the sink limitation hypothesis: additional sinks can relieve sink limitation, e.g., the down-regulation of water splitting and electron transfer due to limited metabolic electron acceptor availability, resulting in enhanced photosynthesis rates [164, 165]. This was also observed for cyclohexane hydroxylation (chapter 4). Here, the reaction rate depended, as shown before [85], on the light availability and could be “switched on” instantly by substrate supply.

Interestingly, the electron sink stimulated the carbon fixation rate similar to the carbon sinks lactate, isopropanol, and sucrose. The stimulation of the carbon fixation rate was found, similar to isopropanol [170], under excess light and carbon availability and not, as in the case of lactate synthesis, under carbon limitation. The quantification of light reaction rates revealed that the stimulation of the carbon fixation rate goes along with an increased AEF over LEF ratio in the cases of lactate synthesis and nitrate assimilation as additional carbon and electron sinks (Fig. 5.1). This ratio allows the estimation of ATP and reduced ferredoxin/ NAD(P)H regeneration rates as both contribute to ATP regeneration but only the LEF is responsible for reduced ferredoxin/ NAD(P)H regeneration. It was hypothesized already before that additional sinks have an impact on the cellular ATP/NAD(P)H balance [144, 170]. Photosynthetic metabolism is believed to be ATP limited as the LEF does not provide ATP and NAD(P)H in a ratio optimal for the Calvin-Benson cycle [167]. The cellular ATP/NAD(P)H balance can be modified by rearranging LEF and AEFs. An additional sink can have different

ATP/NAD(P)H requirements compared to biomass formation (chapter 3 and [144]). In the case of lactate formation, less ATP is required per C compared to biomass formation. Instead, the glycolytic reactions towards lactate regenerate ATP, resulting in significantly increased ATP availability. This was further supported in an increased AEF/LEF ratio. It is hypothesized that the additionally available ATP has the potential to promote the ATP dependent CCM, which explains the increased carbon fixation rate under carbon limitation (chapter 3 and Table 5.1). Similar hints were found for the stimulated carbon fixation rate upon isopropanol synthesis in *Synechocystis* sp. PCC 6803: the intracellular ATP over NAD(P)H concentration ratio increased significantly [170]. Such effects were not found under excess light and carbon availability, presumably due to an already optimal ATP/NAD(P)H ratio or a maximum carbon fixation rate under the selected conditions. Interestingly, the maximum carbon fixation rate was similar for both, the electron and the carbon sink, under excess conditions. This supports the hypothesis that the achieved rate represents the maximum carbon fixation rate under the selected environmental conditions.

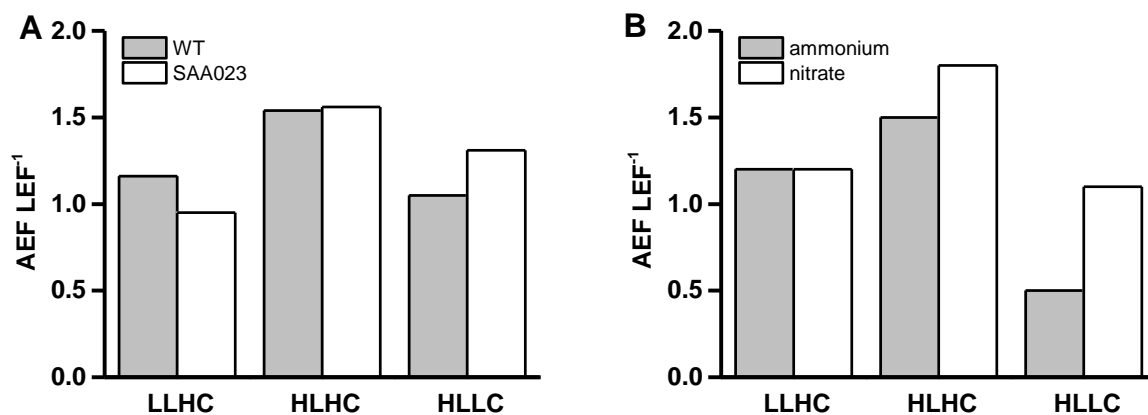


Figure 5.1: The ratio of AEF over LEF for the carbon sink (A, lactate formation) and the electron sink (B, N-sources with different reduction grade) in all tested conditions (LLHC: light limitation, HLHC: excess carbon and light availability, HLLC: carbon limitation).

As said, the AEF over LEF ratio appears to be indicative a stimulation of the carbon fixation rate. Strikingly, the most dominant shift in that ratio was however observed under carbon limitation for nitrate as electron sink. Consequently, the question arises why this shift does not cause a stimulation of the carbon fixation rate. Noticeably, lactate formation as carbon sink did not result in increased growth (chapter 3). The additionally fixed carbon was exclusively channeled towards lactate. It can be hypothesized that underlying mechanisms and cellular modules/functions constrain and limit the biomass formation rate under the chosen carbon limited condition. Assuming this, a beneficial shift in the AEF to LEF ratio

would not result in enhanced carbon fixation rates as the WT would not be able to utilize additional carbon. Considering lactate formation as a *carbon valve* in such a scenario, carbon fixation can be increased even under the premise that biomass formation is limited by other factors than carbon availability. The possibility to uncouple carbon fixation from biomass formation by selecting appropriate light and carbon availabilities is an interesting finding and an interesting target to follow in future photo-biotechnological research.

The investigated examples demonstrate that all additional sinks can cause a (carbon) sink effect that is the stimulation of quantum efficiency, LEF and/or carbon fixation rate. The reason why it was not observed for many other products might simply be that the physiological responses to the respective sinks were not quantified under appropriate conditions. As observed here, lactate formation caused either a distinct stimulation of metabolic rates or no obvious response at all, depending on the applied growth conditions. The same might be the case for other products. Possible physiological responses to the heterologous pathway may depend on the growth conditions and the specific impact on the ATP/NAD(P)H balance. This clearly emphasizes the benefits but also the importance of systematic and quantitative approaches to investigate photosynthesis efficiency. It would be interesting to apply similar approaches for other carbon and electron sinks to verify the hypothesized change in ATP/NAD(P)H balance as underlying mechanisms and combine it with a quantitative determination of intracellular metabolite pools, especially ATP and NAD(P)H. Engineering of the cellular redox metabolism might be a powerful strategy to enhance product formation rates in photosynthetically active cells. Especially, introducing a NAD(P)H oxidase might be an interesting approach to simulate a strong biocatalytic electron withdrawal and shift the ATP/NAD(P)H balance.

The importance of the defined, steady (metabolic) state for a systematic and rational strain characterization and process development

As discussed in this study, the physiological responses of photosynthetically active cells and thereby the metabolic capabilities are highly dependent on the respective metabolic state, i.e., the environmental condition to which the cells are adapted to. Since strain, reaction and process engineering depend on the proper characterization of the whole-cell biocatalyst, it is essential that the metabolic state is well defined and reproducible. This, however, is not given during standard batch cultivation, where increasing cell density leads to shading

effects and thus decreasing light availability and simultaneously varying CO₂ availabilities. Such environmental dynamics lead to a permanent acclimation of the cells [148, 149].

Consequently, stable and steady environmental conditions are the basis for the appropriate determination of physiological changes upon perturbations by metabolic engineering or reaction engineering (temperature, substrate availability including light and CO₂). This was not in focus in the field of photo-biotechnology so far, as exemplified by the small number of systematic and quantitative studies applying continuous and semi-continuous cultivation strategies to gain insights into the quantitative properties of photosynthetically active cells [150, 152-154, 255, 259]. In this study, establishing steady states enabled to quantify the sink effect in *Synechocystis* sp. PCC 6803 and offered explanations for the contradictory observations in literature. Furthermore, the precise and quantitative evaluation of physiological responses to perturbations can provide new targets for further investigations. An example is the increased PSII rate and the enhanced quantum efficiency observed when cells were supplied with nitrate instead of ammonium under low light (chapter 2). This was highly unexpected and contrary to the assumption that quantum efficiency and PSII rates are optimized under low light availability in order to achieve a maximum water oxidation rate to fuel metabolic processes. The reason for that remains unclear but its elucidation might provide hints for further optimization of photosynthesis rates even under low light availabilities. Another aspect is the in-depth investigation of the redox metabolism under defined steady states to clarify the actual impact of sinks, but also of environmental conditions (such as light and carbon availability), on the cellular physiology.

But not only the physiology itself was shown to depend on the steady state conditions. Also the whole-cell activity of *Synechocystis* sp. PCC 6803 was strongly dependent on the metabolic state during the cultivation of the biocatalyst and the assay conditions (chapter 4), with activities ranging from close to zero to around 80 U g_{CDW}⁻¹. This emphasizes that the biocatalyst state and the assay conditions should not be neglected in photo-biocatalysis.

Besides of target identification for strain engineering purposes, the characterization of cellular physiology at steady states demonstrated its potential for reaction and process engineering. The carbon partitioning was shown to not only depend on the pathway properties, but also on the acclimation state of the cells. For instance, carbon partitioning towards lactate could be increased with excess light availability (chapter 3). Additionally, the specific lactate formation rate for the same strain was enhanced by a factor of 12.4 by

modification of growth/reaction conditions in comparison to previous data [135], indicating the potential in increasing product formation rates by the selection of product formation promoting conditions.

Such defined steady state analyses will furthermore promote the application of omics technologies in photo-biotechnology. Even today, at the end of the 2010s, omics approaches are not widely applied in photo-biotechnology even though the benefits are recognized [273]. An example is the field of fluxomics, which is the investigation of the intracellular metabolic rates. This relies heavily on the precise measurement of physiological parameters. The slow progress in experimental data-based MFA [147, 274] in contrast to solely network-based approaches such as FBA [143-146, 275] can be attributed to the limited access to quantitative experimental data. Consequently, network reconstruction and ^{13}C -based MFA will benefit from such cultivation approaches as modelling data can be more easily verified and utilized for projections to optimize cellular fluxes for product formation. Applying systems biology tools in steady states will accelerate in-depth systems knowledge and thereby target identification for a more rational and systematic strain development in photo-biotechnology.

The potential of photo-biotechnology to contribute to the decarbonization of industrial processes

Quantitative data allow estimating the potential of photosynthetically active cells for photo-biotechnology and its potential contribution to the decarbonization of the chemical industry. Here, we take the photo-biotechnological production of lactate directly from CO_2 as a theoretical example. The aim is to produce 10000 t y^{-1} , as it is the case for the fermentative production of the platform chemical succinate in a joint venture between BASF and Corbion Purac [276]. The calculations are based on the following assumptions: i. the carbon fixation rate measured in chapter 3 is the maximum rate achievable, and, ii. excess light is provided 24/7 for continuous process operation. The calculation was further conducted with a biocatalyst concentration of 2 g l^{-1} , which is roughly the cell concentration achieved at the end of batch cultivations of *Synechocystis* sp. PCC 6803. A carbon partitioning of 20% towards lactate, as it was achieved in chapter 3 under light excess conditions, was assumed. With those premises, a plant with a 25661 m^3 reactor would be required to achieve the yearly production of 10000 t of lactate. This is 3.4 times the size of the closed bioreactor system operated by BGG (China) for the photo-biotechnological production of Astaxanthin at

7500 m³ scale. Utilizing glucose as carbon source, the lactate forming heterotrophic *Enterococcus faecalis* can produce the same amount of lactate in a 170 times smaller reactor (150 m³, Table 5.2).

Table 5.2: Estimated bioreactor scales for the production of 10000 t/year of the model compound lactate and varying process and biocatalyst properties.

Carbon partitioning towards lactate [CP]	CP 20%	CP 50%	CP 80%	CP 100%	<i>E. faecalis</i> ^b
Carbon fixation rate ^a / glucose uptake rate [mmol C g _{CDW} ⁻¹ d ⁻¹]	89.9	89.9	89.9	89.9	3440
Carbon fixation rate / glucose uptake rate [mol C g _{CDW} ⁻¹ y ⁻¹]	32.8	32.8	32.8	32.8	1256
Lactate formation rate [mol Lactate g _{CDW} ⁻¹ y ⁻¹]					375
Lactate formation rate [mol Lactate l ⁻¹ y ⁻¹] ^c					
<i>Biocatalyst concentration</i>					
2 g l ⁻¹	4	11	18	22	750
44 g l ⁻¹ ^d	96	241	385	481	16500
100 g l ⁻¹ ^e	219	547	875	1094	75000
Required yearly lactate production rate [million mol lactate y ⁻¹]	112	112	112	112	112
Bioreactor volume [m ³]					
<i>Biocatalyst concentration</i>					
2 g l ⁻¹	25661	10264	6415	5132	150
44 g l ⁻¹ ^d	1166	467	292	233	6.8
100 g l ⁻¹ ^e	513	205	128	103	1.5

Assumptions: a. maximum carbon fixation rate of chapter 3 is reached; b. Parameters determined for *Enterococcus faecalis* CBRD01 in batch cultivation [277]; c. the whole-cell biocatalyst operates at 24/7 under steady conditions (excess light and carbon availability); d. biomass concentration in a phototrophic/heterotrophic mixed species approach on biofilm scale [137]; e: biomass concentration achievable in heterotrophic cell-based bioprocesses.

The biocatalyst concentration would be one of the first parameters to tackle for a process optimization, considering that bioprocesses based on heterotrophic microorganisms are operated at up to 100 g_{CDW} l⁻¹. The highest biomass concentration for *Synechocystis* sp. PCC 6803 was achieved via a biofilm concept involving a mixed species approach. There, a combined biomass concentration of 51.8 g_{CDW} l⁻¹ could be achieved with photosynthetically active *Synechocystis* sp. PCC 6803 cells accounting for 85 percent of the cells [137]. Assuming that a photo-biocatalytically active cell concentration 44 g_{CDW} l⁻¹ can be reached, the reactor volume would decrease to 1166 m³. This is already in a scale which is commercially applied, as seen for the example of BGG (China). But also Roquette (Germany) operates a photo-

bioreactor at half of that size (600 m³). However, such an increase in biomass concentration seems challenging for suspended cultures when taking into account that light and carbon have to be supplied in excess to achieve a homogeneously high lactate formation rate in the whole reactor.

One strategy to further improve the process performance is to optimize the carbon partitioning towards the product, which is actually an obvious main goal in photo-biotechnology [278]. An increase of the carbon partitioning to 80%, as it was achieved for some products in cyanobacteria [173], would result in a decrease of the required reaction volume by approx. 75%. This would simultaneously reduce the biomass production rate and thereby nutrient demand, resulting in an improved life cycle balance of the process. On process level, the application of a biofilm might even allow achieving a carbon partitioning of close to 100%, if growth can be minimized [137, 279]. In such a case, the reactor volume could be reduced to 233 m³, which can be considered feasible for a photo-biotechnological setup. To further improve strain and process performance in future, different parameters can be addressed, such as for example the engineering of the carbon fixation rate [249, 250]. Selecting more suitable strains with intrinsic faster growth rates and consequently higher carbon fixation rates, such as *Synechococcus elongatus* UTEX [280, 281], provide further potential to improve process performance.

However, the theoretical reactor volume of 233 m³ is still 34 times higher than a theoretical process based on *E. faecalis* and glucose as carbon and energy source. This underlines that the cellular productivity of photosynthetically active cells is rather low in comparison to heterotrophic cells, irrespective of the assumptions made here. The central question regarding the implementation of photo-biotechnological processes will be: can the intrinsic advantages of photo-biotechnological systems compensate for the disadvantage of the relatively low productivity? The main advantage is the utilization of the abundant CO₂ instead of glucose or other organic feedstocks and the potential to couple it to carbon dioxide producing processes to create a closed carbon cycle. For the above process frame and the given yield of lactate on glucose, approximately 11300 t glucose would have to be supplied, not taking into account the initial biocatalyst production. This can be considered a major cost factor. The utilization of CO₂ as process feed constitutes an economical advantage: a ton CO₂ is traded with 25 EUR (according to the European Emission Allowances), a ton glucose with 350-600 EUR. Thus utilization of CO₂ can be considered not

only environmentally, but also economically more attractive under the premise that no energy-intensive concentrating processes have to be applied. While the use of CO₂ is an advantage, the cultivation technology in photo-biotechnology represents a major cost factor and requires further research [138-140]. Closed photo-bioreactors are cost intensive and the illumination with light to enable a 24/7 continuous process seems only feasible in a future scenario with cheap and unlimited availability of electricity from renewable energy sources. Cultivation under natural day-night cycles will further result in a reduction of overall growth and thereby carbon fixation rates, up to a factor of 3.5 was described for diverse green algae [282, 283], but allows for a reduction of energy demands for illumination.

Associated costs for the production of organic feedstock, as here for example glucose, have also to be considered for a comprehensive and fair evaluation of photo-biotechnological processes. As in the case of biofuels, organic feedstock for microbial processes has to be produced by agricultural means, resulting in a land use conflict with food production [37-39]. This is an important aspect in the context of the increasing global population and simultaneous decrease of arable land. But not only the land use, but also the energy demand throughout the whole supply chain has to be considered for a comprehensive ecological and economic evaluation of all process options. In the end, a photo-biotechnological process may become favorable in comparison to a heterotrophic process under considerations of the true ecological and economic factors, such as climate and environmental costs. Photo-biotechnology may already represent a feasible alternative to heterotrophic biocatalysis for high priced specialty products with rather low production volumes.

Chapter 6: Conclusion and Outlook

Rational and efficient photo-biotechnological whole-cell biocatalyst and bioprocess development are hindered by insufficient knowledge about photosynthetically active cell systems. Compared to other scientific and industrial workhorses, such as *Escherichia coli*, (quantitative) knowledge about the regulatory networks, the metabolic constraints, and the physiological responses to perturbations, i.e., biocatalytically induced carbon and electron sinks, is missing for photosynthetically active cells.

This study demonstrates the potential of a systematic and quantitative investigation of photosynthetically active cells for future progress in photo-biotechnology. Standard principles in heterotrophic strain and process development [100, 131] were followed in this study, especially the characterization of cellular properties and responses to perturbations in defined and steady states on the basis of cellular rates. This enabled to gain new insights into the interaction of metabolism and biocatalytic activity and contributed knowledge to address old scientific questions, namely the (*carbon*) *sink effect*.

A systematic and quantitative approach in photo-biotechnology will furthermore provide new insights into the cellular capabilities and the responses to perturbations, i.e. environmental conditions, reaction conditions, and biocatalytic activity. Thereby, it will pave the way towards target identification for the optimization of photosynthetically active host organisms on cellular and metabolic level and accelerate strain and bioprocess development in photo-biotechnology.

To sum up, the development of photo-biotechnological processes for the synthesis of bulk chemicals directly from CO₂ based on the presented estimations appears to be challenging, but not impossible in future. The production of high-value compounds, such as fine chemicals and pharmaceutical compounds with lower yearly demand and higher prices, either from CO₂ or in a biotransformation approach, is closer to application. Thinking on the global scale, a total bioreactor volume of 0.82 km³ (under the premises of the given carbon fixation rate, the biocatalyst concentration in biofilms, and 80% carbon partitioning, Table 5.2) would be required to fix the yearly anthropogenic CO₂ emission of 11.3 Gt C y⁻¹. This corresponds roughly to the volume of the German lake Müritz (0,737 km³). The potential contribution of photo-biotechnology to a general decarbonization thus can be considerable. Photo-biotechnology can be an important puzzle-piece contributing to the industrial decarbonization by utilizing CO₂ for the synthesis of value-added compounds and energy carriers.

References

1. BP Statistical Review of World Energy 2018. https://www.bp.com/content/dam/bp/country-sites/de_de/germany/home/pdfs/bp-stats-review-2018-full-report.pdf. 2018.
2. Levi PG, Cullen JM: Mapping global flows of chemicals: From fossil fuel feedstocks to chemical products. *Environ Sci Technol*. 2018;52:1725-34.
3. Le Quéré C, Andrew RM, Friedlingstein P, Sitch S, Hauck J, Pongratz J, et al.: Global Carbon Budget 2018, *Earth Syst. Sci. Data*, 10, 2141-2194, <https://doi.org/10.5194/essd-10-2141-2018>. 2018.
4. Joos F, Spahni R: Rates of change in natural and anthropogenic radiative forcing over the past 20,000 years. *Proc Natl Acad Sci USA*. 2008;105:1425-30.
5. Dlugokencky E, Tans P: Trends in atmospheric carbon dioxide, National Oceanic & Atmospheric Administration, Earth System Research Laboratory (NOAA/ESRL). <http://www.esrl.noaa.gov/gmd/ccgg/trends/global.html>. Accessed on May 6, 2019.
6. Boden TA, Marland G, Andres RJ: Global, regional, and national fossil-fuel CO₂ emissions. Carbon Dioxide Information Analysis Center, Oak Ridge National Laboratory, U.S. Department of Energy, Oak Ridge, Tenn., U.S.A. doi 10.3334/CDIAC/00001_V2017 https://cdiac.ornl.gov/trends/emis/trends_glob_2014.html. 2017.
7. Yin J, Gentile P, Zhou S, Sullivan SC, Wang R, Zhang Y, Guo S: Large increase in global storm runoff extremes driven by climate and anthropogenic changes. *Nat Commun*. 2018;9:4389.
8. Patricola CM, Wehner MF: Anthropogenic influences on major tropical cyclone events. *Nature*. 2018;563:339-46.
9. Min SK, Zhang X, Zwiers FW, Hegerl GC: Human contribution to more-intense precipitation extremes. *Nature*. 2011;470:378-81.
10. Ali H, Fowler HJ, Mishra V: Global observational evidence of strong linkage between dew point temperature and precipitation extremes. *Geophys Res Lett*. 2018;45:12320-30.
11. Schar C, Vidale PL, Luthi D, Frei C, Haberli C, Liniger MA, Appenzeller C: The role of increasing temperature variability in European summer heatwaves. *Nature*. 2004;427:332-6.
12. Zarch MAA, Sivakumar B, Sharma A: Droughts in a warming climate: A global assessment of standardized precipitation index (SPI) and reconnaissance drought index (RDI). *J Hydrol*. 2015;526:183-95.
13. Hansel S, Ustrnul Z, Lupikasza E, Skalak P: Assessing seasonal drought variations and trends over Central Europe. *Adv Water Resour*. 2019;127:53-75.
14. Lewis SL, Maslin MA: Defining the Anthropocene. *Nature*. 2015;519:171-80.
15. Ellis EC, Kaplan JO, Fuller DQ, Vavrus S, Goldewijk KK, Verburg PH: Used planet: A global history. *Proc Natl Acad Sci USA*. 2013;110:7978-85.
16. Rockstrom J, Steffen W, Noone K, Persson A, Chapin FS, Lambin EF, et al.: A safe operating space for humanity. *Nature*. 2009;461:472-5.
17. Steffen W, Richardson K, Rockstrom J, Cornell SE, Fetzer I, Bennett EM, et al.: Sustainability. Planetary boundaries: guiding human development on a changing planet. *Science*. 2015;347:1259855.
18. Thomas CD, Cameron A, Green RE, Bakkenes M, Beaumont LJ, Collingham YC, et al.: Extinction risk from climate change. *Nature*. 2004;427:145-8.
19. Baker HS, Millar RJ, Karoly DJ, Beyerle U, Guillod BP, Mitchell D, et al.: Higher CO₂ concentrations increase extreme event risk in a 1.5 degrees C world. *Nat Clim Change*. 2018;8:604-+.
20. United Nations Framework Convention on Climate Change (UNFCCC): Paris Agreement. FCCC/CP/2015/10/Add. 1. 2015.
21. Pravalie R, Bandoc G: Nuclear energy: Between global electricity demand, worldwide decarbonisation imperativeness, and planetary environmental implications. *Journal of environmental management*. 2018;209:81-92.
22. Kopytko N, Perkins J: Climate change, nuclear power, and the adaptation-mitigation dilemma. *Energ Policy*. 2011;39:318-33.
23. Teravainen T, Lehtonen M, Martiskainen M: Climate change, energy security, and risk-debating nuclear new build in Finland, France and the UK. *Energ Policy*. 2011;39:3434-42.

24. Sanchez J: Nuclear fusion as a massive, clean, and inexhaustible energy source for the second half of the century: brief history, status, and perspective. *Energy Sci Eng.* 2014;2:165-76.
25. Kumar Y, Ringenberg J, Depuru SS, Devabhaktuni VK, Lee JW, Nikolaidis E, Andersen B, Afjeh A: Wind energy: Trends and enabling technologies. *Renew Sust Energ Rev.* 2016;53:209-24.
26. Devabhaktuni V, Alam M, Depuru SSSR, Green RC, Nims D, Near C: Solar energy: Trends and enabling technologies. *Renew Sust Energ Rev.* 2013;19:555-64.
27. Lund JW, Boyd TL: Direct utilization of geothermal energy 2015 worldwide review. *Geothermics.* 2016;60:66-93.
28. Ellabban O, Abu-Rub H, Blaabjerg F: Renewable energy resources: Current status, future prospects and their enabling technology. *Renew Sust Energ Rev.* 2014;39:748-64.
29. Moiola E, Mutschler R, Zuttel A: Renewable energy storage via CO₂ and H₂ conversion to methane and methanol: Assessment for small scale applications. *Renew Sust Energ Rev.* 2019;107:497-506.
30. Emonts B, Reuß M, Stenzel P, Welder L, Knicker F, Grube T, Görner K, Robinius M, Stolten D: Flexible sector coupling with hydrogen: A climate-friendly fuel supply for road transport. *Int J Hydrogen Energ.* 2019;44:12918-30.
31. Pehlken A, Albach S, Vogt T: Is there a resource constraint related to lithium ion batteries in cars? *Int J Life Cycle Ass.* 2017;22:40-53.
32. Andwari AM, Pesiridis A, Rajoo S, Martinez-Botas R, Esfahanian V: A review of battery electric vehicle technology and readiness levels. *Renew Sust Energ Rev.* 2017;78:414-30.
33. Ajanovic A, Haas R: Economic prospects and policy framework for hydrogen as fuel in the transport sector. *Energ Policy.* 2018;123:280-8.
34. Ball M, Weeda M: The hydrogen economy - Vision or reality? *Int J Hydrogen Energ.* 2015;40:7903-19.
35. Staffell I, Scamman D, Abad AV, Balcombe P, Dodds PE, Ekins P, Shah N, Ward KR: The role of hydrogen and fuel cells in the global energy system. *Energ Environ Sci.* 2019;12:463-91.
36. Scarlat N, Dallemand JF, Monforti-Ferrario F, Nita V: The role of biomass and bioenergy in a future bioeconomy: Policies and facts. *Environ Dev.* 2015;15:3-34.
37. Aro EM: From first generation biofuels to advanced solar biofuels. *Ambio.* 2016;45 Suppl 1:S24-31.
38. Murphy R, Woods J, Black M, McManus M: Global developments in the competition for land from biofuels. *Food Policy.* 2011;36:S52-S61.
39. Rathmann R, Szklo A, Schaeffer R: Land use competition for production of food and liquid biofuels: An analysis of the arguments in the current debate. *Renew Energ.* 2010;35:14-22.
40. Malcata FX: Microalgae and biofuels: a promising partnership? *Trends Biotechnol.* 2011;29:542-9.
41. Wijffels RH, Barbosa MJ: An outlook on microalgal biofuels. *Science.* 2010;329:796-9.
42. Reijnders L: Do biofuels from microalgae beat biofuels from terrestrial plants? *Trends Biotechnol.* 2008;26:349-50; author reply 51-2.
43. Nagarajan D, Lee DJ, Kondo A, Chang JS: Recent insights into biohydrogen production by microalgae - From biophotolysis to dark fermentation. *Biores Technol.* 2017;227:373-87.
44. Khetkorn W, Rastogi RP, Incharoensakdi A, Lindblad P, Madamwar D, Pandey A, Larroche C: Microalgal hydrogen production - A review. *Biores Technol.* 2017;243:1194-206.
45. UNESCO: <http://www.unesco.org/new/en/natural-sciences/science-technology/basic-sciences/life-sciences/biotechnology/>. Accessed on May 6, 2019.
46. Boethius A: Something rotten in Scandinavia: The world's earliest evidence of fermentation. *J Archaeol Sci.* 2016;66:169-80.
47. Liu L, Wang J, Rosenberg D, Zhao H, Lengyel G, Nadel D: Fermented beverage and food storage in 13,000 y-old stone mortars at Raqefet Cave, Israel: Investigating Natufian ritual feasting. *Journal of Archaeological Science: Reports.* 2018;21:783-93.
48. Gest H: The discovery of microorganisms by Robert Hooke and Antoni Van Leeuwenhoek, fellows of the Royal Society. *Notes Rec R Soc Lond.* 2004;58:187-201.

49. Hooke R: Micrographia, or some physiological descriptions of minute bodies made by magnifying glasses, with observations and inquiries thereupon. London, Printed by Jo Martyn, and Ja Allestry, printers to the Royal Society, 1665. 1665.
50. Mendel G: Versuche über Pflanzen-Hybriden. Verhandlungen des Naturforschenden Vereins zu Brünn. 1866;4:3-47
51. Bateson W: Genetical analysis and the theory of natural selection. Science. 1922;55:373.
52. Bateson W: An address ON MENDELIAN HEREDITY AND ITS APPLICATION TO MAN: Delivered before the Neurological Society of London, on Thursday, February 1st, 1906. Brit Med J. 1906;2:61-7.
53. Watson JD, Crick FH: The structure of DNA. Cold Spring Harb Symp Quant Biol. 1953;18:123-31.
54. Cohen SN, Chang ACY, Boyer HW, Helling RB: Construction of biologically functional bacterial plasmids *in-vitro*. Proc Natl Acad Sci USA. 1973;70:3240-4.
55. Genentech: First recombinant DNA product approved by The Food And Drug Administration. Press Release <https://www.gene.com/media/press-releases/4193/1982-10-29/first-recombinant-dna-product-approved-b>. 1982.
56. Ikeda M: Amino acid production processes. Adv Biochem Eng Biotechnol. 2003;79:1-35.
57. Singh R: Facts, growth, and opportunities in industrial biotechnology. Org Process Res Dev. 2011;15:175-9.
58. Demain AL: Microbial biotechnology. Trends Biotechnol. 2000;18:26-31.
59. Blankenship RE: Origin and early evolution of photosynthesis. Photosynth Res. 1992;33:91-111.
60. Govindjee, Shevela D: Adventures with cyanobacteria: a personal perspective. Front Plant Sci. 2011;2:28.
61. Savakis P, Hellingwerf KJ: Engineering cyanobacteria for direct biofuel production from CO₂. Curr Opin Biotechnol. 2015;33:8-14.
62. Nozzi NE, Oliver JW, Atsumi S: Cyanobacteria as a platform for biofuel production. Front Bioeng Biotechnol. 2013;1:7.
63. Zhou J, Meng H, Zhang W, Li Y: Production of industrial chemicals from CO₂ by engineering cyanobacteria. Adv Exp Med Biol. 2018;1080:97-116.
64. Angermayr SA, Gorchs Rovira A, Hellingwerf KJ: Metabolic engineering of cyanobacteria for the synthesis of commodity products. Trends Biotechnol. 2015;33:352-61.
65. Gao ZX, Zhao H, Li ZM, Tan XM, Lu XF: Photosynthetic production of ethanol from carbon dioxide in genetically engineered cyanobacteria. Energ Environ Sci. 2012;5:9857-65.
66. Dexter J, Fu PC: Metabolic engineering of cyanobacteria for ethanol production. Energ Environ Sci. 2009;2:857-64.
67. Li XQ, Shen CR, Liao JC: Isobutanol production as an alternative metabolic sink to rescue the growth deficiency of the glycogen mutant of *Synechococcus elongatus* PCC 7942. Photosynth Res. 2014;120:301-10.
68. Lan EI, Liao JC: Metabolic engineering of cyanobacteria for 1-butanol production from carbon dioxide. Metab Eng. 2011;13:353-63.
69. David C, Schmid A, Adrian L, Wilde A, Bühler K: Production of 1,2-propanediol in photoautotrophic *Synechocystis* is linked to glycogen turn-over. Biotechnol Bioeng. 2018;115:300-11.
70. Oliver JWK, Machado IMP, Yoneda H, Atsumi S: Cyanobacterial conversion of carbon dioxide to 2,3-butanediol. Proc Natl Acad Sci USA. 2013;110:1249-54.
71. Savakis PE, Angermayr SA, Hellingwerf KJ: Synthesis of 2,3-butanediol by *Synechocystis* sp. PCC 6803 via heterologous expression of a catabolic pathway from lactic acid- and enterobacteria. Metab Eng. 2013;20:121-30.
72. Ducat DC, Avelar-Rivas JA, Way JC, Silver PA: Rerouting carbon flux to enhance photosynthetic productivity. Appl Environ Microbiol. 2012;78:2660-8.
73. Lan EI, Wei CT: Metabolic engineering of cyanobacteria for the photosynthetic production of succinate. Metab Eng. 2016;38:483-93.

74. Angermayr SA, Paszota M, Hellingwerf KJ: Engineering a cyanobacterial cell factory for production of lactic acid. *Appl Environ Microbiol.* 2012;78:7098-106.
75. Ungerer J, Tao L, Davis M, Ghirardi M, Maness PC, Yu JP: Sustained photosynthetic conversion of CO₂ to ethylene in recombinant cyanobacterium *Synechocystis* 6803. *Energ Environ Sci.* 2012;5:8998-9006.
76. Yoshino T, Liang Y, Arai D, Maeda Y, Honda T, Muto M, Kakunaka N, Tanaka T: Alkane production by the marine cyanobacterium *Synechococcus* sp. NKBG15041c possessing the alpha-olefin biosynthesis pathway. *Appl Microbiol Biot.* 2015;99:1521-9.
77. Santos-Merino M, Garcillan-Barcia MP, de la Cruz F: Engineering the fatty acid synthesis pathway in *Synechococcus elongatus* PCC 7942 improves omega-3 fatty acid production. *Biotechnol Biofuels.* 2018;11:239.
78. Englund E, Shabestary K, Hudson EP, Lindberg P: Systematic overexpression study to find target enzymes enhancing production of terpenes in *Synechocystis* PCC 6803, using isoprene as a model compound. *Metab Eng.* 2018;49:164-77.
79. Gao X, Gao F, Liu D, Zhang H, Nie XQ, Yang C: Engineering the methylerythritol phosphate pathway in cyanobacteria for photosynthetic isoprene production from CO₂. *Energ Environ Sci.* 2016;9:1400-11.
80. Kiyota H, Okudac Y, Ito M, Hirai MY, Ikeuchi M: Engineering of cyanobacteria for the photosynthetic production of limonene from CO₂. *J Biotechnol.* 2014;185:1-7.
81. Korosh TC, Markley AL, Clark RL, McGinley LL, McMahon KD, Pflieger BF: Engineering photosynthetic production of L-lysine. *Metab Eng.* 2017;44:273-83.
82. Zheng LH, Zhang XY, Bai YP, Fan JH: Using algae cells to drive cofactor regeneration and asymmetric reduction for the synthesis of chiral chemicals. *Algal Res.* 2018;35:432-8.
83. Lassen LM, Nielsen AZ, Olsen CE, Bialek W, Jensen K, Moller BL, Jensen PE: Anchoring a plant cytochrome P450 via PsaM to the thylakoids in *Synechococcus* sp. PCC 7002: evidence for light-driven biosynthesis. *PLoS One.* 2014;9:e102184.
84. Xue Y, Zhang Y, Grace S, He QF: Functional expression of an *Arabidopsis* p450 enzyme, *p*-coumarate-3-hydroxylase, in the cyanobacterium *Synechocystis* PCC 6803 for the biosynthesis of caffeic acid. *J Appl Phycol.* 2014;26:219-26.
85. Hoschek A, Toepel J, Hochkeppel A, Karande R, Bühler B, Schmid A: Light-dependent and aeration-independent gram-scale hydroxylation of cyclohexane to cyclohexanol by CYP450 harboring *Synechocystis* sp. PCC 6803. *Biotechnol J.* 2019:e1800724.
86. Königer K, Gómez Baraibar A, Mügge C, Paul CE, Hollmann F, Nowaczyk MM, Kourist R: Recombinant cyanobacteria for the asymmetric reduction of C=C bonds fueled by the biocatalytic oxidation of water. *Angew Chem Int Edit.* 2016;55:5582-5.
87. Rögner M: Metabolic engineering of cyanobacteria for the production of hydrogen from water. *Biochem Soc T.* 2013;41:1254-9.
88. Srirangan K, Pyne ME, Perry Chou C: Biochemical and genetic engineering strategies to enhance hydrogen production in photosynthetic algae and cyanobacteria. *Biores Technol.* 2011;102:8589-604.
89. Bothe H, Winkelmann S, Boison G: Maximizing hydrogen production by cyanobacteria. *Z Naturforsch C.* 2008;63:226-32.
90. Devroe EJ, Kosuri S, Berry DA, Afeyan NB, Skraly FA, Robertson DE, Green B, Ridley CP: US7785861 Hyperphotosynthetic organisms. US Patent 2008.
91. Reppas NB, Ridley CP: US7794969B1 Methods and compositions for the recombinant biosynthesis of n-alkanes. US Patent. 2010.
92. Joule Unlimited: Joule Biotechnologies selected by AlwaysOn as a GoingGreen Top 100 Winner. Press release <http://www.jouleunlimited.com/news/2009/joule-biotechnologies-selected-always-on-going-green-top-100-winner>. 2009.
93. Joule Unlimited: Solar fuel pioneered by Joule named among world's 10 most important emerging technologies. Press release <http://www.jouleunlimited.com/news/2010/solar-fuel-pioneered-joule-named-among-worlds-10-most-important-emerging-technologies>. 2010.

94. Joule Unlimited: Joule named among 50 most innovative companies in the world. Press release <http://www.jouleunlimited.com/news/2010/joule-named-among-50-most-innovative-companies-world>. 2010.
95. Lane J: Heat Death: Joule Unlimited collapses as oil prices flag, time passes, pressure mounts. Biofuel Digest <http://www.biofuelsdigest.com/bdigest/2017/07/18/heat-death-joule-unlimited-collapses-as-oil-prices-fall-time-passes-pressure-mounts/>. 2017.
96. Photanol: Scale up Photanol BV to build demonstration plant at AkzoNobel site in Delfzijl. Press release 7.9.18 <https://www.photanol.com/single-post/2018/09/07/Press-release-7918>. 2018.
97. Lima-Ramos J, Tufvesson P, Woodley JM: Application of environmental and economic metrics to guide the development of biocatalytic processes. *Green Process Synth.* 2014;3:195-213.
98. Tufvesson P, Lima-Ramos J, Al Haque N, Gernaey KV, Woodley JM: Advances in the process development of biocatalytic processes. *Org Process Res Dev.* 2013;17:1233-8.
99. Straathof AJJ, Panke S, Schmid A: The production of fine chemicals by biotransformations. *Curr Opin Biotechnol.* 2002;13:548-56.
100. Lee SY, Kim HU: Systems strategies for developing industrial microbial strains. *Nat Biotechnol.* 2015;33:1061-72.
101. Schmid A, Dordick JS, Hauer B, Kiener A, Wubbolts M, Witholt B: Industrial biocatalysis today and tomorrow. *Nature.* 2001;409:258-68.
102. Kuhn D, Kholiq MA, Heinzle E, Bühler B, Schmid A: Intensification and economic and ecological assessment of a biocatalytic oxyfunctionalization process. *Green Chem.* 2010;12:815-27.
103. Kratzer R, Woodley JM, Nidetzky B: Rules for biocatalyst and reaction engineering to implement effective, NAD(P)H-dependent, whole cell bioreductions. *Biotechnol Adv.* 2015;33:1641-52.
104. Beloqui A, de Maria PD, Golyshin PN, Ferrer M: Recent trends in industrial microbiology. *Curr Opin Microbiol.* 2008;11:240-8.
105. Davids T, Schmidt M, Böttcher D, Bornscheuer UT: Strategies for the discovery and engineering of enzymes for biocatalysis. *Curr Opin Chem Biol.* 2013;17:215-20.
106. Jiang L, Althoff EA, Clemente FR, Doyle L, Rothlisberger D, Zanghellini A, et al.: *De novo* computational design of retro-aldol enzymes. *Science.* 2008;319:1387-91.
107. Kaplan J, DeGrado WF: *De novo* design of catalytic proteins. *Proc Natl Acad Sci USA.* 2004;101:11566-70.
108. Campbell K, Xia JY, Nielsen J: The impact of systems biology on bioprocessing. *Trends Biotechnol.* 2017;35:1156-68.
109. Park JH, Lee KH, Kim TY, Lee SY: Metabolic engineering of *Escherichia coli* for the production of L-valine based on transcriptome analysis and *in silico* gene knockout simulation. *Proc Natl Acad Sci USA.* 2007;104:7797-802.
110. Kuhn D, Fritsch FS, Zhang X, Wendisch VF, Blank LM, Bühler B, Schmid A: Subtoxic product levels limit the epoxidation capacity of recombinant *E. coli* by increasing microbial energy demands. *J Biotechnol.* 2013;163:194-203.
111. Agren R, Otero JM, Nielsen J: Genome-scale modeling enables metabolic engineering of *Saccharomyces cerevisiae* for succinic acid production. *J Ind Microbiol Biot.* 2013;40:735-47.
112. Anfelt J, Hallstrom B, Nielsen J, Uhlen M, Hudson EP: Using transcriptomics to improve butanol tolerance of *Synechocystis* sp. strain PCC 6803. *Appl Environ Microbiol.* 2013;79:7419-27.
113. Julsing MK, Schrewe M, Cornelissen S, Hermann I, Schmid A, Bühler B: Outer membrane protein AlkL boosts biocatalytic oxyfunctionalization of hydrophobic substrates in *Escherichia coli*. *Appl Environ Microbiol.* 2012;78:5724-33.
114. Yim H, Haselbeck R, Niu W, Pujol-Baxley C, Burgard A, Boldt J, et al.: Metabolic engineering of *Escherichia coli* for direct production of 1,4-butanediol. *Nat Chem Biol.* 2011;7:445-52.

115. Kind S, Neubauer S, Becker J, Yamamoto M, Volkert M, von Abendroth G, Zelder O, Wittmann C: From zero to hero - Production of bio-based nylon from renewable resources using engineered *Corynebacterium glutamicum*. *Metab Eng.* 2014;25:113-23.
116. Kadisch M, Julsing MK, Schrewe M, Jehmlich N, Scheer B, von Bergen M, Schmid A, Bühler B: Maximization of cell viability rather than biocatalyst activity improves whole-cell -oxyfunctionalization performance. *Biotechnol Bioeng.* 2017;114:874-84.
117. Woodley JM: Protein engineering of enzymes for process applications. *Curr Opin Chem Biol.* 2013;17:310-6.
118. Blank LM, Ionidis G, Ebert BE, Bühler B, Schmid A: Metabolic response of *Pseudomonas putida* during redox biocatalysis in the presence of a second octanol phase. *FEBS J.* 2008;275:5173-90.
119. Schrewe M, Julsing MK, Lange K, Czarnotta E, Schmid A, Bühler B: Reaction and catalyst engineering to exploit kinetically controlled whole-cell multistep biocatalysis for terminal FAME oxyfunctionalization. *Biotechnol Bioeng.* 2014;111:1820-30.
120. Willrodt C, Hoschek A, Bühler B, Schmid A, Julsing MK: Decoupling production from growth by magnesium sulfate limitation boosts de novo limonene production. *Biotechnol Bioeng.* 2016;113:1305-14.
121. Schügerl K: Integrated processing of biotechnology products. *Biotechnol Adv.* 2000;18:581-99.
122. Keller K, Friedmann T, Boxman A: The bioseparation needs for tomorrow. *Trends Biotechnol.* 2001;19:438-41.
123. Zhao HM, Tan TW: Industrial biotechnology: Tools and applications. *Biotechnol Adv.* 2015;33:1393-4.
124. Ahuja S: Handbook of Bioseparations, Volume 2, 1st Edition. eBook ISBN: 9780080507798. 2000.
125. Brandenbusch C, Bühler B, Hoffmann P, Sadowski G, Schmid A: Efficient phase separation and product recovery in organic-aqueous bioprocessing using supercritical carbon dioxide. *Biotechnol Bioeng.* 2010;107:642-51.
126. Collins J, Grund M, Brandenbusch C, Sadowski G, Schmid A, Bühler B: The dynamic influence of cells on the formation of stable emulsions in organic-aqueous biotransformations. *J Ind Microbiol Biotechnol.* 2015;42:1011-26.
127. Arnold FH: The nature of chemical innovation: new enzymes by evolution. *Q Rev Biophys.* 2015;48:404-10.
128. Packer MS, Liu DR: Methods for the directed evolution of proteins. *Nat Rev Genet.* 2015;16:379-94.
129. Choi KR, Jang WD, Yang D, Cho JS, Park D, Lee SY: Systems metabolic engineering strategies: Integrating systems and synthetic biology with metabolic engineering. *Trends Biotechnol.* 2019.
130. Chae TU, Choi SY, Kim JW, Ko YS, Lee SY: Recent advances in systems metabolic engineering tools and strategies. *Curr Opin Biotechnol.* 2017;47:67-82.
131. Nielsen J, Keasling JD: Engineering cellular metabolism. *Cell.* 2016;164:1185-97.
132. Oliver JW, Atsumi S: Metabolic design for cyanobacterial chemical synthesis. *Photosynth Res.* 2014;120:249-61.
133. Sun T, Li S, Song X, Diao J, Chen L, Zhang W: Toolboxes for cyanobacteria: Recent advances and future direction. *Biotechnol Adv.* 2018;36:1293-307.
134. Angermayr SA, van der Woude AD, Correddu D, Vreugdenhil A, Verrone V, Hellingwerf KJ: Exploring metabolic engineering design principles for the photosynthetic production of lactic acid by *Synechocystis* sp. PCC6803. *Biotechnol Biofuels.* 2014;7:99.
135. Angermayr SA, Hellingwerf KJ: On the use of metabolic control analysis in the optimization of cyanobacterial biosolar cell factories. *J Phys Chem B.* 2013;117:11169-75.
136. Hoschek A, Bühler B, Schmid A: Stabilization and scale-up of photosynthesis-driven ω -hydroxylation of nonanoic acid methyl ester by two-liquid phase whole-cell biocatalysis. *Biotechnol Bioeng.* 2019.

137. Hoschek A, Heuschkel I, Schmid A, Bühler B, Karande R, Bühler K: Mixed-species biofilms for high-cell-density application of *Synechocystis* sp. PCC 6803 in capillary reactors for continuous cyclohexane oxidation to cyclohexanol. *Biores Technol.* 2019;282:171-8.
138. Grobbelaar JU: Factors governing algal growth in photobioreactors: the "open" versus "closed" debate. *J Appl Phycol.* 2009;21:489-92.
139. Huang QS, Jiang FH, Wang LZ, Yang C: Design of photobioreactors for mass cultivation of photosynthetic organisms. *Engineering-Proc.* 2017;3:318-29.
140. Morweiser M, Kruse O, Hankamer B, Posten C: Developments and perspectives of photobioreactors for biofuel production. *Appl Microbiol Biot.* 2010;87:1291-301.
141. Borirak O, de Koning LJ, van der Woude AD, Hoefsloot HCJ, Dekker HL, Roseboom W, de Koster CG, Hellingwerf KJ: Quantitative proteomics analysis of an ethanol- and a lactate-producing mutant strain of *Synechocystis* sp. PCC 6803. *Biotechnol Biofuels.* 2015;8.
142. Janasch M, Asplund-Samuelsson J, Steuer R, Hudson EP: Kinetic modeling of the Calvin cycle identifies flux control and stable metabolomes in *Synechocystis* carbon fixation. *J Exp Bot.* 2019;70:973-83.
143. Knoop H, Gründel M, Zilliges Y, Lehmann R, Hoffmann S, Lockau W, Steuer R: Flux balance analysis of cyanobacterial metabolism: the metabolic network of *Synechocystis* sp. PCC 6803. *PLoS Comput Biol.* 2013;9:e1003081.
144. Knoop H, Steuer R: A computational analysis of stoichiometric constraints and trade-offs in cyanobacterial biofuel production. *Front Bioeng Biotechnol.* 2015;3:47.
145. Knoop H, Zilliges Y, Lockau W, Steuer R: The metabolic network of *Synechocystis* sp. PCC 6803: systemic properties of autotrophic growth. *Plant Physiol.* 2010;154:410-22.
146. Nogales J, Gudmundsson S, Knight EM, Palsson BO, Thiele I: Detailing the optimality of photosynthesis in cyanobacteria through systems biology analysis. *Proc Natl Acad Sci USA.* 2012;109:2678-83.
147. Young JD, Shastri AA, Stephanopoulos G, Morgan JA: Mapping photoautotrophic metabolism with isotopically nonstationary C-13 flux analysis. *Metab Eng.* 2011;13:656-65.
148. Schuurmans RM, Matthijs JC, Hellingwerf KJ: Transition from exponential to linear photoautotrophic growth changes the physiology of *Synechocystis* sp. PCC 6803. *Photosynth Res.* 2017;132:69-82.
149. Straka L, Rittmann BE: Effect of culture density on biomass production and light utilization efficiency of *Synechocystis* sp. PCC 6803. *Biotechnol Bioeng.* 2018;115:507-11.
150. Kwon JH, Rögner M, Rexroth S: Direct approach for bioprocess optimization in a continuous flat-bed photobioreactor system. *J Biotechnol.* 2012;162:156-62.
151. Kim HW, Vannela R, Zhou C, Rittmann BE: Nutrient acquisition and limitation for the photoautotrophic growth of *Synechocystis* sp. PCC 6803 as a renewable biomass source. *Biotechnol Bioeng.* 2011;108:277-85.
152. Touloupakis E, Cicchi B, Torzillo G: A bioenergetic assessment of photosynthetic growth of *Synechocystis* sp. PCC 6803 in continuous cultures. *Biotechnol Biofuels.* 2015;8.
153. Zavrel T, Ocnasova P, Cerveny J: Phenotypic characterization of *Synechocystis* sp. PCC 6803 substrains reveals differences in sensitivity to abiotic stress. *PLoS One.* 2017;12:e0189130.
154. Zavrel T, Sinetova MA, Buzova D, Literakova P, Cerveny J: Characterization of a model cyanobacterium *Synechocystis* sp. PCC 6803 autotrophic growth in a flat-panel photobioreactor. *Eng Life Sci.* 2015;15:122-32.
155. Yano J, Yachandra V: Mn4Ca cluster in photosynthesis: Where and how water is oxidized to dioxygen. *Chem Rev.* 2014;114:4175-205.
156. Fischer WW, Hemp J, Johnson JE: Evolution of oxygenic photosynthesis. *Annu Rev Earth Pl Sc.* 2016;44:647-83.
157. Mondal J, Bruce BD: Ferredoxin: the central hub connecting photosystem I to cellular metabolism. *Photosynthetica.* 2018;56:279-93.
158. Curien G, Flori S, Villanova V, Magneschi L, Giustini C, Forti G, et al.: The water to water cycles in microalgae. *Plant Cell Physiol.* 2016;57:1354-63.

159. Allahverdiyeva Y, Isojarvi J, Zhang P, Aro EM: Cyanobacterial oxygenic photosynthesis is protected by flavodiiron proteins. *Life*. 2015;5:716-43.
160. Allahverdiyeva Y, Ermakova M, Eisenhut M, Zhang PP, Richaud P, Hagemann M, Cournac L, Aro EM: Interplay between flavodiiron proteins and photorespiration in *Synechocystis* sp. PCC 6803. *Journal of Biological Chemistry*. 2011;286:24007-14.
161. Shimakawa G, Shaku K, Nishi A, Hayashi R, Yamamoto H, Sakamoto K, Makino A, Miyake C: FLAVODIIRON2 and FLAVODIIRON4 proteins mediate an oxygen-dependent alternative electron flow in *Synechocystis* sp. PCC 6803 under CO₂-limited conditions. *Plant Physiol*. 2015;167:472-U732.
162. Allahverdiyeva Y, Mustila H, Ermakova M, Bersanini L, Richaud P, Ajlani G, Battchikova N, Cournac L, Aro EM: Flavodiiron proteins Flv1 and Flv3 enable cyanobacterial growth and photosynthesis under fluctuating light. *Proc Natl Acad Sci USA*. 2013;110:4111-6.
163. Bersanini L, Battchikova N, Jokel M, Rehman A, Vass I, Allahverdiyeva Y, Aro EM: Flavodiiron protein Flv2/Flv4-related photoprotective mechanism dissipates excitation pressure of PSII in cooperation with phycobilisomes in cyanobacteria. *Plant Physiol*. 2014;164:805-18.
164. Wilhelm C, Selmar D: Energy dissipation is an essential mechanism to sustain the viability of plants: The physiological limits of improved photosynthesis. *J Plant Physiol*. 2011;168:79-87.
165. Paul MJ, Foyer CH: Sink regulation of photosynthesis. *J Exp Bot*. 2001;52:1383-400.
166. Lea-Smith DJ, Bombelli P, Vasudevan R, Howe CJ: Photosynthetic, respiratory and extracellular electron transport pathways in cyanobacteria. *Biochimica et Biophysica Acta, Bioenergetics*. 2016;1857:247-55.
167. Kramer DM, Evans JR: The importance of energy balance in improving photosynthetic productivity. *Plant Physiol*. 2011;155:70-8.
168. Abramson BW, Kachel B, Kramer DM, Ducat DC: Increased photochemical efficiency in cyanobacteria via an engineered sucrose sink. *Plant Cell Physiol*. 2016;57:2451-60.
169. Berepiki A, Hitchcock A, Moore CM, Bibby TS: Tapping the unused potential of photosynthesis with a heterologous electron sink. *Acs Synth Biol*. 2016;5:1369-75.
170. Zhou J, Zhang FL, Meng HK, Zhang YP, Li Y: Introducing extra NADPH consumption ability significantly increases the photosynthetic efficiency and biomass production of cyanobacteria. *Metab Eng*. 2016;38:217-27.
171. Oliver JWK, Atsumi S: A carbon sink pathway increases carbon productivity in cyanobacteria. *Metab Eng*. 2015;29:106-12.
172. Xiong W, Morgan JA, Ungerer J, Wang B, Maness PC, Yu JP: The plasticity of cyanobacterial metabolism supports direct CO₂ conversion to ethylene. *Nature Plants*. 2015;1.
173. Angermayr SA, Rovira AG, Hellingwerf KJ: Metabolic engineering of cyanobacteria for the synthesis of commodity products. *Trends Biotechnol*. 2015;33:352-61.
174. Kaneko T, Sato S, Kotani H, Tanaka A, Asamizu E, Nakamura Y, et al.: Sequence analysis of the genome of the unicellular cyanobacterium *Synechocystis* sp. strain PCC 6803. II. Sequence determination of the entire genome and assignment of potential protein-coding regions (supplement). *DNA Res*. 1996;3:185-209.
175. Trautmann D, Voss B, Wilde A, Al-Babili S, Hess WR: Microevolution in cyanobacteria: re-sequencing a motile substrain of *Synechocystis* sp. PCC 6803. *DNA Res*. 2012;19:435-48.
176. Ding Q, Chen G, Wang Y, Wei D: Identification of specific variations in a non-motile Strain of cyanobacterium *Synechocystis* sp. PCC 6803 originated from ATCC 27184 by whole genome resequencing. *Int J Mol Sci*. 2015;16:24081-93.
177. Kanesaki Y, Shiwa Y, Tajima N, Suzuki M, Watanabe S, Sato N, Ikeuchi M, Yoshikawa H: Identification of substrain-specific mutations by massively parallel whole-genome resequencing of *Synechocystis* sp. PCC 6803. *DNA Res*. 2012;19:67-79.
178. Wang B, Eckert C, Maness PC, Yu J: A genetic toolbox for modulating the expression of heterologous genes in the cyanobacterium *Synechocystis* sp. PCC 6803. *Acs Synth Biol*. 2018;7:276-86.

179. Sebesta J, Werner A, Peebles CAM: Genetic engineering of cyanobacteria: Design, implementation, and characterization of recombinant *Synechocystis* sp. PCC 6803. *Methods Mol Biol.* 2019;1927:139-54.
180. Liu D, Pakrasi HB: Exploring native genetic elements as plug-in tools for synthetic biology in the cyanobacterium *Synechocystis* sp. PCC 6803. *Microb Cell Fact.* 2018;17:48.
181. Albers SC, Gallegos VA, Peebles CA: Engineering of genetic control tools in *Synechocystis* sp. PCC 6803 using rational design techniques. *J Biotechnol.* 2015;216:36-46.
182. Abe K, Sakai Y, Nakashima S, Araki M, Yoshida W, Sode K, Ikebukuro K: Design of riboregulators for control of cyanobacterial (*Synechocystis*) protein expression. *Biotechnol Lett.* 2014;36:287-94.
183. Zang X, Liu B, Liu S, Arunakumara KK, Zhang X: Optimum conditions for transformation of *Synechocystis* sp. PCC 6803. *J Microbiol.* 2007;45:241-5.
184. Cheah YE, Albers SC, Peebles CA: A novel counter-selection method for markerless genetic modification in *Synechocystis* sp. PCC 6803. *Biotechnol Progr.* 2013;29:23-30.
185. Ruffing AM: Engineered cyanobacteria: teaching an old bug new tricks. *Bioeng Bugs.* 2011;2:136-49.
186. Fujisawa T, Narikawa R, Maeda SI, Watanabe S, Kanesaki Y, Kobayashi K, et al.: CyanoBase: a large-scale update on its 20th anniversary. *Nucleic Acids Res.* 2017;45:D551-D4.
187. Nakamura Y, Kaneko T, Hirose M, Miyajima N, Tabata S: CyanoBase, a WWW database containing the complete nucleotide sequence of the genome of *Synechocystis* sp. PCC 6803. *Nucleic Acids Res.* 1998;26:63-7.
188. You L, Berla B, He L, Pakrasi HB, Tang YJ: C-13-MFA delineates the photomixotrophic metabolism of *Synechocystis* sp PCC 6803 under light-and carbon-sufficient conditions. *Biotechnol J.* 2014;9:684-92.
189. You L, He L, Tang YJ: Photoheterotrophic fluxome in *Synechocystis* sp. PCC 6803 and its implications for cyanobacterial bioenergetics. *J Bacteriol.* 2015;197:943-50.
190. Yoshikawa K, Kojima Y, Nakajima T, Furusawa C, Hirasawa T, Shimizu H: Reconstruction and verification of a genome-scale metabolic model for *Synechocystis* sp. PCC 6803. *Appl Microbiol Biot.* 2011;92:347-58.
191. Hernandez-Prieto MA, Semeniuk TA, Giner-Lamia J, Futschik ME: The transcriptional landscape of the photosynthetic model cyanobacterium *Synechocystis* sp. PCC 6803. *Sci Rep-Uk.* 2016;6:22168.
192. Hernandez-Prieto MA, Futschik ME: CyanoEXpress: A web database for exploration and visualisation of the integrated transcriptome of cyanobacterium *Synechocystis* sp. PCC 6803. *Bioinformatics.* 2012;8:634-8.
193. Branco Dos Santos F, Du W, Hellingwerf KJ: Corrigendum: *Synechocystis*: not just a plug-bug for CO₂, but a green *E. coli*. *Front Bioeng Biotechnol.* 2016;4:32.
194. Branco Dos Santos F, Du W, Hellingwerf KJ: *Synechocystis*: not just a plug-bug for CO₂, but a green *E. coli*. *Front Bioeng Biotechnol.* 2014;2:36.
195. Stephenson PG, Moore CM, Terry MJ, Zubkov MV, Bibby TS: Improving photosynthesis for algal biofuels: toward a green revolution. *Trends Biotechnol.* 2011;29:615-23.
196. Mullineaux CW: Electron transport and light-harvesting switches in cyanobacteria. *Front Plant Sci.* 2014;5.
197. Roach T, Krieger-Liszka A: Regulation of photosynthetic electron transport and photoinhibition. *Curr Protein Pept Sc.* 2014;15:351-62.
198. Tikkanen M, Grieco M, Nurmi M, Rantala M, Suorsa M, Aro EM: Regulation of the photosynthetic apparatus under fluctuating growth light. *Philos Trans R Soc Lond B Biol Sci.* 2012;367:3486-93.
199. Wagner H, Jakob T, Fanesi A, Wilhelm C: Towards an understanding of the molecular regulation of carbon allocation in diatoms: the interaction of energy and carbon allocation. *Philos T R Soc B.* 2017;372.

200. Wilhelm C, Jakob T: From photons to biomass and biofuels: evaluation of different strategies for the improvement of algal biotechnology based on comparative energy balances. *Appl Microbiol Biot.* 2011;92:909-19.
201. Rosgaard L, de Porcellinis AJ, Jacobsen JH, Frigaard NU, Sakuragi Y: Bioengineering of carbon fixation, biofuels, and biochemicals in cyanobacteria and plants. *J Biotechnol.* 2012;162:134-47.
202. Hoschek A, Bühler B, Schmid A: Overcoming the gas-liquid mass transfer of oxygen by coupling photosynthetic water oxidation with biocatalytic oxyfunctionalization. *Angew Chem Int Edit.* 2017;56:15146-9.
203. Böhmer S, Köninger K, Gómez-Baraibar A, Bojarra S, Mügge C, Schmidt S, Nowaczyk MM, Kourist R: Enzymatic oxyfunctionalization driven by photosynthetic water-splitting in the cyanobacterium *Synechocystis* sp. PCC 6803. *Catalysts.* 2017;7.
204. Wlodarczyk A, Gnanasekaran T, Nielsen AZ, Zulu NN, Mellor SB, Luckner M, et al.: Metabolic engineering of light-driven cytochrome P450 dependent pathways into *Synechocystis* sp. PCC 6803. *Metab Eng.* 2016;33:1-11.
205. Itoh K, Nakamura K, Aoyama T, Matsuba R, Kakimoto T, Murakami M, et al.: Photobiocatalyzed asymmetric reduction of ketones using *Chlorella* sp. MK201. *Biotechnol Lett.* 2012;34:2083-6.
206. Savakis P, Tan X, Du W, Branco dos Santos F, Lu X, Hellingwerf KJ: Photosynthetic production of glycerol by a recombinant cyanobacterium. *J Biotechnol.* 2015;195:46-51.
207. Raven JA, Wollenweber B, Handley LL: A comparison of ammonium and nitrate as nitrogen sources for photolithotrophs. *New Phytol.* 1992;121:19-32.
208. Ohmori M, Ohmori K, Strotmann H: Inhibition of nitrate uptake by ammonia in a blue-green alga, *Anabaena cylindrica*. *Arch Microbiol.* 1977;114:225-9.
209. Dortch Q: The interaction between ammonium and nitrate uptake in phytoplankton. *Mar Ecol Prog Ser.* 1990;61:183-201.
210. Flynn KJ: Algal carbon-nitrogen metabolism: a biochemical basis for modeling the interactions between nitrate and ammonium uptake. *J Plankton Res.* 1991;13:373-87.
211. Bienfang PK: Steady state analysis of nitrate-ammonium assimilation by phytoplankton. *Limnol Oceanogr.* 1975;20:402-11.
212. Dai GZ, Qiu BS, Forchhammer K: Ammonium tolerance in the cyanobacterium *Synechocystis* sp. strain PCC 6803 and the role of the psbA multigene family. *Plant Cell Environ.* 2014;37:840-51.
213. Markou G, Depraetere O, Muylaert K: Effect of ammonia on the photosynthetic activity of *Arthrospira* and *Chlorella*: A study on chlorophyll fluorescence and electron transport. *Algal Res.* 2016;16:449-57.
214. Drath M, Kloft N, Batschauer A, Marin K, Novak J, Forchhammer K: Ammonia triggers photodamage of photosystem II in the cyanobacterium *Synechocystis* sp. strain PCC 6803. *Plant Physiol.* 2008;147:206-15.
215. Ludwig M, Bryant DA: Acclimation of the global transcriptome of the cyanobacterium *Synechococcus* sp. strain PCC 7002 to nutrient limitations and different nitrogen sources. *Front Microbiol.* 2012;3:145.
216. Slovacek RE, Hind G: Energetic factors affecting carbon dioxide fixation in isolated chloroplasts. *Plant Physiol.* 1980;65:526-32.
217. Jakob T, Wagner H, Stehfest K, Wilhelm C: A complete energy balance from photons to new biomass reveals a light- and nutrient-dependent variability in the metabolic costs of carbon assimilation. *J Exp Bot.* 2007;58:2101-12.
218. Wagner H, Jakob T, Wilhelm C: Balancing the energy flow from captured light to biomass under fluctuating light conditions. *New Phytol.* 2006;169:95-108.
219. Gilbert M, Wilhelm C, Richter M: Bio-optical modelling of oxygen evolution using *in vivo* fluorescence: Comparison of measured and calculated photosynthesis/irradiance (P-I) curves in four representative phytoplankton species. *J Plant Physiol.* 2000;157:307-14.

220. Halsey KH, O'Malley RT, Graff JR, Milligan AJ, Behrenfeld MJ: A common partitioning strategy for photosynthetic products in evolutionarily distinct phytoplankton species. *New Phytol.* 2013;198:1030-8.
221. Rippka R, Deruelles J, Waterbury JB, Herdman M, Stanier RY: Generic assignments, strain histories and properties of pure cultures of cyanobacteria. *J Gen Microbiol.* 1979;111:1-61.
222. Porra RJ, Thompson WA, Kriedemann PE: Determination of accurate extinction coefficients and simultaneous-equations for assaying chlorophylls *a* and *b* extracted with 4 different solvents - verification of the concentration of chlorophyll standards by atomic absorption spectroscopy. *Biochimica et Biophysica Acta, Bioenergetics* 1989;975:384-94.
223. Schreiber U, Klughammer C, Kolbowski J: Assessment of wavelength-dependent parameters of photosynthetic electron transport with a new type of multi-color PAM chlorophyll fluorometer. *Photosynth Res.* 2012;113:127-44.
224. Baker NR: Chlorophyll fluorescence: A probe of photosynthesis *in vivo*. *Annu Rev Plant Biol.* 2008;59:89-113.
225. Campbell D, Hurry V, Clarke AK, Gustafsson P, Oquist G: Chlorophyll fluorescence analysis of cyanobacterial photosynthesis and acclimation. *Microbiol Mol Biol Rev.* 1998;62:667-83.
226. Schuurmans RM, van Alphen P, Schuurmans JM, Matthijs HC, Hellingwerf KJ: Comparison of the photosynthetic yield of cyanobacteria and green algae: Different methods give different answers. *PLoS One.* 2015;10:e0139061.
227. Acuna AM, Snellenburg JJ, Gwizdala M, Kirilovsky D, van Grondelle R, van Stokkum IHM: Resolving the contribution of the uncoupled phycobilisomes to cyanobacterial pulse-amplitude modulated (PAM) fluorometry signals. *Photosynth Res.* 2016;127:91-102.
228. Ogawa T, Misumi M, Sonoike K: Estimation of photosynthesis in cyanobacteria by pulse-amplitude modulation chlorophyll fluorescence: problems and solutions. *Photosynth Res.* 2017;133:63-73.
229. Blache U, Jakob T, Su W, Wilhelm C: The impact of cell-specific absorption properties on the correlation of electron transport rates measured by chlorophyll fluorescence and photosynthetic oxygen production in planktonic algae. *Plant Physiol Bioch.* 2011;49:801-8.
230. Gilbert M, Domin A, Becker A, Wilhelm C: Estimation of primary productivity by chlorophyll *a* *in vivo* fluorescence in freshwater phytoplankton. *Photosynthetica.* 2000;38:111-26.
231. Goldman JAL, Kranz SA, Young JN, Tortell PD, Stanley RHR, Bender ML, Morel FMM: Gross and net production during the spring bloom along the Western Antarctic Peninsula. *New Phytol.* 2015;205:182-91.
232. Feist AM, Palsson BO: The biomass objective function. *Curr Opin Microbiol.* 2010;13:344-9.
233. Ohashi Y, Shi W, Takatani N, Aichi M, Maeda S, Watanabe S, Yoshikawa H, Omata T: Regulation of nitrate assimilation in cyanobacteria. *J Exp Bot.* 2011;62:1411-24.
234. Flores E, Guerrero MG, Losada M: Photosynthetic nature of nitrate uptake and reduction in the cyanobacterium *Anacystis nidulans*. *Biochim Biophys Acta.* 1983;722:408-16.
235. Asada K: The water-water cycle as alternative photon and electron sinks. *Philos Trans R Soc Lond B Biol Sci.* 2000;355:1419-30.
236. Zhang P, Eisenhut M, Brandt AM, Carmel D, Silen HM, Vass I, Allahverdiyeva Y, Salminen TA, Aro EM: Operon *flv4-flv2* provides cyanobacterial photosystem II with flexibility of electron transfer. *Plant Cell.* 2012;24:1952-71.
237. Chukhutsina V, Bersanini L, Aro EM, van Amerongen H: Cyanobacterial *flv4-2* operon-encoded proteins optimize light harvesting and charge separation in photosystem II. *Mol Plant.* 2015;8:747-61.
238. Allen JF: Cyclic, pseudocyclic and noncyclic photophosphorylation: new links in the chain. *Trends Plant Sci.* 2003;8:15-9.
239. Pfannschmidt T, Nilsson A, Allen JF: Photosynthetic control of chloroplast gene expression. *Nature.* 1999;397:625-8.
240. Fujita Y, Murakami A, Ohki K: Regulation of photosystem composition in the cyanobacterial photosynthetic system - the regulation occurs in response to the redox state of the electron pool located between the 2 photosystems. *Plant Cell Physiol.* 1987;28:283-92.

241. Li H, Sherman LA: A redox-responsive regulator of photosynthesis gene expression in the cyanobacterium *Synechocystis* sp. strain PCC 6803. *J Bacteriol.* 2000;182:4268-77.
242. Oliver NJ, Rabinovitch-Deere CA, Carroll AL, Nozzi NE, Case AE, Atsumi S: Cyanobacterial metabolic engineering for biofuel and chemical production. *Curr Opin Chem Biol.* 2016;35:43-50.
243. Knoot CJ, Ungerer J, Wangikar PP, Pakrasi HB: Cyanobacteria: Promising biocatalysts for sustainable chemical production. *J Biol Chem.* 2018;293:5044-52.
244. Veetil VP, Angermayr SA, Hellingwerf KJ: Ethylene production with engineered *Synechocystis* sp. PCC 6803 strains. *Microb Cell Fact.* 2017;16:34.
245. Lindberg P, Park S, Melis A: Engineering a platform for photosynthetic isoprene production in cyanobacteria, using *Synechocystis* as the model organism. *Metab Eng.* 2010;12:70-9.
246. Liu XY, Sheng J, Curtiss R: Fatty acid production in genetically modified cyanobacteria. *Proc Natl Acad Sci USA.* 2011;108:6899-904.
247. Wang B, Pugh S, Nielsen DR, Zhang WW, Meldrum DR: Engineering cyanobacteria for photosynthetic production of 3-hydroxybutyrate directly from CO₂. *Metab Eng.* 2013;16:68-77.
248. Jacobsen JH, Frigaard NU: Engineering of photosynthetic mannitol biosynthesis from CO₂ in a cyanobacterium. *Metab Eng.* 2014;21:60-70.
249. Liang FY, Englund E, Lindberg P, Lindblad P: Engineered cyanobacteria with enhanced growth show increased ethanol production and higher biofuel to biomass ratio. *Metab Eng.* 2018;46:51-9.
250. Liang F, Lindblad P: *Synechocystis* PCC 6803 overexpressing RuBisCO grow faster with increased photosynthesis. *Metab Eng Commun.* 2017;4:29-36.
251. Woolston BM, Edgar S, Stephanopoulos G: Metabolic engineering: past and future. *Annu Rev Chem Biomol.* 2013;4:259-88.
252. Blank LM: Let's talk about flux or the importance of (intracellular) reaction rates. *Microb Biotechnol.* 2017;10:28-30.
253. Schrewe M, Julsing MK, Bühler B, Schmid A: Whole-cell biocatalysis for selective and productive C-O functional group introduction and modification. *Chem Soc Rev.* 2013;42:6346-77.
254. van Alphen P, Najafabadi HA, dos Santos FB, Hellingwerf KJ: Increasing the photoautotrophic growth rate of *Synechocystis* sp. PCC 6803 by identifying the limitations of its cultivation. *Biotechnol J.* 2018;13.
255. Zavrel T, Knoop H, Steuer R, Jones PR, Cervený J, Trtilek M: A quantitative evaluation of ethylene production in the recombinant cyanobacterium *Synechocystis* sp. PCC 6803 harboring the ethylene-forming enzyme by membrane inlet mass spectrometry. *Biores Technol.* 2016;202:142-51.
256. Grund M, Jakob T, Wilhelm C, Bühler B, Schmid A: Electron balancing under different sink conditions reveals positive effects on photon efficiency and metabolic activity of *Synechocystis* sp. PCC 6803. *Biotechnol Biofuels.* 2019;12:43.
257. Running JA, Bansal K: Oxygen transfer rates in shaken culture vessels from fernbach flasks to microtiter plates. *Biotechnol Bioeng.* 2016;113:1729-35.
258. Gaden EL: Improved shaken flask performance. *Biotechnol Bioeng.* 1962;4:99-103.
259. Kim HW, Vannela R, Zhou C, Harto C, Rittmann BE: Photoautotrophic nutrient utilization and limitation during semi-continuous growth of *Synechocystis* sp. PCC 6803. *Biotechnol Bioeng.* 2010;106:553-63.
260. Burnap RL, Hagemann M, Kaplan A: Regulation of CO₂ Concentrating Mechanism in Cyanobacteria. *Life.* 2015;5:348-71.
261. Burnap RL, Nambudiri R, Holland S: Regulation of the carbon-concentrating mechanism in the cyanobacterium *Synechocystis* sp. PCC 6803 in response to changing light intensity and inorganic carbon availability. *Photosynth Res.* 2013;118:115-24.
262. Norena-Caro D, Benton MG: Cyanobacteria as photoautotrophic biofactories of high-value chemicals. *J Co2 Util.* 2018;28:335-66.

263. Russo DA, Zedler JAZ, Jensen PE: A force awakens: exploiting solar energy beyond photosynthesis. *J Exp Bot.* 2019;70:1703-10.
264. Nielsen AZ, Mellor SB, Vavitsas K, Wlodarczyk AJ, Gnanasekaran T, de Jesus MPRH, King BC, Bakowski K, Jensen PE: Extending the biosynthetic repertoires of cyanobacteria and chloroplasts. *Plant J.* 2016;87:87-102.
265. Grund M, Jakob T, Toepel J, Schmid A, Wilhelm C, Bühler B: Heterologous lactate synthesis in *Synechocystis* sp. PCC 6803 causes a condition-dependent increase of photosynthesis rates. submitted.
266. Karande R, Salamanca D, Schmid A, Bühler K: Biocatalytic conversion of cycloalkanes to lactones using an *in-vivo* cascade in *Pseudomonas taiwanensis* VLB120. *Biotechnol Bioeng.* 2018;115:312-20.
267. Salamanca D, Karande R, Schmid A, Dobslaw D: Novel cyclohexane monooxygenase from *Acidovorax* sp. CHX100. *Appl Microbiol Biot.* 2015;99:6889-97.
268. Yamanaka R, Nakamura K, Murakami A: Reduction of exogenous ketones depends upon NADPH generated photosynthetically in cells of the cyanobacterium *Synechococcus* PCC 7942. *AMB Express.* 2011;1.
269. Jones PR: Genetic instability in cyanobacteria - an elephant in the room? *Front Bioeng Biotechnol.* 2014;2:12.
270. Cano M, Holland SC, Artier J, Burnap RL, Ghirardi M, Morgan JA, Yu J: Glycogen synthesis and metabolite overflow contribute to energy balancing in cyanobacteria. *Cell Rep.* 2018;23:667-72.
271. Tamagnini P, Axelsson R, Lindberg P, Oxelfelt F, Wünschiers R, Lindblad P: Hydrogenases and hydrogen metabolism of cyanobacteria. *Microbiol Mol Biol Rev.* 2002;66:1-20, table of contents.
272. Carrieri D, Wawrousek K, Eckert C, Yu J, Maness PC: The role of the bidirectional hydrogenase in cyanobacteria. *Biores Technol.* 2011;102:8368-77.
273. Gudmundsson S, Nogales J: Cyanobacteria as photosynthetic biocatalysts: a systems biology perspective. *Molecular bioSystems.* 2015;11:60-70.
274. Shastri AA, Morgan JA: A transient isotopic labeling methodology for ¹³C metabolic flux analysis of photoautotrophic microorganisms. *Phytochemistry.* 2007;68:2302-12.
275. Shastri AA, Morgan JA: Flux balance analysis of photoautotrophic metabolism. *Biotechnol Progr.* 2005;21:1617-26.
276. Succinity: Succinity produziert erste kommerzielle Mengen biobasierter Bernsteinsäure. Press release https://www.basf.com/global/documents/de/news-and-media/news-releases/2014/03/P-14-0303-CI_Succinity.pdf. 2014.
277. Subramanian MR, Talluri S, Christopher LP: Production of lactic acid using a new homofermentative *Enterococcus faecalis* isolate. *Microb Biotechnol.* 2015;8:221-9.
278. Melis A: Carbon partitioning in photosynthesis. *Curr Opin Chem Biol.* 2013;17:453-6.
279. Halan B, Bühler K, Schmid A: Biofilms as living catalysts in continuous chemical syntheses. *Trends Biotechnol.* 2012;30:453-65.
280. Mueller TJ, Ungerer JL, Pakrasi HB, Maranas CD: Identifying the metabolic differences of a fast-growth phenotype in *Synechococcus* UTEX 2973. *Sci Rep-Uk.* 2017;7.
281. Yu JJ, Liberton M, Cliften PF, Head RD, Jacobs JM, Smith RD, Koppelaar DW, Brand JJ, Pakrasi HB: *Synechococcus elongatus* UTEX 2973, a fast growing cyanobacterial chassis for biosynthesis using light and CO₂. *Sci Rep-Uk.* 2015;5.
282. de Winter L, Cabanelas ITD, Martens DE, Wijffels RH, Barbosa MJ: The influence of day/night cycles on biomass yield and composition of *Neochloris oleoabundans*. *Biotechnol Biofuels.* 2017;10:104.
283. Krzeminska I, Pawlik-Skowronska B, Trzcinska M, Tys J: Influence of photoperiods on the growth rate and biomass productivity of green microalgae. *Bioprocess Biosyst Eng.* 2014;37:735-41.

Supplemental Information

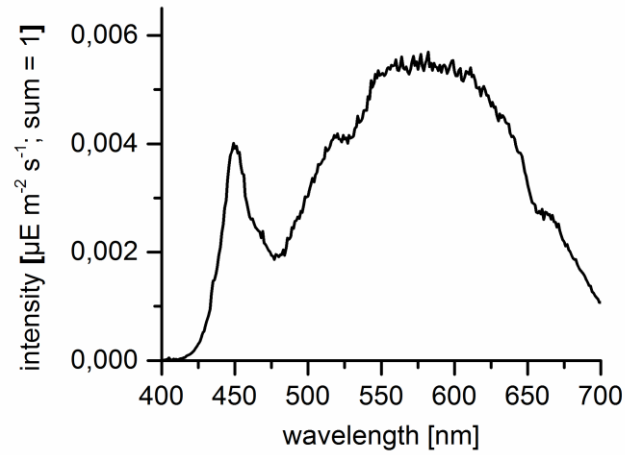


Figure S1: Emission spectrum of the bioreactor LED panel used in this study normalized to $1 \mu\text{mol photons m}^{-2} \text{s}^{-1}$ PAR.

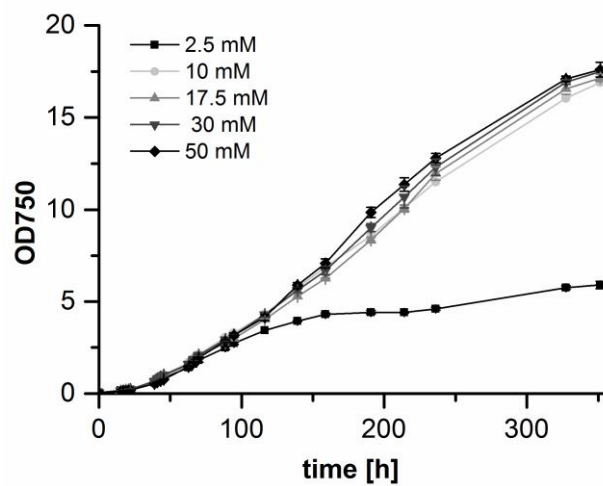


Figure S2: Growth of PCC6803 at different ammonium concentrations. No negative effect on growth in batch mode was observed up to an ammonium concentration of 50 mM. PCC6803 was cultivated in shake flasks at $50 \mu\text{mol photons m}^{-2} \text{s}^{-1}$ in YBG11 supplemented with 50 mM HEPES at pH 7.8 and different concentrations of ammonium chloride ranging from 2.5 to 50 mM.

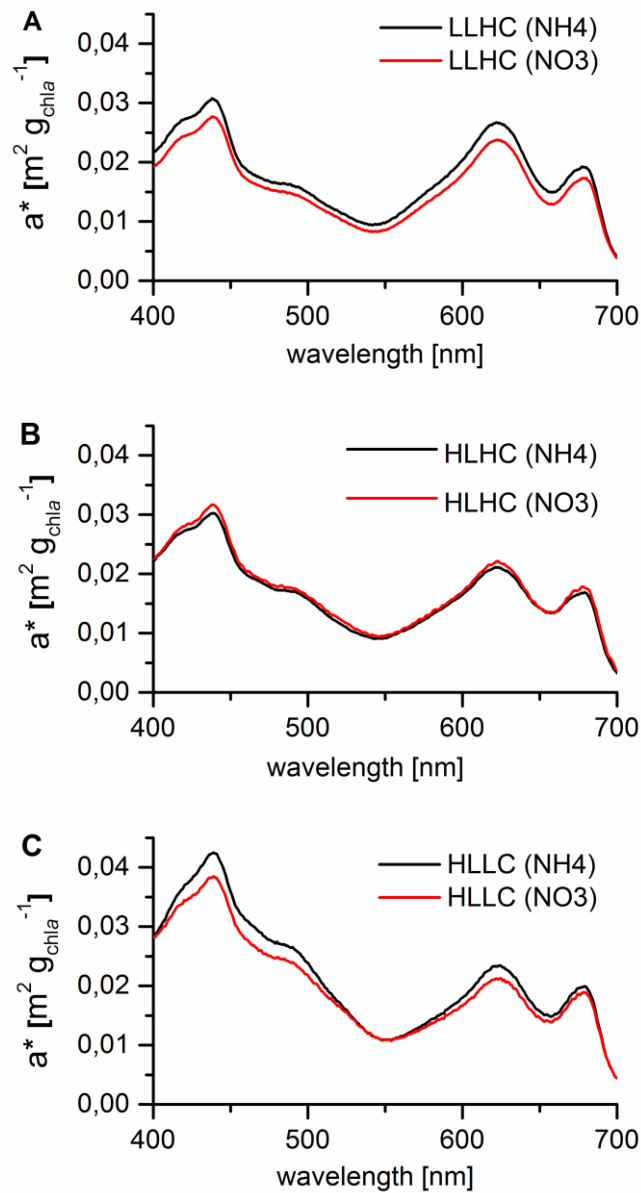


Figure S3: Chlorophyll *a*-specific absorption spectra of PCC6803 under different sink-source availabilities. The spectra were measured for cells in the investigated metabolic states low light high carbon (LLHC, panel A), high light high carbon (HLHC, panel B), and high light low carbon (HLLC, panel C).

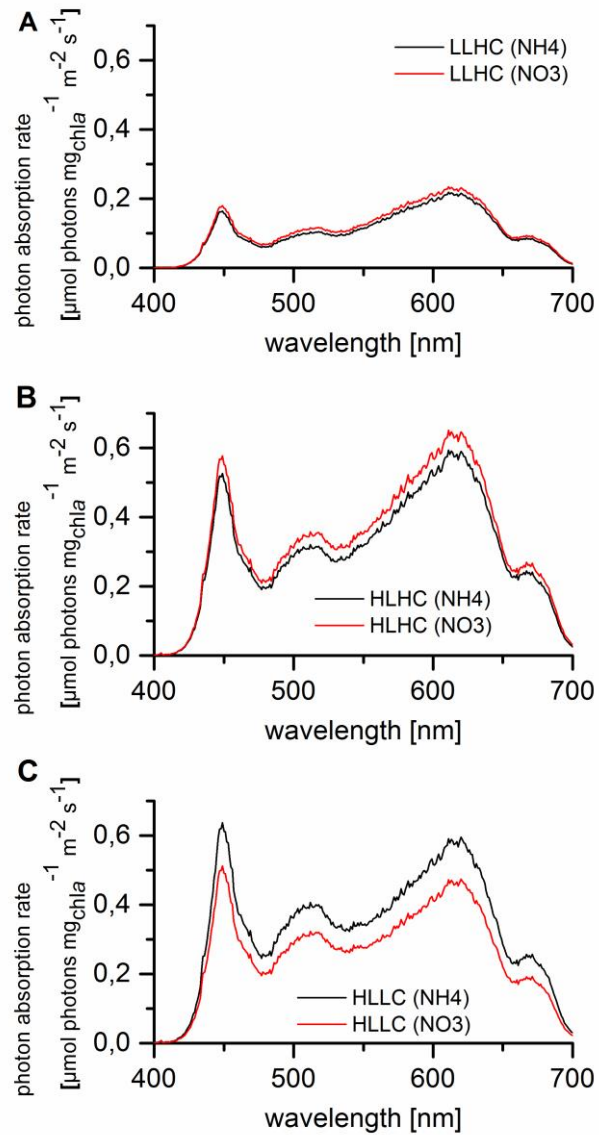


Figure S4: Wavelength-dependent quantum uptake rate (Q_{phar}) of PCC6803 under different sink-source availabilities. Spectra were measured on three different days per condition and averaged: low light high carbon (LLHC, panel A), high light high carbon (HLHC, panel B), and high light low carbon (HLLC, panel C).

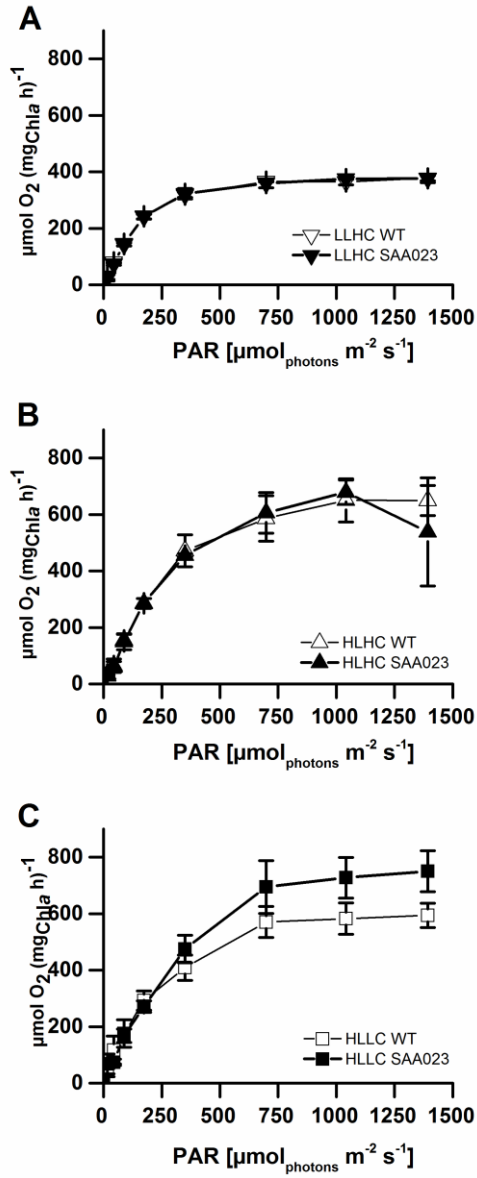


Figure S5: Light induction curves (LIC) of PCC6803 WT and SAA023 under the tested conditions. LICs were performed for cells grown in the conditions light limitation (LLHC, panel A), excess availability of light and carbon (HLHC, panel B), and carbon limitation (HLLC, panel C).

Curriculum Vitae

Personal Data

Name Marcel Grund
Born July 17, 1986 in Hagen
Nationality German
Academic degree Diplom Ingenieur (Bioingenieurwesen)

Education

2013 –2019 **PhD studies** at MLU Halle-Wittenberg & in the group Applied Biocatalysis in the Department of Solar Materials, Helmholtz-Centre for Environmental Research (UFZ), Leipzig, Germany
2011 –2012 **Diploma thesis** at the Australian Institute for Bioengineering and Nanotechnology, The University of Queensland, Brisbane, Australia
2006 –2012 **Study of Biochemical Engineering** at TU Dortmund University, Dortmund, Germany
1997 –2006 **Abitur** at Ruhrtal-Gymnasium Schwerte, Schwerte, Germany

Publications

Grund, M.; Jakob, T.; Toepel, J.; Schmid, A.; Wilhelm, C.; Bühler, B.:
„Heterologous lactate synthesis in *Synechocystis* sp. PCC 6803 causes a condition-dependent increase of photosynthesis rates in *Synechocystis* sp. PCC 6803.”
Submitted

Grund, M.; Jakob, T.; Wilhelm, C.; Bühler, B.; Schmid, A. (2019):
„Electron balancing under different sink conditions reveals positive effects on photon efficiency and metabolic activity of *Synechocystis* sp. PCC 6803.”
BMC Biotechnology for Biofuels, 12, 43

Collins, J.; Grund, M.; Brandenbusch, C.; Sadowski, G.; Schmid, A.; Bühler, B. (2015):
„The dynamic influence of cells on the formation of stable emulsions in organic–aqueous Biotransformations.”
Journal of Industrial Microbiology & Biotechnology, 42(7), 1011-1026

Ebert, B. E.; Kurth, F.; Grund, M.; Blank, L. M.; Schmid A. (2011):
„Response of *P. putida* KT2440 to increased NADH and ATP demand.”
Applied and Environmental Microbiology, Vol. 77(18), 6597-6605

Eiden, F.; Grund, M.; Blank, L. M. (2011):
„Synthetische Biologie: Wege zur Synthese von Ganzzellbiokatalysatoren.”
GIT Labor-Fachzeitschrift 4/2011, 252–253, GIT VERLAG GmbH & Co. KG, Darmstadt

Presentations

„The Sink-Effect in Cyanobacteria – from Myths to Facts: A Systematic and Quantitative Investigation in the Model Organism *Synechocystis* sp. PCC 6803.”

Photobiotechnology Symposium, 10. - 11.12.2018, Leipzig, Germany

„The Influence of additional Energy Sinks on the Energy Distribution in the Model Cyanobacterium *Synechocystis* sp. PCC 6803.”

2nd International Solar Fuels Conference (ISF-2), 06. - 10.07.2017, San Diego, USA

Poster

Grund, M.; Jakob, T.; Wagner, H.; Wilhelm, C.; Bühler, B.; Schmid, A.:

„Quantitative Physiology in Cyanobacteria - Can we uncouple energy and carbon metabolism in cyanobacteria?”

HIGRADE Conference 2017, 10.05.2017, Leipzig, Germany

Grund, M.; Frick, O.; Bühler, B.; Schmid, A.:

„Towards quantitative physiology in cyanobacteria by isotopically instationary ¹³C-metabolic flux analysis.”

DECHEMA Summer School Quantitative Biology 2015, 20. - 24.07.2015, Berlin, Germany

Grund, M.; Krabbe, P.; Frick, O.; Bühler, B.; Schmid, A.:

„Towards quantitative physiology in cyanobacteria.”

1st International Solar Fuels Conference (ISF-1), 26.04. - 01.05.2015, Uppsala, Sweden

Grund, M.; Frick, O.; Bühler, B.; Schmid, A.:

„Metabolic Engineering of Cyanobacteria as Efficient Industrial Biocatalysts.”

UFZ EnergyDays 2015, 24. - 25.02.2015, Leipzig, Germany

Grund, M.; Frick, O.; Bühler, B.; Schmid, A.:

„Metabolic Engineering of Cyanobacteria as Efficient Industrial Biocatalysts.”

DECHEMA Summer School Biotransformations 2014, 24. - 27.08.2014, Bad Herrenalb, Germany

David, C.; Grund, M.; Bühler, B.; Bühler, K.; Schmid, A.:

„Applied Biocatalysis & Bio-Artificial Photosynthesis.”

POF III Evaluation Meeting, 04.02.2014, Berlin, Germany